

**DEVELOPMENT OF SUITABLE FAILURE CRITERIA
FOR DESIGNING SUFFICIENT MUD WEIGHTS
FOR NIGER DELTA WELL**

BY

NWANRO CHIDINDU PEACE (B.Eng)

20134937848

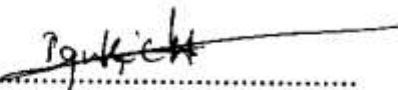
**A THESIS SUBMITTED TO THE POSTGRADUATE SCHOOL,
FEDERAL UNIVERSITY OF TECHNOLOGY, OWERRI**

**IN PARTIAL FULFILLMENT OF THE REQUIREMENTS FOR THE
AWARD OF THE DEGREE OF MASTERS OF ENGINEERING, (M.Eng)
IN PETROLEUM ENGINEERING**

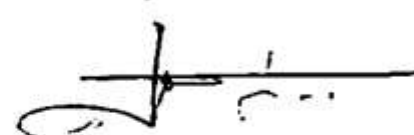
FEBRUARY, 2022

CERTIFICATION

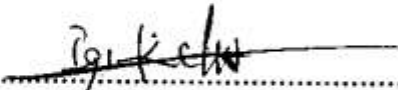
This is to certify that this work "Development of Suitable Failure Criteria for Designing Sufficient Mud Weights in Niger Delta" was carried out by NWANRO PEACE CHIDINDU with Reg. No. 20134937848 in partial fulfillment for the award of the degree of M.Eng in Petroleum Engineering in the Department of Petroleum Engineering, School of Engineering of the Federal University of Technology, Owerri.


.....
Engr. Dr. Kevin C. Igwilo
Principal Supervisor

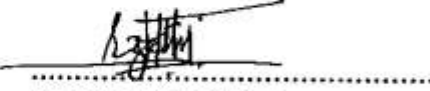
12/02/2022
.....
Date


.....
Engr. Dr. N.P. Ohia
Co-Supervisor

10/02/2022
.....
Date


.....
Engr. Dr. Kevin C. Igwilo
HOD, Petroleum Engineering

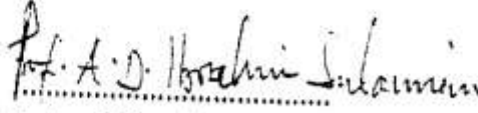
12/02/2022
.....
Date

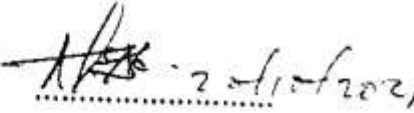

.....
Engr. Prof. J. C. Ezeh
Dean, SEET

08/12/2022
.....
Date

.....
Prof. C.C. Eze
Dean, Postgraduate School

.....
Date


.....
External Examiner


.....
Date

DEDICATION

I dedicate this thesis to Almighty God, who through His infinite mercy and Grace this thesis is realized. May all glory, honour and adoration be ascribed unto His holy name, in Jesus name.

Amen,

ACKNOWLEDGEMENT

I am very thankful to my energetic principal supervisor and Head of Petroleum Engineering Department, Engr. Dr. Kevin Igwilo and Co-supervisor Engr Dr P.N. Ohia for their unalloyed support, encouragements and timely review of the work. My thanks also go to Engr. Dr Anthony Kerunwa for his encouragement.

TABLE OF CONTENTS

Certification page	ii
Dedication	iii
Acknowledgment	iv
Abstract	v
Table of Contents	vi
List of Tables	viii
List of Figures	ix
CHAPTER ONE: INTRODUCTION	1
1.1 Background of the Study	1
1.2 Problem Statement	3
1.3 Study Objectives	3
1.4 Significance of the Study	4
1.5 Scope of the Study	4
CHAPTER TWO: LITERATURE REVIEW	5
2.1 Drilling Fluids	5
2.2 Fluid Selection Factors	23
2.3 Well Bore Stress	27
2.4 Rock Failure Modes	35
2.5 Rock Failure Criteria	36
CHAPTER THREE: MATERIALS AND METHODOLOGY	45
3.1 Materials	45
3.2 Method	45
CHAPTER FOUR: RESULTS AND DISCUSSIONS	59
4.1 Results	59
CHAPTER FIVE: CONCLUSIONS AND RECOMMENDATIONS	76
5.1: CONCLUSIONS	76
5.2: RECOMMENDATIONS	77
5.3: CONTRIBUTION TO KNOWLEDGE	78
REFERENCES	79
NOMENCLATURE	87
Appendix 1	91

LIST OF TABLES

Table 2.1: Drilling mud additives, functions and examples	17-18
Table 4.1: Results of in-situ stresses for the 5 wells	59
Table 4.2: Relatives Magnitude and Stress Regimes	60
Table 4.3: Results of the local stresses for the 5 wells	61
Table 4.4 Results of the actual and model predicted mud weight for well T-101	67
Table 4.5: Results of the actual and model predicted mud weight forWell A-33	69
Table 4.6: Results of the actual and model predicted mud weight forWell D-705	71
Table 4.7 Results of the actual and model predicted mud weight forWell Z-47	74
Table 4.8 Results of the actual and model predicted mud weight forWell Q-01	75

LIST OF FIGURES

Figure 1.1: The concept of safe mud weight windows for drilling	2
Figure 2.2: Flow curve for different fluid types	19
Figure 2.3 Stress components showing the normal and shear stress	28
Figure 3.1: work flow chart for developing a suitable model based criteria for Designing sufficient mud weight	46
Figure 4.1: Plot of Failure Criterion vs Mud Weight for Well T-101	62
Figure 4.2: Plot of Failure function vs Mud Weight for Well A-33	63
Figure 4.3: Plot of Failure function vs Mud Weight for Well D-705	64
Figure 4.4: Plot of Failure function vs Mud Weight for Well Z-47	65
Figure 4.5: Plot of Failure function vs Mud Weight for Well Q-01	66
Figure 4.6 Effects of different failure criteria on minimum mud weight for Well T-101	68
Figure 4.7: Effects of different failure criteria on maximum mud weight for Well T-101	69
Figure 4.8: Effects of different failure criteria on minimum mud weight for Well A-33	70
Figure 4.9: Effects of different failure criteria on maximum mud weight for Well A-33	71
Figure 4.10: Effects of different failure criteria on minimum mud weight for Well D-705	73
Figure 4.11: Effects of different failure criteria on maximum mud weight for Well D-705	73

ABSTRACT

Drilling the well to the target depth comes with it a lot of challenges; part of the issues related to drilling both vertical and deviated wellbores is related to the type of formation failures and well problems observed during drilling. Wellbore direction and deviation changes during drilling while the formation is the same, the effect of transformed stresses around the wellbore wall will be different. This is obvious that neither rock properties nor in-situ stresses can be changed to mitigate the failures of the wellbore. However, the density of the drilling mud can significantly control the situation. Large wellbore pressure due to using high mud density could enforce the formation to open in tensile mode, which in due course may result in mud loss or ultimately fracturing the formation. Also, using a low density mud, corresponding to low wellbore pressure may result in rock failure in shear mode and consequently breakouts. Most drilling engineers do not incorporate thorough wellbore stability analysis as part of well planning due to the complexity of wellbore stability models and thus employs the traditional practice which is identifying the pore pressure and adding extra pressure typically 100-200psi in mud equivalent as safety margin. Predicted mud weights in this manner end up in failed states resulting in several types of problems such as stuck pipe, lost circulation, formation damage and well control problems simply because either the mud weights designed are not sufficiently screened or those operating them lack the basic understanding of such mud systems. Five case studies were considered in this work to analyze the well and mud data from previously drilled wells with typical wellbore stability issues in the Niger Delta Region. A problem diagnostic was conducted to determine the main cause of the instability issues in these wells. Based on our findings, an excel based spreadsheet was developed for all the data and to perform all calculations. A coupled Mogi-Coulomb criterion further developed predicts the safe mud weight window in an iterative manner and describes the rock failure more accurately than does the traditional Mohr-Coulomb criterion which is independent of the intermediate principal stress, and presents a very slim mud weight window. Results of this study can help well trajectory optimization, proper mud weight determination, hydraulic fracturing job, sanding analysis and reduce non-productive time (NPT) while drilling.

Key Words: Vertical and Deviated wellbores, Stresses, Wellbore Instability, Safe Mud window and Rock failure.

CHAPTER ONE

INTRODUCTION

1.1 Background of the Study

Drilling deep wellbores in oil and gas industry is to access the reservoir formation for production purposes. While drilling vertical wells is a common approach, sometimes it is necessary to drill deviated or horizontal wells when more production is required as it provides maximum reservoir contact. Drilling non-vertical wells is more important in unconventional reservoirs such as shale gas or tight formations as the hydrocarbon bearing formations in such reservoirs exhibit very low permeability and having large exposure to the wellbore wall is essential for economical production rate (Joshi, 2003).

Almost every drilling problem has a link, directly or indirectly with the performance of the drilling fluid. This is not to say that the drilling fluid can be traced as the source or solution of all problems encountered during drilling operations, rather, as a tool that can often be used to alleviate a difficult drilling situation. Therefore in general, a drilling fluid should be seen as a very vital and intricate part of the whole drilling process that should be used to complement other aspects of the operation.

For any drilling operation to be termed successful, care must be taken during the selection and application of the drilling fluid which are key factors that should be considered. Any actions contrary to carefully selection and application of drilling fluids could have very dire consequences ranging from destruction of the drilling rig equipment, non-productive time leading to financial losses, damage to environment and loss of lives of crew workers, therefore the properties of drilling fluids must from the onset of the drilling operation, and at regular intervals, be monitored, tested and investigated to ascertain they have the desired qualities all the way, and in most cases, drilling mud agents are added to the muds if needed to necessitate a successful drill operation.

Drilling the well to the target depth comes with it a lot of challenges, part of the issues related to drilling both vertical and deviated wellbores is related to the type of formation failures and well problems observed during drilling. However, as the wellbore direction and deviation changes, while the formation is the same, the effect of transformed stresses around the wellbore wall will be different. This is obvious that neither rock properties nor in-situ stresses can be changed to mitigate the failures of the wellbore. However, the density of the drilling mud can significantly control the situation. Large wellbore pressure, due to using high mud density could enforce the formation to open in tensile mode, which in due course may result in mud loss or ultimately fracturing the formation. Also, using a low density mud, corresponding to low wellbore pressure may result in rock failure in shear mode and consequently breakouts. Very low mud weight of below the reservoir pressure will result in a kick (Nas, 2011). Therefore there is a safe mud weight window (MWW) to be used for drilling with minimum instability or safety issues.

In order to develop a suitable criteria for designing a given mud weight used for drilling or perform a complete wellbore stability analysis, as explained above, we need these sets of information: the formation mechanical properties (i.e. Young's modulus, Poisson's ratio, compression and tensile strength) and the state of in-situ stresses (i.e. magnitude of vertical and maximum and minimum horizontal stresses) and the direction of maximum stress, plus the magnitude of pore pressure. Normally, the output of these is used for various studies including determination of the mud weight window for drilling, hydraulic fracturing job and sanding analysis (Rasouli et al., 2010).

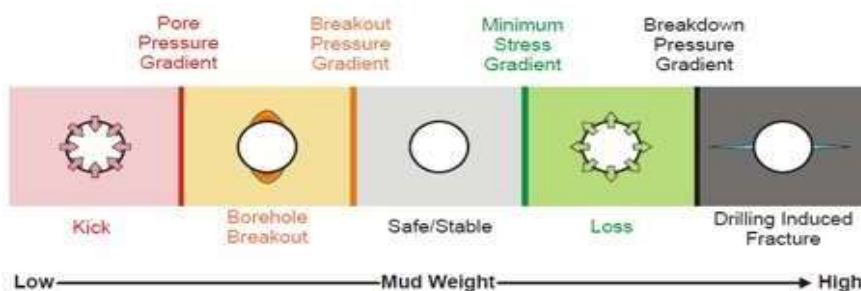


Figure 1.1: The concept of safe mud weight windows for drilling (Rasouli et al., 2010).

1.2 Problem Statement

A good drilling mud whether for conventional or challenging environments has to fulfill some basic requirements, it has to be generally simple with a number of additives, and it is worth knowing that the performance of a drilling mud should be driven more by engineering than of the product used. Most often, during drilling operations exotic mud systems end up in failed states resulting in several types of problems such as stuck pipe, lost circulation, borehole instability, pipe failures, formation damage and well control problems simply because either the mud weights designed are not sufficiently screened or those operating them lack the basic understanding of such mud systems (Azar and Robello, 2007). The type of mud chosen for a particular well depends on three important factors; cost, technical performance and environmental impact. The cost of products is very important, but should only be considered on a cost-performance basis. Most important of all three is the technical performance of the drilling mud (Hawker 2001; Devereux 1999). Each of these problems as mentioned above can lead to significant high nonproductive time (NPT), which in return leads to a high additional cost of the operation. By designing an appropriate mud density and subjecting it to thorough suitability screening, it is possible to control the well problems to a certain degree.

1.3 Study Objectives

The main objective of this research is to develop suitable criteria for designing sufficient mud weights in Niger Delta Region. The specific objectives are:

- i. To conduct an extensive literature study on mud rheology, wellbore stability and failure criterion
- ii. To determine the major cause of problem in the studied wells
- iii. To analyze the well, geo-mechanical and mud data from selected previously drilled wells in the Niger Delta Region.
- iv. To create a wellbore stability model applicable in the studied area using well data, drilling report geo-mechanical and geological data.

- v. To develop a suitable criterion and perform thorough wellbore stability analyses to understand the causes of well problems on the selected case studies.
- vi. To generate safe mud weight window for the 5wells in the case study
- vii. To compare new model results prediction against an existing failure model

1.4 Significance of the Study

The main drilling management goals are expected to be achieved in this study which include minimizing non-productive time (NPT) and reduction in overall cost of the operation by shying away from well stability problems. This research is representing a quantum leap forward in drilling economics, by marrying all the benefits realized with this simple robust and reliable mud design selection criterion.

1.5 Scope of the Study

The study would focus on a number of drilled wells in the Niger Delta Region. Based on available drilling reports, some wells drilled with mud will be selected and all the well and drill mud data documented will be screened and used for the analysis.

CHAPTER TWO

LITERATURE REVIEW

2.1 Drilling Fluids

Fink (2011) defined drilling fluid as a circulating fluid used in rotary drilling to perform any or all of the various functions required in drilling operations. It is the single most essential system in safe, efficient, and economic well drilling. The drilling fluid consists of a mixture of natural and synthetic compounds used for a variety of purposes.

2.1.1 Types of Drilling Fluids

Currently in the industry, there are four common types of drilling fluids available, which are (Economides, Watters and Dunn-Norman, 1998):

- i. Water-based mud (WBM)
- ii. Oil-based mud (OBM)
- iii. Synthetic-based mud
- iv. Pneumatic drilling fluids

2.1.1.1 Water Base Muds (WBM)

Water Base Muds also referred to as aqueous drilling fluid, which is 90–95 % of fresh water, salt or sea water and several dissolved substances meaning that water is the continuous phase here (Skalle 2010; Devereux 1999). It is predominantly used in the industry due to its environmentally acceptable nature, and also because it is relatively cheap to operate with. WBM is the drilling mud type which would be focused on and used in this project. There are several types of WBM as seen below;

- i. Dispersed Muds– These mud type are basically used at greater depths requiring higher densities or in problematic hole conditions where heightened treatments are required. The mud system would be dispersed with specific additives to give specific properties to the mud e.g. thinners or dispersants.

- ii.** Non – Dispersed Muds - These mud type are basically applied for shallow wells or top hole sections. Clear or native water is used and examples are spud muds, natural muds and other lightly treated systems. The use of thinners or dispersants to disperse drilled solids and clay particles is not required, rather, the water is allowed to react with formations containing shales/clays so that the mud will form solids content and density naturally.
- iii.** Salt water Muds – This could either be a saturated salt system with chlorides concentration around 190,000 mg/l, which is suitable for salt formation drilling in order to prevent dissolving, or a saltwater system where chloride concentration lies between 10,000 and 190,000 mg/l(Van Dyke & Baker 1998; Hawker 2001).
- iv.** Polymer Muds – Long chain polymers such as cellulose and acrylamide are used in mud systems to provide a number of functions; increase viscosity, prevent dispersion by acting as encapsulating agents to drilled solids, minimize fluid loss, and inhibit or prevent sloughing of shales by coating. Example of such is KCl/NaCl muds which are inhibited salts that stabilize shale formations.
- v.** Low solids Mud – This mud system is significantly used to control or improve the rates of penetration. These are systems where the amounts of solids are intentionally controlled with a range of 6 to 10 % total solids volume and clay volume not more than 3 %. They typically use polymer additives as viscosifier and are non-dispersed.
- vi.** Calcium Muds – The presence of calcium or magnesium in fresh water drilling muds inhibits swelling and hydration of clays and shales, but with higher levels of dissolved calcium, the problems of shale sloughing and hole enlargement are greatly reduced. Calcium treated muds also resist contamination and are therefore suitable for use in drilling gypsum/anhydrite lithologies. However, they are susceptible to gelling and solidifying at elevated temperatures.

2.1.1.2 Oil Base Muds (OBM)

These muds have oil as their continuous phase, usually diesel oil, mineral oil or low toxicity mineral oil, and although they may pick up formation water, no additional water or brine is added. This is due to the fact that they contain water-emulsifying agents. Oil-based mud is known for having good inhibitive properties against shale formations and granting drill string lubrication, which both assists in providing a good drilling performance. The chances of experiencing drilling related problems such as corrosion and stuck pipe can be reduced and to some degree avoided by using oil-based mud (Skjeggestad, 1989). This kind of mud is very effective when drilling in scenarios such as; highly reactive shale and evaporite, as long as the salinity of the emulsified water is higher than the salinity of the water in the formation (Skjeggestad, 1989), extended reach wells, and high-pressure, high temperature wells exposed to hydrogen sulfide (H₂S), which will get neutralized due to the high content of calcium hydroxide (Ca(OH)₂) in OBM (Skjeggestad, 1989; Economides et al., 1998).

2.1.1.3 Synthetic Base Muds (SBM)

Out of an increased desire to reduce the environment impact of offshore drilling operations, synthetic-base muds were developed but without sacrificing the cost-effectiveness of oil-based systems. They (synthetic oils and mineral oils) provide much of the performance advantages of hydrocarbon oil systems but have none of the associated environmental concerns (Fink, 2011). Like OBMs, SBMs can be applied to minimize wellbore stability problems arising from reactive shales, maximize the rate of penetration and increase lubricity in directional and horizontal wells. Examples of synthetic mud systems are esters, ethers and poly or isomerized alpha olefins. These have high biodegradability and low toxicity and as such, are good base fluids for environmental performance.

2.1.2 Functions of Drilling Fluids

Drilling fluids should have the following functions in every drilled well at some point in time.

2.1.2.1 Formation Pressure Control

The proper restraint of formation pressures depend upon the density or the weight of the mud column in the well. The density of the drilling mud must be such that the hydrostatic pressure exerted by the mud column will prevent flow into the well bore. As the formation pressures increase, the density of the drilling fluid is increased to help maintain a safe margin and prevent “kicks” or “blowouts.” However, if the density of the fluid becomes too heavy, the formation can break down. If drilling fluid is lost in the resultant fractures, a reduction of hydrostatic pressure occurs. This pressure reduction also can lead to an influx from a pressured formation. Therefore, maintaining the appropriate fluid density for the wellbore pressure regime is critical to safety and wellbore stability.

The well is said to be “**balanced**” if the mud hydrostatic pressure is equal to the formation pressure. It is said to be “**underbalanced**” if the mud hydrostatic pressure is less than the formation pressure and “overbalanced” if the mud hydrostatic pressure is greater than the formation pressure (Van Dyke & Baker 1998; Devereux 1999). Control of formation pressure remains a very big issue when it comes to drilling mud function because it does not only consist of controlling the formation and hydrostatic pressures in the well bore, it also consists of controlling pressure build dissipated in frictional losses along the entire flow path. As a result, the sum of the hydrostatic pressure and the circulating pressure drop from a particular point to the exit point make up the total pressure in a circulating system.

Equivalent Circulating Density (ECD) represents the total-actual bottom hole pressure exerted on the formation being drilled and is usually given in terms of equivalent density (Skalle 2010). ECD is the cumulative sum of the static density, the density or weight of drill cuttings in the annulus and the effect of pressure drop along the annulus. Figure 2.1 shows the graphical effects of ECD.

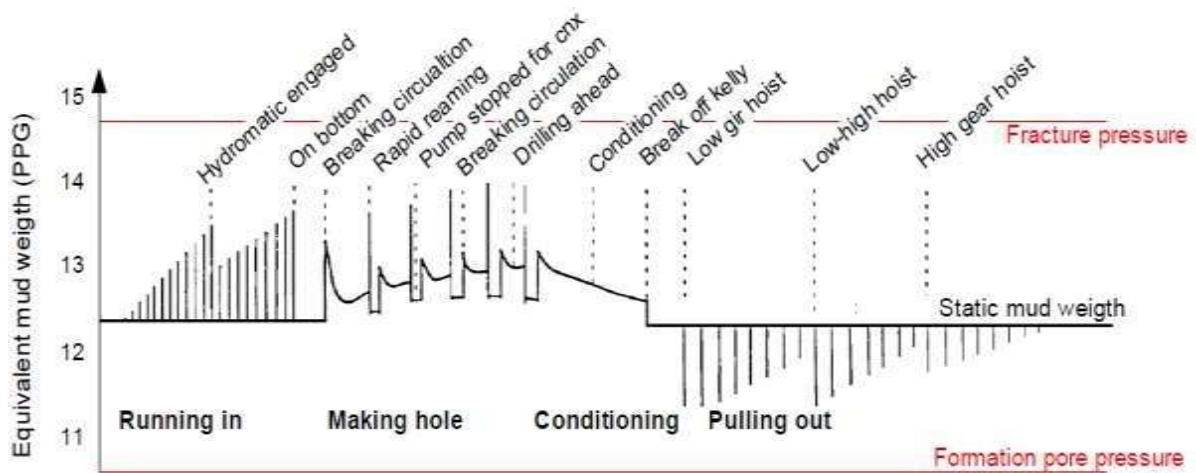


Figure 2.1: Graphical view of pressure variation during tripping and drilling (Skalle 2010).

2.1.2.2 Cooling and Lubricating Drill String and Bit

The circulation of mud down the drill string cools the bottom of the well bore. The mud should have sufficient thermal properties (heat capacity and thermal conductivity) to absorb heat down hole by convection, convey this absorbed heat to the surface and release it to the atmosphere by radiation. As the geothermal bottom-hole temperature is higher than the maximum mud temperature during circulation, it is important to know that the point of maximum circulating temperature is not at the bottom of the hole as many would imagine, but say about two-thirds the way down the hole. This fact is particularly important when additives which are influence by temperature are used, because it could be possible to have a mud additive which may perform satisfactorily at circulating temperatures, but at the geothermal bottom-hole temperature, becomes absolutely unstable or vice-versa (Potash & Nygren 1993; Max and Annis 1996).

Furthermore, the circulating mud also gets rid of frictional heat produced in large quantities by the drill bits and string and provides some lubricating effects as well which is aimed at increasing drilling efficiency and improving the bit's life. When using a diamond bit for example which happens to be very expensive, then it is very essential to keep the temperature below a certain critical value because at higher temperatures, graphitization of diamond could be induced which

would lead to the destruction of the diamond structure hence reducing tool life and drilling efficiency (Max and Annis 1996).

The following factors are reasons lubrication is very important;

- i. Excessive torque and drag: The drill string, during drilling, may develop an unacceptable rotational torque and drag, often caused by key seats, improper hole cleaning and bit balling, which would make twisting and rotating very difficult thereby limiting horizontal displacement of the hole. This would give rise to a very high COF (Coefficient of friction) hence the need for lubricant effect.
- ii. Stuck pipe: In this case, the drill string cannot be rotated, neither can it be raised or lowered. This problem could be caused by a number of factors:
 - a. Unexpected differential formation pressure.
 - b. Buildup of drill cuttings or sloughing in the well bore.
 - c. Embedding of part of the drill string into wall cakes caused by irregular well bore development.
 - d. An under gauge borehole.

In the event that the drill pipe becomes embedded or stuck in the mud wall cake opposite a permeable zone, then this is termed “**Differential Pressure Sticking**”. The pipe gets stuck in place as a result of difference between the hydrostatic pressure in the drill pipe and the formation pressure. Differential pressure sticking could be prevented and a stuck pipe freed with the use of oil based mud or water based surfactant composition (Max and Annis 1996). This composition performs functions as permeating drilling mud wall cake, reducing differential pressure, reducing friction resistance and destroying binding wall cake. Unfortunately, the uses of these are severely limited by environmental concerns and high costs.

2.1.2.3 Seal Permeable Formations

Drilling mud should possess the quality of depositing filter cake on the wall of the well bore to consolidate the formation which is almost always permeable and to retard the flow of well bore fluid into the formation. This fluid is often referred to as “**fluid loss or filtrate loss**”. As the cake becomes thicker, sealing occurs thus decreasing the flow rate into the formation. This causes a reduction of the amount of fluid lost to the formation, with the filter cake progressively building up causing some other problems. For this reason, the filtration properties of mud should be measured and controlled.

In summary, a good mud must keep the loss of fluid to the formation as minimal as possible while preventing excessively thick filter cake. Thinner and less permeable are thus the desired characteristics of a good filter cake. The following are some of the problems associated with thick filter cakes;

- i. **Differential pressure sticking:** With increase in the wall cake thickness comes this problem of differential pressure sticking. Here, the contact area of pipe and the wall cake is increased resulting in decreased hole diameter and increased sticking force. The incidence of pipe sticking would be drastically reduced if thin and low permeable cakes durable enough are deposited on the wall of the hole.
- ii. **Lost circulation:** With increased wall cake thickness to an appreciable extent comes an increment in the circulating pressure drop due to the decreased clearance between the wall and the pipe. During swabbing or pulling out of the drill string, there would be an increase in pressure and even greater problems with increased surge pressure which could lead to a fractured formation resulting in escape of mud into the formation.
- iii. **Logging problems:** The feedback of some logging tools are affected by thick wall cakes as the tendency for the tools to be stuck is heightened and in some cases, the tools cannot be lowered down because of drag on a thick wall cake.

Other problems created by thick wall cakes include torque and drag, difficulty in running casing in the whole and poor cement jobs (Max and Annis 1996).

2.1.2.4 Well Bore Stability

A good combination of chemical composition and mud properties would provide a stable well bore. Also, pressure is a key player when it comes to well bore stability as the formation pore pressure must be balanced. Most peculiar with instability issues are shale formations as they are water-sensitive.

Mechanism of shale destabilization

Failure of shale formation is caused by a combination of 2 effects (Fink 2011; Skalle 2010);

- i. **Stress induction:** With the absorption of water by a shale formation, stress is induced into the formation. Increased absorption leads to a corresponding increase in the stress level until it eventually overcomes the peak strength of the rock. This yield in rock strength gives way to failure of the formation.
- ii. **Weakening effects:** Absorption of water goes into the grain boundaries and eventually penetrates the grain interstitials causing softening of the grains of the formation and an increased stress level. This weakening accelerates the occurrence of the rock failure.

In general, well bore instability is caused by reaction between drilling fluid and the formation due to discrepancies in their chemical make-up. Shale formations have a high affinity for water therefore they tend to be destabilized much easier than any other type of formation. Below are some of the causes of instability and some that aid instability as well.

- i. **Erosion**, which involves washing away a part of the shale formation by drilling fluid, may cause an already weakened formation to slough enlarging the hole. By reducing the annular velocities, these erosion effects can be lowered because there would be a change in the flow regime from turbulent to laminar.
- ii. **Swabbing** can also cause sloughing in an already weakened zone because during swabbing, hydrostatic pressure is reduced adding more stress imbalance at the wall. This

pulling out action of the drill string causes the fluid motion to act downwards on its own weight which is a deviation from normal. This may lead to displacement of rock particles in the drilled hole causing hole enlargement.

2.1.2.5 Drilled Cuttings Removal from the Annulus and Bit

This is the most basic function of mud which involves the mud being able to lift cuttings of various sizes out of the drilling hole. For this to be achieved, the mud must possess a high suspension capacity to ensure that during moments of non-circulation, the cuttings and commercially added solids as barite, do not sink to the bottom, the mud circulation rate must be adequate to prevent excessive increase in mud viscosity or density as a result of drilled solids being dispersed into it especially when they become finer. This would give rise to an increase in equivalent circulating density of the mud in the annulus exceeding the fracture gradient causing lost circulation. To reduce the effect of increased density and viscosity by these drilled solids, the rate of circulation can be increased, but this would in turn increase the ECD. In the event that the ECD is greater than the fracture gradient, the rate of drilling must be reduced. The chemical properties of the mud should be such that it helps to prevent or minimize dispersion of drilled solids so they can be efficiently be rid-off at the surface.

It is very vital that cuttings are being removed from the annulus because of reasons listed below (Max and Annis 1996; Hawker 2001);

- i. Maintaining minimum annular pressure
- ii. Permitting the drill string to move and rotate easily.
- iii. Preventing loading of the annulus.
- iv. Transporting drilled cuttings to the surface in proper conditions to aid in formation evaluation by geologists.

The annular velocity, the yield point and gel strength of the mud are the key determinants of cuttings removal with other factors as pipe rotation, hole inclination, size, colour, shape and density of drilled cuttings being secondary.

2.1.2.6 Cleaning Beneath the Bit

At high speeds and pressures, the rock surface is crushed by the drilling bit and in order to maintain the tempo of crushing, the cuttings must be removed in an efficient manner at the same or even greater rate than they are produced. Two types of energy namely mechanic and hydraulic energy are brought from the surface to the rock surface and the former takes care of the rock crushing process, while the latter, the cuttings removal process. Investigations have shown that drilling rate is increased significantly with increased hydraulic energy which could be as jet velocity through the bit nozzles or hydraulic horse-power.

2.1.2.7 Formation Evaluation

This function of mud which focuses on discovering and evaluating potential reservoir zones unfortunately is not being given so much focus as should be as attentions are being shifted to the drill rates and costs, which often lead to programs being implemented that have a detrimental side blow on formation evaluation. The drilled cuttings brought up the surface by the drilling mud are analyzed for information gathering about the formation. This could be for:

- i. **Cutting Analysis:** For accurate geological analysis, the best cuttings should be aimed at being transported out of the hole. This is one of the areas where the mud viscosity plays a very vital role as it determines how well the cuttings are being lifted and transported from the hole. Smooth laminar flows are preferred to turbulent flow patterns to reduce the degree of erosion and structural alteration of the cuttings (Hawker 2001). Typically, for production of high quality cuttings, then it is advisable to use oil bas muds as water base systems can react with most of the clay minerals.
- ii. **Wireline logs and production Tests:** It is necessary that both formation evaluation and mud programs are synchronized to be consistent with one another. Regardless of mud type, logs which can be run would be affected when in the well bore. The salinity of water base muds as well as the degree of flushing of the zone around the wellbore are important evaluation considerations.

2.1.2.8 Formation Damage

This function of drilling mud is concerned more with the type of filtrate than it is with the amount of fluid loss to a formation. A restriction in permeability will result if there is a reaction between the filtrate and the formation solids or fluids, because this would block the pore throats and pore spaces. Only a very narrow layer of damage around the well bore is sufficient to cause serious restriction of fluid flow, however, if the damaged zone is sufficiently narrow that the pore openings extend beyond it, then, the well could still produce effectively. This problem is normally associated with water sensitive formations which are mainly sands with appreciable clay solids content. Several factors are responsible for the degree of damage; the types of clay present in the pore space, their reaction with the filtrate, and of course, their mobility. On reacting with the filtrate, a change in the salinity or ionic level of the water present in the pores may result to either swelling or shrinking or the clay particles making them mobile. This will certainly cause damage. In solving the problem of formation damage, there is unfortunately no one best type of mud to prevent damage. This is because the type of clay and ionic content of the residual or connate water differs in a wide range from one formation to another. In some cases, special types of muds are used and they could work effectively in one scenario but badly in others e.g. saturated salt water appears to reduce damage in some sands but may not be appropriate in others. The same can be said of potassium chloride types of muds. Oil muds have been found to be suitable for preventing damage in water sensitive sands, but they have a drawback in that their use is not universal (Max and Annis 1996).

2.1.3 Properties of Drilling Fluids

It is very important to measure the mud properties (physico-chemical) when trying to design and maintain a mud system to perform a particular function. Since there are various mud properties, it is normal to carry out measurements on these properties by running tests and correlating the results with the functions of the mud. These mud tests are done mainly to simulate closely, downhole conditions or to predict the downhole mud properties from surface condition

measurements. Since drilling mud normally have multifunctional requirements, it is necessary to have both physical and compositional tests in order to properly monitor a mud system. Some of the mud properties are discussed in details below.

2.1.3.1 Density

The density of a fluid is temperature and pressure dependent. This means that as the pressure is increased the density of the fluid will also increase, and as the temperature is increase there will be a decrease in the density of the fluid.

2.1.3.2 Viscosity

Viscosity can be described as the internal resistance to flow. The resistance to flow is caused by both mechanical friction and electrochemical forces between the molecules. The viscosity is dependent on several factors, such as temperature, pressure and the physical/chemical composition of the fluid.

2.1.3.3 Plastic Viscosity

The plastic viscosity (PV) is the part of the flow resistance that is determined the mechanical friction in the fluid. The mechanical friction can be caused by the friction between the particles in the fluid as well as the friction between the liquid surface and the particles.

2.1.3.4 Apparent Viscosity

The apparent viscosity (AV) is the relationship between shear stress and shear rate, and provides information about the total viscosity of the fluid.

2.1.3.5 Yield Stress

The yield stress (YS) is the part of the resistance that is developed due to the electrochemical forces between the molecules in the fluid.

2.1.3.6 YS/PV Ratio

The ratio of yield stress to plastic viscosity is used as a measure of thinning of the fluid (Darley and Gray, 1988). When comparing fluids, a higher ratio will express a greater shear thinning.

2.1.4 Drilling Fluid Additives

Additives are added to mud to enhance its performance by changing its properties and composition particularly when the driller would like the mud to carry out specific function(s) to optimize the drilling operation. Several mud additives exist some performing more than one function, but only a few would be discussed subsequently. Some common mud additives and their functions are given in table 2.1 (Skalle 2010; Hawker 2001).

Table 2.1: Drilling Mud Additives, Functions and Examples

Type	Purpose	Agents
Surface active agents	Reduce interfacial tension between contacting faces (water/oil, water/air, water/solid).	Emulsifiers, de-emulsifiers, wetting agents, flocculants or deflocculants, depending on the surfaces involved.
Temperature stability	Increase rheological and filtration stability in fluids exposed to high temperatures.	Acrylic or sulphenated polymers, lignite, lignosulphate, tannin
Thinners or dispersants	They modify the relationship between viscosity and solids volume reducing gel strength and increasing the pumpability of a fluid. More specifically, they act as deflocculants to reduce attraction of clay particles that cause high viscosity and gelation.	Tannins, lignite and lignosulphates, polyphosphates.
Viscosifiers	Increase viscosity providing better solid suspension and hole cleaning.	Bentonite, CMC, attapulgite clays and polymers.
Weighting agents	To provide necessary density to control formation pressures, provide hole stability and to prevent u-tubing when pulling the drillpipe.	Barite, lead compounds, iron oxides, calcium carbonate.

Alkalinity, pH control	To control acidity and alkalinity of fluid	Lime, caustic soda, soda ash, bicarbonate of soda
Bactericides	Used to reduce bacteria count	Para formaldehyde, caustic soda, lime and starch preservatives.
Calcium removers	To prevent and overcome contaminating effects of anhydrite, gypsum and calcium sulphates.	Caustic soda, soda ash, bicarbonate of soda and certain polyphosphates.
Corrosion inhibitors	Prevent corrosion, pH control, neutralize hazardous acid gases such as H ₂ S, prevent formation of scale in drilling fluid.	Hydrated lime, amine or phosphate based products.
Defoamers	Reduce foaming action especially in brackish or saturated saltwater muds.	
Emulsifiers	To create a heterogeneous mixture of two insoluble liquids.	Oil based muds – fatty acids, amine-based chemicals. Water based muds – detergents, soaps, organic acids.
Filtrate loss	Reduce water loss from the drilling mud into the formation.	Bentonite clay, CMC, lignite, polyacrylate, pregelatinized starch.
Flocculants	Increase viscosity, improve hole cleaning, de-water or clarify low-solids fluids. Particles in suspension will aggregate into flocs causing solids to settle out.	Salt, hydrated lime, gypsum, soda ash, bicarbonate of soda, polymers.
Foaming agents	Permit air or gas drilling through water-bearing formations.	Surfactants (foamers).
Lost circulation materials	To plug the zone of loss in the formation.	
Lubricants	Increase horsepower transmitted to the bit by reducing the coefficient of friction, also reduces torque and drag.	Oils, graphite, synthetic liquids, glycol or surfactants.
Pipe-freezing agents	Increase lubricity and reduce friction where a pipe sticks and inhibit formation swelling.	Detergents, soaps, oils and surfactants
Shale inhibitors	Reduce shale hydration when drilling water sensitive shales, thereby preventing excessive wellbore enlargement and caving of shale.	Gypsum, sodium silicate and calcium lignosulfonates, lime and salt.

2.1.5 Drilling Fluid Rheology and Models

The term rheology is an expression used for the study of deformation and suspension properties of a flow in pipes or other conduits. In order to move the drilling fluid through the longer, slender pipes and annuli in the drilling process, the large viscous forces must be overcome. A means to describe the flow behaviour can be done by the rheological model, which gives a description of the relationship between the shear rate and the shear stress. The Newtonian and non-Newtonian fluids are illustrated in Figure 2.2 below. Pseudo-plastic (Power Law) is a shear thinning fluid, while dilatant is a shear thickening fluid:

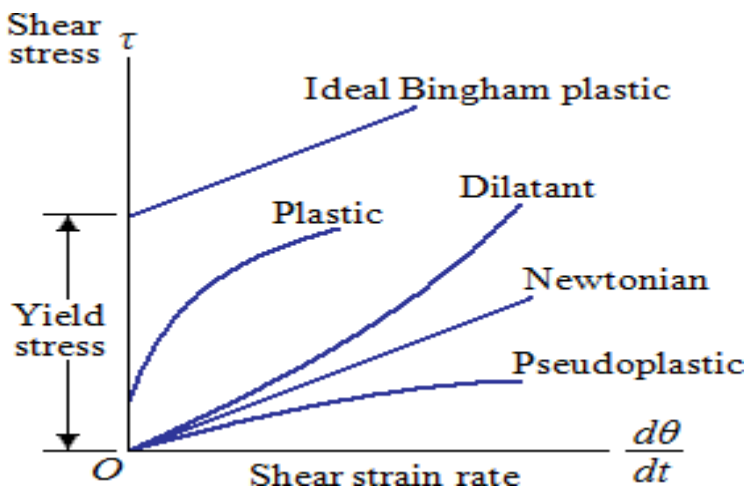


Figure 2.2: Flow curve for different fluid types (Viera and Peres, 2012).

2.1.5.1 Newtonian Model

Newtonian fluids are fluids that do not contain particles greater than molecules, such as clean water, glycerin and oils. These fluids will exhibit a constant viscosity at any shear rate when the fluid is exposed to a constant pressure and temperature. Therefore, by plotting shear stress versus shear rate for a Newtonian fluid, a straight line through the origin will be obtained. The model for Newtonian fluid can be described by the following equation (Skjeggstad, 1989):

$$\tau = \mu \cdot \gamma \tag{2.1}$$

Where:

τ = Shear stress

γ = Shear rate

μ = Newtonian viscosity

2.1.5.2 Non-Newtonian Models

Non-Newtonian fluids contains particles with a size greater than molecules, an example is drilling fluids. The models used for Non-Newtonian fluids will be described in the following section.

2.1.5.2.1 Bingham Plastic Model

The Bingham plastic model is similar to the Newtonian model in a sense that the relationship between the shear stress and shear rate is linear. However, in order to initiate flow of the fluid, a finite stress is required. The finite stress is the yield stress.

The model can be described by equation 2.2 (Skjeggstad, 1989; Caenn, Darley and Gray, 2011):

$$r = r_y + \mu_p * \gamma \quad 2.2$$

Where

τ_y = Yield stress (lbs/100 ft²)

μ_p = Plastic viscosity (cP)

These two parameters above can be calculated by equation 2.3 and 2.4 (Skjeggstad, 1989):

$$\mu_p = R_{600} - R_{300} \quad 2.3$$

$$r_y = F_{300} - \mu_p \quad 2.4$$

2.1.5.2.2 Power Law Model

The Power law model can be used in order to describe pseudoplastic fluids, which are fluids that have a reduction in viscosity as the shear rate increases. This model is better at describing fluids than the

Bingham plastic model, especially at lower shear rates. The equation used to describe the model is (Skjeggstad, 1989; Mitchell and Miska, 2011):

$$r = k\gamma^n \quad 2.5$$

Where

k = Consistency index

n = Flow behavior index

The value of n will determine what flow model the power law describes (Caenn, Darley and Gray 2011):

$n < 1$, pseudoplastic fluid, effective viscosity decreases with shear rate.

$n = 1$, Newtonian fluid, constant fluid viscosity

$n > 1$, dilatant fluid, effective viscosity increases with shear rate

In order to find the n and k values, equation 2.5 is rewritten by taking the logarithm of each term, resulting in the following equation.

$$\log r = \log k + n \log \gamma \quad 2.6$$

The equation is now linearized, and the n and k value can be found graphically, as the slope of the curve and intercept on the y-axis respectively.

The two values can also be estimated from Fann35 data, by using the following equations (Skjeggestad, 1989):

$$n = 3.32 \log (R_{600}/R_{300}) \quad 2.7$$

$$k = R_{300}/511^n = R_{600}/1022^n \quad 2.8$$

2.1.5.2.3 Herschel-Bulkley Model

The Herschel-Bulkley model applies the characteristics of both the Bingham and Power-law model, and uses three parameters in order to characterize a fluid. The model is defined by equation 2.9 (Mitchell and Miska, 2011):

$$r = r_y + k\gamma^n \quad 2.9$$

It can also be rewritten by taking the logarithm of each term:

$$\log (r - r_y) = \log k + n \log \gamma \quad 2.10$$

In order to obtain a value for τ_y , Versan and Tolga (2005) proposed the following approach, where

$\tau_y = \tau_0$:

$$r_o = \frac{c^{*2} - c_{min} * c_{max}}{2 * c^* - c_{min} - c_{max}} \quad 2.11$$

Where

τ^* = Shear stress value that corresponds to the geometric mean of the shear rate, γ^* .

$$\gamma^* = \sqrt{\gamma_{min} * \gamma_{max}} \quad 2.12$$

The τ^* is then found by interpolating the γ^* value with the shear stress values.

2.1.5.2.4 Unified Model

The unified model is a new rheological model designed for the drilling industry, which is based upon the Herschel-Bulkley model (Zamora and Power, 2002). The equation is expressed below, with its linearized counterpart:

$$r = r_y + k\gamma^n \quad 2.13$$

$$\log r - r_y = \log k + n \log \gamma \quad 2.14$$

What differentiates the unified model from the Herschel-Bulkley model is how to estimate the yield stress, τ_y . Zamora and Power proposed the following method for solving yield stress, by taking τ_y as the low-shear yield point (τ_{yL}):

$$\tau_{yL} = (2R_3 - R_6)1.066 \quad 2.15$$

Where

τ_{yL} = Low-shear yield point

1.066 = Conversion factor from laboratory units to field units

2.1.5.2.5 Robertson-Stiff Model

The Robertson-Stiff model was proposed by Robertson and Stiff (1976) in an attempt to give a better description of the yield-pseudoplastic fluids. The model is defined as:

$$r = (\gamma + C)^B \quad 2.16$$

Where

A, B and C = Model parameters

From equation 2.16, the parameters A and B act similar to the K and n parameters for the Power Law model. The C parameter is a correction of shear rate, where $(\gamma + C)$ is considered as the effective shear rate.

By transforming equation 2.16 into the logarithmic form, it will be possible to achieve a straight line in a log-log plot.

$$\log r = \log A + B \log(\gamma + C) \quad 2.17$$

From equation 2.17 above, A will be the intercept and B will be the slope. The last model parameter, C, can be found from the following equation:

$$C = \frac{\gamma_{min} * \gamma_{max} - \gamma^{*2}}{2\gamma^{*} - \gamma_{min} - \gamma_{max}} \quad 2.18$$

Where

γ^{*} = Shear rate value that corresponds to the geometric mean of the shear stress, τ^{*} .

In order to find γ^{*} , the geometric mean of the shear stress must first be calculated, and then this value has to be interpolated with the values of shear rates. The equation used to find τ^{*} is shown below (Robertson and Stiff, 1976):

$$r^{*} = \sqrt{r_{min} * r_{max}} \quad 2.19$$

2.2 Fluid Selection Factors

Drilling fluid selection can require consideration of numerous factors. The most important are safety, evaporate zones, high temperatures and pressures, environment, loss zones, shale problems, well trajectory and economics. Taking these one at a time and in order, will in most cases lead to a proper choice of drilling fluid.

2.2.1 Safety Issues (Well Control, Gas Hydrates and H₂S)

Safety is paramount. The fluid must be able to carry the mud weight required to control the well, and circulating, surge, and swab pressures must not be excessive. Speed and ease with which a mud will accept weighting materials can be important in kick situations. Although most mud types are satisfactory in these respects, at mud weights above about 15 lbm/gal, polymer muds will need some dispersant and oil muds will need oil/water ratios higher than 50/50.

Gas hydrates can interfere mechanically with well-control operations in deep-water drilling. Salt muds are currently the fluids of choice in deep water because high salinity tends to suppress hydrate formation Barker and Gomez (1989). The effect of mud composition in preventing hydrates is the subject of ongoing research in several laboratories. The safest fluids for drilling H₂S bearing zones contain at least 10 lbm/bbl excess lime plus a sulfide scavenger. Lime and oil muds are the only two mud types that are truly compatible with this requirement (Barker and Gomez, 1989).

2.2.2 Evaporite Zones

Massive evaporite zones tend to leach out excessively into water-based drilling fluids unless the fluids are pre saturated with the evaporite before the zone is drilled. Gypsum muds are a natural choice for massive anhydrite sections. Thick salt sections require a saturated salt mud or an oil mud. A properly formulated oil mud is a good choice for any evaporite zone.

2.2.3 High Temperatures and Pressures.

High temperature gelation and fluid-loss-control problems occur for most water-based mud types at downhole temperatures of 250 to 350°F. Specially formulated water-based muds are stable to 400 to 450°F at mud weights up to 18 lbm/gal. Oil muds are a viable, and sometimes less costly, alternative at these elevated temperatures and pressures.

2.2.4 Environmental Considerations

Permit restrictions can limit the choice of mud type. Environmental considerations are many and varied, depending on the well location. They have led to avoidance of oil muds in some areas, salt muds in others, and high-pH or chromium-treated muds in still others. Drilling- fluid bioassay tests are useful for assessing the toxicity of special additives (Leuterman et al., 1989). Although acceptable substitutes have been developed for some additives, the search for adequate replacements for environmentally objectionable systems continues to be the highest research priority in drilling fluids (Lorenz, 1989).

2.2.5 Severe Loss Zones

Lost-circulation materials are added to muds to seal off thief zones when mud losses occur downhole. Some zones may be known in advance as being prone to losses and difficult to seal. If it is anticipated that large volumes of mud may be lost in an interval, the mud type should be simple and inexpensive if possible. This tends to rule out oil muds and heavily treated water-based muds. In subnormal-pressured intervals, aerated fluids may merit consideration (Westennark, 1986).

2.2.6 Shale Problems

Kelly (1968) in his work mentioned that shale formations can swell, disperse, or slough into the hole. Indeed, shale problems are probably the most common and vexing mud-related drilling problem encountered around the world. Some shale problems are basically mechanical in nature, and increased mud weight is then essential to the solution. More often than not, the mud type is at least equally important in avoiding a serious shale problem. Experience and theory suggest that dissolved salts (such as KCl) reduce shale swelling, long-chain water-soluble polymers reduce dispersion, and asphaltic materials reduce sloughing (Kelly, 1968). The applicability of this wisdom can depend on the particular shale drilled, with sometimes subtle difference between shale being the controlling factor. Laboratory tests on the swelling and dispersive characteristics of the problem shale in various fluids often are helpful in choosing a fluid where offset experience is

inadequate. Although no water-based mud has been universally successful, many shale problems have been solved through the use of potassium, polymer, lime, gypsum, and salt muds, muds treated with asphaltic additives, and combinations of these. In most cases, oil muds eliminate shale problems, provided that mud weight is adequate and the salinity of the aqueous internal phase is high enough. To prevent osmotic transfer of water into the formation, the aqueous phase salinity should equal or exceed that of the water in the pore spaces of the shale drilled.

2.2.7 Well Trajectory

Recent studies on hole cleaning in high-angle holes underscored the role played by low-shear-rate viscosities (Seeberger, Matlock and Hanson, 1989). Certain additives can elevate low-shear-rate viscosities with minimal increases in plastic viscosity and yield point. Some polymer muds have naturally elevated low-shear-rate viscosities but may require a lubricant for long-reach wells. Oil muds have good lubricity characteristics and can be treated to raise low-shear-rate viscosities.

2.2.8 Economics

The factors previously discussed dominate economic considerations: ignoring them invites lost drilling time. Loss of hole, or worse. With these factors duly considered, the remaining viable drilling fluid candidates can be subjected to a direct economic comparison. This should include the cost of the base fluid, makeup and maintenance costs, mud-related disposal costs, and for oil muds, buy-back provisions. Disposal costs have become increasingly important in such calculations. Certain other cost-requirement differences between systems, such as better solids control or mud mixing equipment, can be offset by increases in expected penetration rates or reduced mud-material consumption. Many wells do not require expensive, complicated muds. Examples of low-cost muds for problem-free areas include unweighted-gel freshwater muds, lignite muds, lightly treated lignosulfonate muds, and native-brine starch muds.

Other Factors. In some areas, experience has repeatedly shown that one drilling mud type offers significant penetration-rate advantages over another. Additional factors influencing selection

include differential-sticking tendencies, formation-damage concerns, or special logging requirements.

2.3 Well Bore Stress

The subsurface formations are subjected to a stress field that is largely influenced by the overburden formation, topography, tectonic activities, rock material behavior, and geological history. Accurate knowledge of in-situ stress state in creating geomechanical model is important to prepare for the effects of subsurface conditions prior to the drilling. Important parameters in understanding in-situ stress state in the subsurface formations and around the wellbore will be reviewed

2.3.1 Stress

Stress is defined as force acting per unit area which pushes or pulls a body of a material. The magnitude of the force and the properties of the material determine the response of the material toward the applied stress. In general, the equation for stress is:

$$\sigma = \frac{\text{Force}}{\text{Area}} = \frac{F}{A} \quad 2.20$$

In earth sciences, stress commonly measured in psi or megapascals (MPa). The area of the cross section and the direction of the force is important in defining the state of stress. The force that is acting on the area can be divided into two components: F_n which is acting in the normal direction to the cross section, and F_s which is acting parallel to the section.

The normal stress is quantified as:

$$\sigma_n = \frac{F_n}{A} \quad 2.21$$

While the parallel stress is also known as shear stress and is quantified as

$$\tau = \frac{F_s}{A} \quad 2.22$$

Material failure can be caused by the normal stress (tensile or compressive failure), or the shear stress (shear failure) by shearing the material along a plane, as shown in Figure 3.1.

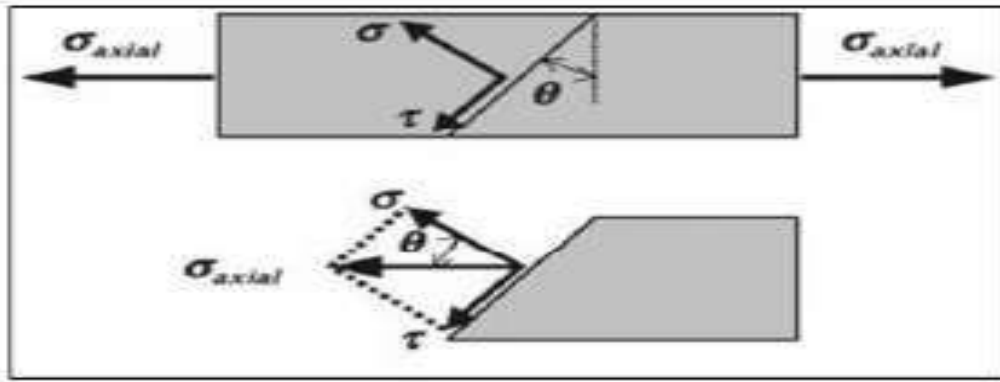


Figure 2.3: Stress components showing the normal and shear stress (Aadnoy and Loyeh 2011).

3.2.1.1 Stress around a Vertical Wellbore

During the drilling process, the excavation and removal of material from the borehole cause the formation surrounding the wellbore wall to be subjected to stress concentrations whose magnitude varies based on the position around the well. The stress alteration around the wellbore can cause compressive failure in the form of wellbore breakouts or tensile failure of the wellbore wall. Therefore, the induce stresses should be adjusted through mud pressure. In severe condition these breakouts can lead into major wellbore instability problems, such as stuck pipe and hole enlargement. The formation response toward drilling is dependent on its rock strength and the in-situ stress field.

As reported in Aadnoy and Loyeh (2011), a theoretical approach was introduced by Kirsch in 1898. The approach is widely used to mathematically determine the stresses around a wellbore of a previously stressed virgin rock. Kirsch's equations are based on liner elasticity and assume the rock properties are homogeneous and isotropic. He calculates the effective stresses at a point in cylindrical coordinate (r, θ) around the wellbore, which can be described as:

$$\sigma_{rr} = \frac{\sigma^0 + \sigma^0}{2} \left(1 - \frac{a^2}{r^2}\right) + \left(\frac{x}{2} - \frac{y}{2}\right) \left(1 + 3\frac{a^2}{r^2} - 4\frac{a^2}{r^2}\right) \cos 2\theta + \sigma_{xy}^0 \left(1 + 3\frac{a^4}{r^4} - 4\frac{a^2}{r^2}\right) \sin 2\theta - P \frac{a^2}{w_r^4} \quad 2.23$$

$$\sigma_{\theta\theta} = \left(\frac{\sigma_x^0 - \sigma_y^0}{2} \right) \left(1 + \frac{a^2}{r^2} \right) - \left(\frac{\sigma_x^0 - \sigma_y^0}{2} \right) \left(1 + 3 \frac{a^4}{r^4} \right) \cos 2\theta - \sigma_{xy}^0 \left(1 + 3 \frac{a^4}{r^4} \right) \sin 2\theta - P_w \frac{a^2}{r^2} \quad 2.24$$

$$\sigma_{zz} = \sigma_z^0 - \nu \left[2(\sigma_x^0 - \sigma_y^0) \frac{a^2}{r^2} \cos 2\theta + 4\sigma_{xy}^0 \frac{a^2}{r^2} \sin 2\theta \right] \quad 2.25$$

$$r_{r\theta} = \left[- \left(\frac{\sigma_x^0 - \sigma_y^0}{2} \right) \left(1 - 3 \frac{a^4}{r^4} + 2 \frac{a^2}{r^2} \right) \sin 2\theta \right] + r_{xy}^0 \left(1 - 3 \frac{a^4}{r^4} \right) \cos 2\theta \quad 2.26$$

$$r_{rz} = (r_{xz} \cos \theta + r_{yz} \sin \theta) \left(1 - \frac{a^2}{r^2} \right) \quad 2.27$$

$$r_{\theta z} = (r_{xz} \sin \theta + r_{yz} \cos \theta) \left(1 - \frac{a^2}{r^2} \right) \quad 2.28$$

Where “a” is the radius of the wellbore, r is distance from the borehole, P_w is the internal wellbore pressure, and ν is poisson’s ratio, angle θ is measured clockwise from x-axis, σ_{rr} is the radial stress, $\sigma_{\theta\theta}$ is tangential stress, σ_{zz} is axial stress, $r_{\theta z}$, and r_{rz} are three components of the shear stress.

At the wellbore of anisotropic rock, where $a=r$, Kirsch equations can be written as:

$$\sigma_{rr} = P_w \quad 2.29$$

$$\sigma_{zz} = (\sigma_x^0 + \sigma_y^0) - 2(\sigma_x^0 + \sigma_y^0) \left(1 + 3 \frac{a^4}{r^4} \right) \cos 2\theta - 4\sigma_{xy}^0 \sin 2\theta - 4\sigma_{xy}^0 \sin 2\theta - P_w \quad 2.30$$

$$\sigma_{zz} = \sigma_x^0 - 2\nu(\sigma_x^0 - \sigma_y^0) \cos 2\theta - 4\nu r_{xy}^0 \sin 2\theta \quad 2.31$$

$$r_{r\theta} = 0 \quad 2.32$$

$$r_{rz} = 0 \quad 2.33$$

$$r_{\theta z} = 2(r_{xz}^0 \sin \theta + r_{yz}^0 \cos \theta) \quad 2.34$$

2.3.1.2 Stress Distribution Around Inclined Wellbore

For inclined wells, stress components should be transformed and adjusted to the well inclination from vertical (γ), geographical azimuth of the wellbore (φ), and the wellbore position from the x-axis (θ). Aadony and Looyeh (2011) explained the coordinate transformation of the in-situ stresses in inclined wellbore into a new Cartesian coordinate system, as shown in figure 3.4. This transformation is important before deriving the stresses around the wellbore using Kirsch concept. The stress transformation is written as follows:

$$\sigma_x = (\sigma_{Hmax} \cos 2\varphi + hmin \sin 2\varphi) \cos 2\gamma + \sigma_v \sin 2\gamma$$

$$\sigma_x \sigma_{Hmax} \sin 2\varphi + \sigma_{hmin} \cos 2\varphi \tag{2.35}$$

$$\sigma_{zz} = (\sigma_{Hmax} \cos 2\varphi + hmin \sin 2\varphi) \sin 2\gamma + \sigma_v \cos 2\gamma \tag{2.36}$$

$$r_{xy} = 0.5(\sigma_{Hmax} - \sigma_{Hmax}) \sin 2\varphi \cdot \cos \gamma \tag{2.37}$$

$$r_{xz} = 0.5(\sigma_{Hmax} \cos 2\varphi + hmin \sin 2\varphi - \sigma_v) \sin 2\gamma \tag{2.38}$$

$$r_{yz} = 0.5(\sigma_{Hmax} - \sigma_{Hmax}) \sin 2\varphi \cdot \sin \gamma \tag{2.39}$$

Where, σ_x , σ_y , σ_{zz} , t_{xy} , t_{xz} and t_{yz} are the transformation stress components. σ_{Hmax} , σ_{hmin} , σ_v , are the principle stresses, φ is the wellbore azimuth from the direction of σ_{Hmax} , and γ is the wellbore inclination from the vertical.

Equations 3.35-3.239 can also be shown in matrix format:

$$\begin{bmatrix} \sigma_x \\ \sigma_y \\ \sigma_{zz} \end{bmatrix} = \begin{bmatrix} \cos^2\varphi \cos^2\gamma & \sin^2\varphi \cos^2\gamma & \sin^2\gamma \\ \sin^2\varphi & \cos^2\varphi & 0 \\ \cos^2\varphi \sin 2\gamma & \sin^2\varphi \sin 2\gamma & \cos^2\gamma \end{bmatrix} \begin{bmatrix} S_{Hmax} \\ S_{hmin} \\ S_v \end{bmatrix} \tag{2.40}$$

$$\begin{bmatrix} t_{xy} \\ t_{xz} \\ t_{yz} \end{bmatrix} = \begin{bmatrix} \sin^2\varphi \cos^2\gamma & \sin^2\varphi \cos^2\gamma & 0 \\ -\cos^2\varphi \sin 2\gamma & \sin^2\varphi \sin 2\gamma & -\sin 2\gamma \\ -\sin 2\varphi \sin \gamma & \sin^2\varphi \sin 2\gamma & 0 \end{bmatrix} \begin{bmatrix} S_{Hmax} \\ S_{hmin} \\ S_v \end{bmatrix} \tag{2.41}$$

After the transformation, these components are converted into stresses components in Kirsch's cylindrical coordinate system, as follows:

$$\begin{aligned} \sigma_r = & \frac{1}{2}(\sigma_x + \sigma_y) \left(1 - \left(\frac{a}{r}\right)^2\right) - \frac{1}{2}(\sigma_x - \sigma_y) \left(1 + 3\left(\frac{a}{r}\right)^4 - 4\left(\frac{a}{r}\right)^4 \cos 2\theta + r_{xy} \left(1 + 3\left(\frac{a}{r}\right)^4\right.\right. \\ & \left.\left. - 4\left(\frac{a}{r}\right)^2 \sin 2\theta + \Delta p_w \left(\frac{a}{r}\right)^2\right), \right. \end{aligned} \quad 2.42$$

$$\begin{aligned} \sigma_\theta = & \frac{1}{2}(\sigma_x + \sigma_y) \left(1 + \left(\frac{a}{r}\right)^2\right) - \frac{1}{2}(\sigma_x - \sigma_y) \left(1 + 3\left(\frac{a}{r}\right)^4 \cos 2\theta + r_{xy} \left(1 + 3\left(\frac{a}{r}\right)^4\right.\right. \\ & \left.\left. + \Delta p_w \left(\frac{a}{r}\right)^2\right), \right. \end{aligned} \quad 2.43$$

$$\sigma_z = \sigma_{zz} - 2\nu(\sigma_x + \sigma_y) \left(\frac{a}{r}\right)^2 \cos 2\theta + 4\nu r_{xy} \left(\frac{a}{r}\right)^2 \sin 2\theta \quad 2.44$$

$$r_{\theta z} = (r_{xy} \cos \theta - r_{yz} \sin \theta) \left(1 + \left(\frac{a}{r}\right)^2\right) \quad 2.45$$

$$r_{rz} = (r_{xy} \cos \theta - r_{yz} \sin \theta) \left(1 + \left(\frac{a}{r}\right)^2\right) \quad 2.46$$

$$r_{r\theta} = \left(\frac{1}{2}(\sigma_x + \sigma_y) \sin 2\theta + r_{xy} \cos 2\theta\right) \left(1 - 3\left(\frac{a}{r}\right)^4 + 2\left(\frac{a}{r}\right)^2\right), \quad 2.47$$

Where a is the radius wellbore, r is the outer radius, θ is the wellbore position from the x-axis, Δp_w is the internal wellbore pressure which is the different between the wellbore pressure and pore pressure:

$$\Delta p_w = P_w - P_p \quad 2.48$$

For the stresses component at the wellbore wall, where $a=r$, the equation become:

$$\sigma_r = \Delta p_w \quad 2.49$$

$$\sigma_\theta = (\sigma_x + \sigma_y - \Delta p_w) - 2(\sigma_x - \sigma_y) \cos 2\theta - 4\nu r_{xy} \sin 2\theta \quad 2.50$$

$$\sigma_z = \sigma_{zz} - 2\nu(\sigma_x - \sigma_y) \cos 2\theta - 4\nu r_{xy} \sin 2\theta \quad 2.51$$

$$r_{r\theta} = r_{rz} = 0 \quad 2.52$$

$$r_{\theta z} = 2(r_{xy} \cos \theta - r_{yz} \sin \theta) \quad 2.53$$

The arbitrarily effective principle stresses at the wellbore wall can be calculated using the following equations:

$$\sigma_{tmax} = \frac{1}{2}(\sigma_{\theta} + \sigma_z) + \frac{1}{2}\sqrt{(\sigma_{\theta} - \sigma_z)^2 + 4r_{\theta z}^2} \quad 2.54$$

$$\sigma_{tmin} = \frac{1}{2}(\sigma_{\theta} + \sigma_z) - \frac{1}{2}\sqrt{(\sigma_{\theta} - \sigma_z)^2 + 4r_{\theta z}^2} \quad 2.55$$

$$\sigma_{rr} = \sigma_r = \Delta p_w \quad 2.56$$

Where σ_{tmax} and σ_{tmin} respectively are the largest and the smallest principle stresses around the wellbore.

3.2.2 Effect of Chemical interaction, and flow-induced stresses

3.2.2.1 Chemical interaction

The difference between the chemical composition of the drilling mud and the formation fluids may cause chemical interaction between them. Chemical interaction in shale formation can be critical because of the reactive swelling clay minerals. Therefore, careful mud selection should be conducted to minimize the interaction. The low permeability of shale makes creating mud cake at the wellbore wall difficult, causing water and pressure (Mese and Tutuneu 2011). This increase in pore pressure can lead to stress alteration at the wellbore and cause yielding of shale. When the mud pressure applied within the wellbore cannot support the formation fluid pressure, shale yielding can take place in the form of sloughing into the wellbore. Depending on the compatibility of the chemical composition of the formation of the formation fluid pressure, shale formation creates an additional pressure called “swelling pressure” that needs to also be included in the mud pressure calculations and drilling fluid

design. Hence, the effects of chemical interaction on the stress state around the wellbore should be considered in the calculation.

To calculate the effect of chemical interaction, numeral equations for osmotic pressure cab be derived from several equations by (Chen, Chenevert, Sharma, et al. 2001) and equations provided in the well integrity class (Tutuncu, 2015), as follows:

$$\sigma_{r'} = 0 \quad 2.57$$

$$\sigma_{\theta'} = a \frac{1-2\nu}{1-\nu} \Delta\Pi \quad 2.58$$

$$\sigma_{z'} = a \frac{1-2\nu}{1-\nu} \Delta\Pi \quad 2.59$$

Where σ_r , $\sigma_{y\theta}$, and σ_{zz} are the alteration of radial, hoop and axial stresses due to the introduction of the osmotic pressure, a is the Biot's coefficient, ν is Poisson's ratio, and $\Delta\Pi$ is the osmotic pressure.

The effects of excess pore pressure of the osmotic potential can be expressed as (Tutuneu), 2014):

$$\Delta\Pi = I_m * \frac{(RT\phi)}{V_w} \ln \left(\frac{a_{w,df}}{a_{w,sh}} \right) \quad 2.60$$

Where I_m is a reactivity coefficient which characterize member efficiency, a dimensionless parameter and ranges from 0 to 1, R is the universal gas constant and equals 8.314 J/K. mole, T_o is the absolute temperature, K. V_w is the molar volume of the water (18.104 m³), $a_{w,df}$ and $a_{w,sh}$ are chemical activities of the drilling fluid and shale pore water equals to 1, and for salt water is less than 1.

3.2.2.2 Temperature Alteration

Circulation of cold drilling fluid into the wellbore can cause stress alteration due to rock temperature change. Aadnoy and Looyeh (2011) calculate the thermal stress induced as follows:

$$\sigma_T = \frac{a_m * E(T - T_o)}{1-\nu} \quad 2.61$$

Where ν is the Poisson's ratio, E is Young modulus, α_m is a volumetric thermal expansion coefficient of rock matrix ($^{\circ}\text{K}^{-1}$), T is the circulation temperature and ($^{\circ}\text{K}$), and T_o is virgin rock temperature ($^{\circ}\text{K}$).

3.2.2.3 Flow Induced Stress

Kadyrov (2012) describes the effects of flow-induced stresses in the equations that define the stress alteration at the wellbore when a radial flow is introduced or underbalanced drilling.

$$\sigma_r'' = 0 \quad 2.62$$

$$\sigma_{\theta}'' = 1(1 - \alpha) \frac{1-2\nu}{1-\nu} (P_w - P_o) \quad 2.63$$

$$\sigma_z'' = 1(1 - \alpha) \frac{1-2\nu}{1-\nu} (P_w - P_o) \quad 2.64$$

Where $P_w - P_o = \Delta P_w$

By adding the effects of chemical interaction, temperature interaction, and flow induced stress, the numerical model can be expressed as:

$$\sigma_r = \Delta P_w \quad 2.65$$

$$\sigma_{\theta} = (\sigma_x + \sigma_y - \Delta p_w) - 2(\sigma_x - \sigma_y) \cos 2\theta$$

$$-4\nu t_{xy} \sin 2\theta + \alpha \frac{1-2\nu}{1-\nu} \Delta \Pi + \frac{\alpha m * E * (T - T_o)}{1-\nu} - (1 - \alpha) \frac{1-2\nu}{1-\nu} (P_w - P_o) \quad 2.66$$

$$\sigma_z = \sigma_{zz} - 2\nu(\sigma_x - \sigma_y) \cos 2\theta - 4\nu t_{xy} \sin 2\theta \alpha \frac{1-2\nu}{1-\nu} \Delta \Pi + \frac{\alpha m * E * (T - T_o)}{1-\nu}$$

$$-(1 - \alpha) \frac{1-2\nu}{1-\nu} (P_w - P_o) \quad 2.67$$

$$r_{r\theta} = r_{rz} = 0 \quad 2.68$$

$$r_{\theta z} = 2(r_{yz} \cos \theta - r_{xz} \sin \theta) \quad 2.69$$

2.4 Rock Failure Modes

Understanding the types and reasons of formation failures is important as prevention and also for mitigation. Wellbore log data such as caliper and image logs are helpful to provide information identifying wellbore failures during drilling. Analyzing wellbore image data also help in proving reliable information about the failure mode, whether it is tensile, compressional, or shear failure.

2.4.1 Tensile Failure

Tensile failure in a wellbore occurs when the tensile strength acting across the plain exceed the maximum limit of the rock tensile strength. One of the examples of tensile failure is drilling induced hydraulic fractures. These fractures are occurs due to the concentration of in-situ regional stresses, pore pressure, drilling mud pressure, and thermal stresses due to cooling of borehole during drilling. Tensile strength has the same unit as stress, usually rocks have very low tensile strength is assumed to be zero.

2.4.2 Shear Failure

Shear failure is also known as compressive failure; it takes place when the compressive loading makes the shear stress along the plane high enough to cause the rock undergo shear failure. Borehole collapse during drilling is an example of shear failure. The shape of the collapse is determined by the stresses around the wellbore. If the mud pressure in the well is the same as the formation pore pressure, the wellbore will still be in the circular shape. In the case when the stresses are different, the shape of the wellbore will be elongated due to collapse. In a vertical well wellbore, breakout will occur in the direction of the minimum in-situ stress direction.

2.4.3 Creep Failure

Creep failure takes place when the rock formation undergoes deformation under constant stress over time. There are three stages of creep failure based on the mechanism for creep applies to a specific

case. The first stage is transient creep, when the stresses cause micro-fractures in the rock, but if the stresses are reduced to zero, the deformation will eventually disappear.

2.5 Rock Failure Criteria

Determining the appropriate drilling fluid density by rock failure analysis is an essential step to control wellbore instability. To determine wellbore failure stresses, rock strength must be known, an appropriate constitutive model should be selected, and an accurate rock failure criterion must be chosen. There are numerous rock failure criteria that have been used in wellbore stability analysis to determine the minimum drilling fluid density, but there is no agreement on which failure criterion should be used. Based on the different characteristics of the rock failure criteria, the results for the minimum drilling fluid density might be significantly different. Previous studies on the evaluation of rock failure criteria were mainly focused on quantitative comparison or determination of the best fitting parameters for the different rock failure criteria based on triaxial test results data. One of the first studies for the evaluation of rock failure criteria was conducted by (Mclean and Addis., 1990). They compared Mohr-Coulomb and different forms of Drucker-Prager to predict the minimum mud weight. Results showed a criterion can predict a realistic result in one situation but give unrealistic results for other conditions. The Mohr-Coulomb failure criterion was recommended for wellbore stability analysis because of the more realistic results compared with the different forms of Drucker-Prager (Mclean and Addis, 1990).

Ewy (1999) developed the Modified-Lade Failure Criterion and presented the advantages of this new criterion over Mohr-Coulomb and Drucker-Prager. Colmenares and Zoback (2002) evaluated seven different rock failure criteria based on polyaxial test data, and they concluded that the Modified Lade and the Modified Wiebols-Cook fit best with polyaxial test data. Al Ajmi and Zimmerman (2005) developed the linear form of Mogi-Coulomb and compared that with the Mohr-Coulomb failure criterion. They proposed the use of Mogi-Coulomb over Mohr-Coulomb with regard to fitting polyaxial test data as well as prediction of the borehole breakout pressure. Yi, Ong and Russell (2005)

compared three common rock failure criteria based on minimum mud weight estimation. They concluded that a failure criterion which best fits the polyaxial test data can better describe rock failure, and therefore provide more reliable results for the minimum required mud weight. Based on their results, no specific failure criterion can consistently estimate higher or lower minimum mud weight compared with the other failure criteria. Benz and Schwab (2008) optimized the material parameters for six rock failure criteria to obtain the best fit with polyaxial test data. Zhang and Radha (2010) compared minimum mud weight prediction of five common rock failure criteria. They recommended Mogi-Coulomb and Hoek-Brown to be used for wellbore stability analysis. Nawrocki (2010) predicted borehole breakout pressure based on evaluation of four rock failure criteria. He recommended Modified Lade as a reliable failure criterion for wellbore stability analysis. A review of previous studies reveals that some failure criteria, including Stassi d'Alia, have not been considered. Also, in some previous studies, hypothetical data sets were used for the stress data, rock mechanical properties, and well depth which caused results to be unrealistic in some cases. For example, true vertical well depths of 12,000 m or 28,000 m, were chosen for analysis and therefore, the results were not directly applicable to the stability of wells for petroleum exploitation (Zhang et al., 2010). Furthermore, quantitative comparisons have been previously studied on some failure criteria, but few evaluations of the failure criteria were based on typical petroleum related situations. Thirteen of the most common rock failure criteria used for wellbore stability analysis have been statistically evaluated for three rock lithologies including shale, sandstone, and siltstone. Rock mechanical and stress data from the Rulsion field in western Colorado were used (Higgins, 2006). Results of the statistical analysis are presented using the percentage difference method and table of contradiction.

Rock failure criterion specifies stress conditions at failure. Common rock failure criteria can be classified based on two main characteristics. Some rock failure criteria have linear form, such as Tresca, while other failure criteria have nonlinear form, such as Drucker-Prager. The second characteristic involves considering the effect of intermediate principal stress on the rock strength.

Mohr-Coulomb and Hoek-Brown are examples of rock failure criteria that do not consider the effects of intermediate principal stress. In contrast, rock failure criteria such as Modified Lade and Mogi-Coulomb consider the effect of intermediate principal stress on rock failure.

2.5.1 Mohr-Coulomb

Linear Mohr-Coulomb is the most commonly used failure criterion in geo-mechanics. The following is the governing equation for Mohr-Coulomb criterion based on the shear and normal stress components:

$$\tau = \mu\sigma + c \quad 2.70$$

$$\mu = \tan \varphi \quad 2.71$$

The parameter c is the cohesion of rock and μ is the coefficient of the internal angle of friction. In terms of principal stresses, Mohr Coulomb failure criterion can be expressed in the following form (Jaeger et al., 2007):

$$\sigma_1 = q\sigma_3 + c_0$$

Where c_0 is the uniaxial compressive strength (UCS) and q is the flow factor parameter which is a function of the internal angle of friction:

$$q = \frac{1 + \sin\varphi}{1 - \sin\varphi} \quad 2.72$$

$$c_0 = \frac{2c \cos\varphi}{1 - \sin\varphi} \quad 2.73$$

Mohr-Coulomb criterion does not consider the effect of intermediate principal stress in contrast to the triaxial stress state of rock.

2.5.2 Mogi-Coulomb

Based on the Mogi's theory on the effect of intermediate principal stress on the rock strength (Mogi, 1971), Al-Ajmi (2005) found a linear relation which can fit polyaxial test data in $\tau_{\text{oct}} - \sigma_{m,2}$ space:

$$\tau_{\text{oct}} = a + b\sigma_{m,2} \quad 2.74$$

$$\sigma_{m,2} = 1/3(\sigma_1 + \sigma_3) \quad 2.75$$

$$\tau_{oct} = 1/3\sqrt{(\sigma_1 - \sigma_2)^2 + (\sigma_1 - \sigma_3)^2 + (\sigma_2 - \sigma_3)^2} \quad 2.76$$

The τ_{oct} is octahedral shear stress and $\sigma_{m,2}$ is mean normal stress. Parameters a and b can be evaluated based on the Mohr-Coulomb parameter c_0 and q:

$$a = \frac{2\sqrt{2}c_0}{3q+1} \quad 2.77$$

$$b = \frac{2\sqrt{2}q-1}{3q+1} \quad 2.78$$

2.5.3 Tresca

The simplest failure criterion based on the Mohr's theory is Tresca which assumes failure would occur if maximum shear failure inside any plane of rock reaches a critical value, c (Fjaer Holt, Horsrud, Raaen, and Risnes, 2008).

$$\frac{(\sigma_1 - \sigma_3)}{2} = c = \tau_{max} \quad 2.79$$

$$\frac{c_0}{2} = c \quad 2.80$$

Tresca can be considered a special case of the Mohr-Coulomb failure criterion when the internal angle of friction is equal to zero.

$$\sigma_1 = q\sigma_1 + c_0 \quad 2.81$$

When $\phi = 0$,

$$q = \frac{1 + \sin\phi}{1 - \sin\phi} = 0, \quad 2.82$$

$$\sigma_1 - \sigma_3 = c_0 \quad 2.83$$

2.5.4 Von Mises

Von Mises proposed his failure criterion by assuming that rock fails when the invariant of the deviatoric stress (J_2) reaches a critical value (Jaeger, Cook and Zimmerman, 2007)

$$\sqrt{J_2} = \frac{c_0}{3} \quad 2.84$$

$$\sqrt{J_2} = \sqrt{\frac{(\sigma_1 - \sigma_3)^2 + (\sigma_2 - \sigma_3)^2 + (\sigma_1 - \sigma_2)^2}{6}} = \frac{c_0}{3} \quad 2.85$$

Von Mises hypothetically included the effect of intermediate principal stress by using rotational symmetry in the three dimensional stress space.

2.5.5 Drucker-Prager

As an extension of Von Mises theory, Drucker and Prager presented their failure criterion in the following form (Drucker, 1952 & Zoback, 2007):

$$\sqrt{J_2} = k + \alpha J_1 \quad 2.86$$

The parameters k and α are the material constants and is the mean effective confining stress:

$$J_1 = \frac{(\sigma_1 + \sigma_2 + \sigma_3)}{3} \quad 2.87$$

The material parameters α and k can be determined from the slope and the intercept of the failure envelope plotted in the (J_1) and $(\sqrt{J_2})$ space. The parameter α is related to the frictional angle of rock and k is related to the cohesion of rock. Therefore Mohr-Coulomb criterion parameters could be used to determine Drucker-Prager criterion parameters. Based on comparison with the Mohr-Coulomb criterion in a three dimensional stress space, the Drucker-Prager criterion can be divided into Circumscribed Drucker-Prager and Inscribed Drucker-Prager. The solution of α and k parameters for Inscribed Drucker-Prager presented by (Vekeens, Walters, Kenter and Davies, 1989).

$$\alpha = \frac{3 \sin \phi}{\sqrt{9 + 3 \sin^2 \phi}} \quad 2.88$$

$$k = \frac{3 c_0 \cos \phi}{2 \sqrt{q} \sqrt{9 + 3 \sin^2 \phi}} \quad 2.89$$

Zhou (1994) found the following solution for α and k parameters in the Circumscribed Drucker-Prager:

$$\alpha = \frac{\sqrt{3}(q-1)}{(2+q)} \quad 2.90$$

$$\alpha = \frac{\sqrt{3}c_0}{2+q} \quad 2.91$$

2.5.6 Hoek-Brown

Hoek and Brown (1980) presented their empirical rock failure criterion for fractured rocks based on the wide range of experimental data in following form:

$$\sigma_1 = \sigma_3 + \sqrt{mc_0\sigma_3 + sc_0^2} \quad 2.92$$

Where m and s are constant depending on both rock and fracture properties and parameter s for intact rock is equal to 1. It should be noted that Hoek-Brown failure criterion does not consider the effect of the intermediate principal stress.

2.5.7 Modified Lade

Lade (1977) developed his criterion in terms of the first and third stress invariants:

$$\left(\frac{I_1^3}{I_3} - 27\right) \left(\frac{I_1}{P_a}\right)^m = \eta_1 \quad 2.93$$

The parameter m and η_1 are material constants and P_a is atmospheric pressure. The stress invariant parameters, I_1 and I_3 are defined as:

$$I_1 = (\sigma_1 + \sigma_2 + \sigma_3) \quad 2.94$$

$$I_3 = (\sigma_1 \cdot \sigma_2 \cdot \sigma_3) \quad 2.95$$

The Modified Lade criterion was developed by Ewy (1999). He neglected material constant in order to obtain a criterion that predicts linear shear strength increases with increasing first stress tensor I_1 . Furthermore, Ewy (1999) considered the effect of pore pressure and included effective stress components in the criterion. Since the original Lade criterion was for cohesion-less soil, Ewy introduced parameter as the function of cohesion to extend application of the Lade criterion to cohesive rocks. The Modified Lade criterion was presented in following form:

$$\frac{I_1^3}{I_3} = \eta_1 + 27 \quad 2.96$$

Where the appropriate stress tensors and are in following form:

$$I''_1 = (\sigma_1 + S) + (\sigma_2 + S) + (\sigma_3 + S) \quad 2.97$$

$$I''_3 = (\sigma_1 + S) \cdot (\sigma_2 + S) \cdot (\sigma_3 + S) \quad 2.98$$

The parameters S and η can be determined by Mohr Coulomb criterion parameters, cohesion and internal angle of friction:

$$S = \frac{c}{\tan\phi} \quad 2.99$$

$$\eta = \frac{4\tan^2\phi(9-7\sin\phi)}{(1-\sin\phi)} \quad 2.100$$

2.5.8 Modified Wiebols-Cook

Wiebols and Cook developed a model that describes the impact of the σ_2 on the rock strength (Wiebols and Cook 1968). By considering shear strain energy of micro cracks in the rock, they provided a physical description of sliding micro crack surfaces that cause failure when the stress condition meets the frictional criterion. Zhou developed a nonlinear criterion as an extension of circumscribed Drucker-Prager that is named Modified Wiebols-Cook due to similarities to the original model by Wiebols and Cook (Zhou, 1994):

$$\sqrt{J_2} = A + BJ_1 + CJ_1^2 \quad 2.101$$

The Mohr-Coulomb criterion parameters, including uniaxial compressive strength (c_0) and flow factor (q), can be used as input data to determine A, B, and C parameters:

$$C = \frac{\sqrt{27}}{2c_1 + (q-1)\sigma_3 - c_0} \left(\frac{c_1 + (q-1)\sigma_3 - c_0}{2c_1 + (2q-1)\sigma_3 - c_0} - \frac{q-1}{q+2} \right) \quad 2.102$$

The parameter c_1 is the function of frictional angle and uniaxial compressive strength (c_0):

$$C_1 = (1 + 0.6\mu) C_0 \quad 2.103$$

Where μ is the coefficient of internal angle of friction.

$$B = \frac{\sqrt{3}(q-1)}{q+2} - \frac{c}{3} (2c_0 + (q+2)\sigma_3) \quad 2.104$$

And parameter A is a function of B and C:

$$A = \frac{c_0}{\sqrt{3}} - \frac{c_0}{3} B - \frac{c_0^2}{9} C \quad 2.105$$

2.5.9 Griffith

Analysis of micro-cracks in a two dimensional model was Griffith's idea for developing his failure model (Fjaer et al., 2008). Expansion of micro-cracks as the onset of failure is a function of tensile stress at the tip of a crack. Original Griffith criterion has been developed in Mohr space and in terms of principal stresses and uniaxial tensile strength, T_0 :

$$(\sigma_1 - \sigma_3)^2 = 8T_0(\sigma_1 + \sigma_3) \quad 2.106$$

$$\sigma_3 = -T_0 \text{ if } \sigma_1 + 3\sigma_3 < 0 \quad 2.107$$

$$T_0 = C_0/8 \quad 2.108$$

In $\tau - \sigma$ plane, Griffith criterion is presented in the following form:

$$\tau^2 = 4T_0(\sigma + T_0) \quad 2.109$$

The constant ratio of uniaxial compressive strength to uniaxial tensile strength, which has been presented by Griffith, is lower but close to the typical range of this ratio, 10 to 15, from experimental observation (Fjaer et al., 2008). One of the disadvantages of this failure criterion is its dependence on a single variable which makes it harder to fit polyaxial test data. The second shortcoming of the Griffith criterion is the lack of consideration of the effect that intermediate principal stress has on the rock strength.

2.5.10 Modified Griffith

Under compression, shear failure due to the closure of a crack can occur before tensile stress reaches a critical level at the tip of a crack to initiate fracture (Brace, 1960). McClintock and Walsh (1962) included the effect of friction between crack faces. By neglecting the stress required to close cracks, Modified Griffith would be reduced to the following form:

$$\sigma_1(\sqrt{\mu^2 + 1} - \mu) - \sigma_3(\sqrt{\mu^2 + 1} + \mu) = 4T_0 \quad 2.110$$

$$\frac{c_0}{T_0} = \frac{4}{\sqrt{\mu^2 + 1} - \mu} \quad 2.111$$

By including the frictional behavior, Modified Griffith shows similarity to the Mohr-Coulomb Criterion. As it is shown in Eq.2.71, the ratio of uniaxial compressive strength to tensile strength is a function of internal angle of friction. The effect of intermediate principal stress is not considered in the Modified Griffith criterion since failure theory has been modeled in two-dimensional space.

2.5.11 Murrel

Murrel (1963) introduced a new criterion based on Griffith theory by including the intermediate principal stress as a contributing factor in the rock strength. He extended the Griffith criterion to three-dimensional stress space:

$$(\sigma_1 - \sigma_3)^2 + (\sigma_1 - \sigma_2)^2 + (\sigma_2 - \sigma_3)^2 = 24T_0(\sigma_1 + \sigma_2 + \sigma_3) \quad 2.112$$

The ratio between uniaxial compressive strength and uniaxial tensile strength in the Murrel criterion is close to the typical range of the experimental observation:

$$T_0 = \frac{c_0}{12} \quad 2.113$$

In terms of octahedral stresses, the Murrel criterion can be written in the following form. The σ_{oct} is equal to mean confining stress, J_1 .

$$\tau_{oct}^2 = 8T_0\sigma_{oct} \quad 2.114$$

2.5.12 Stassi d'Alia

Stassi d'Alia (1967) developed his failure criterion in terms of tensile strength and uniaxial compressive strength.

$$(\sigma_1 - \sigma_3)^2 + (\sigma_1 - \sigma_2)^2 + (\sigma_2 - \sigma_3)^2 = 2(c_0 - T_0)(\sigma_1 + \sigma_2 + \sigma_3) + 2C_0T_0 \quad 2.115$$

In his study, the modified Griffith assumption (Eq.2.111) was used for determination of tensile requirement in Eq.2.115

CHAPTER THREE

MATERIALS AND METHODOLOGY

3.1 Materials

The materials used in this research were data obtained for the following parameters: formation mechanical properties (i.e. Young's modulus, Poisson's ratio, compression and tensile strength) and state of in-situ stresses (i.e. magnitude of vertical and maximum and minimum horizontal stresses) and direction of maximum stress, plus the magnitude of pore pressure and these data were gotten from five (two vertical and three directional) wells in the Niger Delta area

3.2 Method

Selection of Mud weight for pressure control and wellbore stability requires knowledge of not only pore pressure gradient and fracture gradient but also collapse gradient of formation.

The mud weight window which is the value or range of values that might be used to keep safe operation while drilling has three specific paths to attain wellbore stability. Minimum values of this window correspond to the minimum weight required to avoid collapse formation in the borehole, maximum values addressed to prevent hydraulic fracturing while drilling and optimum weight is the suggested mud weight to perform drilling. This research therefore tends to develop a suitable model based criteria for designing sufficient mud weights in Niger Delta Region. The approach utilized to realize this work is through the development of workflow and the workflow is given below in Figure 3.1:

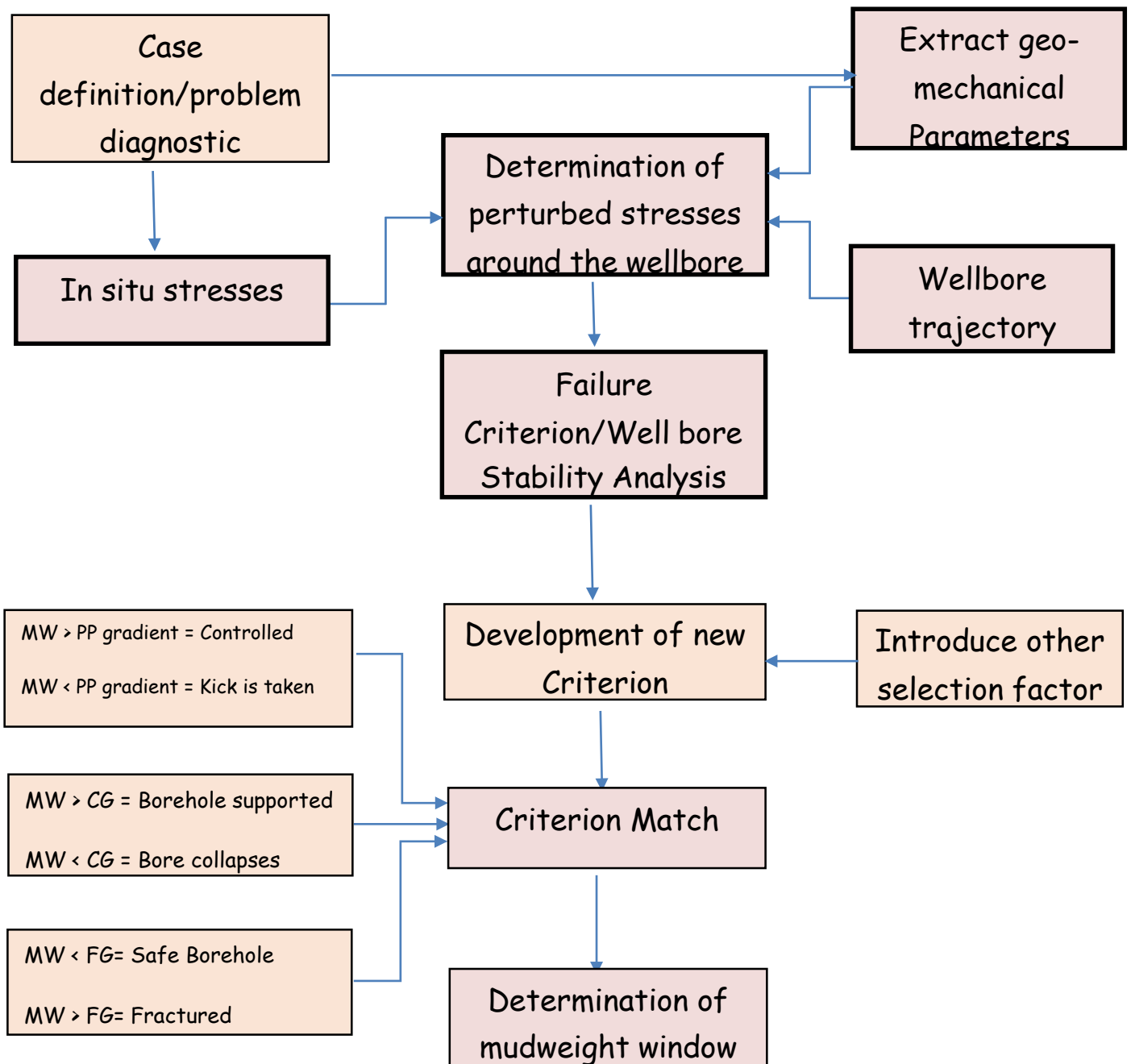


Figure 3.1: work flow chart for developing a suitable model based criteria for designing sufficient mud Weight

3.2.1. Case Definition and Problem Diagnostic

The cases considered in this work analyze the well and mud data from selected previously drilled wells with typical wellbore instability issues in the Niger Delta Region. The effort to drill these wells as part of the field development plan was quite challenging because of the unusual rate of well failures during the drilling phase. Out of the wells that were drilled in different block where these wells were selected, five (5) had experienced severe wellbore stability issues, failed to reach the target depth, and eventually were abandoned because of mechanical issues encountered. A problem diagnostic was conducted to determine the main cause of the instability issues in these fields. To identify the causes of instability problems, a problem diagnostic procedure was performed, which includes studying the well plans, drilling programs, daily drilling reports, and various logs for all well. The key operational data that will be analyzed for this problem diagnosis are the nonproductive time at a horizon or lithology, measured depth (MD), true vertical depth (TVD), mud weight, borehole inclination, azimuth, and lithology.

3.2.1.1 Well T-101 Case Study

Well T-101 was drilled for oil production. The initial plan for the well is a directional well with azimuth N 80° and inclination 50°. The kick off point starts at 7200ft, with final depth at 12750ft MD. According to the plan, the drilling process would have taken 32 days to complete. The designed mud weight for this section was 10.34ppg. This mud weight was relatively high however, wellbore instabilities still occurred in this section. The first problem happened while pulling out the BHA, there was indication of pack off which led to stuck BHA at 11330ft MD. With an over pull of 60 ton, jarring and optimized circulation failed to release the BHA, and finally it was decided to cut the BHA at 11000ft MD. The wellbore was then plugged, and a new drilling program for a sidetrack well was prepared.

3.2.1.2 Well A-33 Case Study

Well A-33 is a development oil well, the drilling of well A-33 successfully reached the target depth, although with some wellbore instability issues during drilling. The well was drilled directional with inclination 35° and azimuth N 98°. The first wellbore instability problem occurred at 8830ft MD (shale formation) with mud weight of 9.05ppg. After successfully releasing the BHA, the drilling of this section was done by using mud weight 9.2ppg until it reaches the pay section. Another pack off happened at 9660ft MD at shale formation (below the target reservoir). Pack off detected followed by stuck BHA. The mud weight used at this section was 9.49ppg

3.2.1.3 Well D- 705 Case Study

Well D-705 was proposed as development gas condensate well with expected production of 5 MMSCFD gas and 10 BCFD of condensate from this Sand. The well was planned to be drilled directionally with azimuth N 305° and inclination 25°. The kick off point starts at 6600ft, with final depth at 10940ft MD. According to the plan, the drilling process would have taken 28 days to complete. The mud weight used in this section is 9.1ppg. Severe wellbore-stability issues were experienced while drilling this section that led to BHA stuck at 9530ft MD due to pack-off. Several types of efforts were done to overcome this problem including optimizing the mud circulation, jarring, and utilizing the dissolving chemicals. All of these efforts were unable to free the stuck pipe and the hole was plugged. A new sidetrack well program was then prepared for this well with increased mud weight from 9.01ppg to 9.22ppg. The sidetrack window was drilled at 9870ft MD using 9.33ppg mud weight, first indication of wellbore instabilities occurred at 10080ft MD, shale cuttings were observed at shale shakers and BHA got stuck. Optimization of mud circulation successfully freed the stuck BHA. However, while running the BHA back into the current depth, the BHA sat at 10200ft MD. The drilling fluid from the wash down operation indicated that the hole was filled with shale cutting. Unfortunately the next pack off and over pull at 10940ft MD cannot be surmounted, the BHA was cut with top of fish (TOF) at 10620ft MD,

and the hole was plugged with top of cement (TOC) at 10440ft MD. The amount of shale cuttings from drilling fluid circulation indicated that they were the causes of pack off in both occurrences.

3.2.1.4 Well Z-47 Case study

The field where well Z-47 was drilled has shown past history of wellbore instability in spite of increasing level of chemical inhibition. Hence, previously drilled wells in the field experienced critical hole pack-offs, stuck pipe incidents and above all larger unanticipated non-productive time. As per Well Z-47 which was planned a vertical well, the pore pressure were hydrostatic (0.462psi/ft) and the mud weight needed from the traditional well design approach was 0.4664psi/ft to drill up to 9200ft MD with less than 3degrees inclination. The well was drilled to 8820ft MD towards the 8½ inches section and then observed cavings at shale shakers after pumping tandem pills and circulating bottoms-up done. All efforts proved by engineers to optimize the drilling parameters proved abortive, conclusion was that the mud weight was insufficient in spite of the inhibition of the mud leading to a critical stuck pipe incident.

3.2.1.5 Well Q--01 Case study

Well Q-01 originally planned to be vertical development oil well, the first wellbore instability problem occurred at 6250ft MD (shale formation) with mud weight 9.12ppg. After successfully freeing the BHA, the drilling of this section was done by using mud weight 9.33ppg until it reaches the sandstone formation (target reservoir). Mud weight slightly increased above fracture gradient caused the formation to fracture at 6560 m MD at shale formation (below the target reservoir) causing a severe lost circulation. The mud weight used at this section was 9.47ppg.

3.2.2 Extraction/Determination of Rock Mechanical Properties

For the selected case studies, the studied rocks interval range in depth from 5000ft to 13000ft in the subsurface. It falls within the Agbada Formation whose stratigraphic succession consists of interbedded sandstone and shale.

Determination of rock mechanical properties including elastic and inelastic properties was carried out using density and sonic compressional (ΔTC) and shear (ΔTS) transit times as. The elastic

properties included Poisson ratio (ν), elastic modulus (E) shear/rigidity modulus (G), bulk and matrix/grain moduli (K_b and K_m), bulk and grain compressibility (C_b and C_r), and Biot's coefficient. The inelastic properties determined were fracture gradient and rock strength which include uniaxial compressive strength, tensile and cohesive strengths, and frictional angle. Poisson's ratio and Young's Modulus (E), Shear Modulus (G), Bulk Modulus (K_b) and Matrix/Grain Bulk Modulus (K_m) were obtained from the wireline logs using empirical relationships. Poisson's ratio and Young's modulus were determined from P- and S- wave velocity. Where shear transit times data were not available, interval transit time of the shear wave (ΔT_s) was estimated and used to derive the shear wave velocity (V_s). This was achieved using the relationships in equations 3.1 to 3.3

$$V_p = \frac{304878}{\Delta T_c} \quad 3.1$$

$$V_s = \frac{304878}{\Delta T_s} \quad 3.2$$

$$V_s = (0.804 * V_p) - 0.856 \quad 3.3$$

3.2.2.1 Poisson Ratio (ν)

Poisson ratio (ν) was computed from acoustic measurements including the slowness of the compressional wave (ΔT_c) and shear wave (ΔT_s) ratio using the expression below;

$$\nu = 0.5 \left(\frac{V_p}{V_s} \right)^2 - \frac{1}{\left(\frac{V_p}{V_s} \right)^2} - 1 \quad 3.4$$

3.2.2.2 Shear Modulus (G)

The shear modulus (G) which is the ratio of the shear stress to the shear strain was estimated from the formula in equation 3.5

$$G = \frac{a \rho_b}{\Delta T_s} \quad 3.5$$

Where coefficient $a = 13464$, ρ_b = bulk density, ΔT_s = shear sonic transit time.

3.2.2.3 Bulk Modulus (K_b)

The bulk modulus (K_b) was computed from the sonic and density logs using equation 3.6

$$K_b = \rho_b \left(\frac{1}{\Delta T_C^2} - \frac{4}{3\Delta T_S^2} \right) \quad 3.6$$

Where ΔT denotes sonic transit times for compressional and shear waves

3.2.2.4 Matrix/Grain Bulk Modulus (K_m)

This was determined from the empirical relationship in equation 3.7

$$K_m = \frac{KS\rho_{ma}}{\frac{1}{\Delta T_{Cma}^2} - \frac{4}{3\Delta T_{Sma}^2}} \quad 3.7$$

3.2.2.5 Young's Modulus (E)

Young's modulus or modulus of elasticity was determined from shear modulus and Poisson's ratio as in equation 3.8

$$E = 2G(1 + \nu) \quad 3.8$$

3.2.2.6 Bulk Compressibility (C_b)

Bulk Compressibility with porosity was determined by the relationship in equation 3.9

$$C_b = \frac{1}{K_b} \quad 3.9$$

3.2.2.7 Rock Compressibility (C_r)

Rock Compressibility with zero porosity was obtained from equation 3.10 as:

$$C_r = \frac{1}{\rho \log \left(\frac{1}{\Delta T_{Cma}^2} - \frac{4}{3\Delta T_{Sma}^2} \right)} \quad 3.10$$

3.2.2.8 Biot Constants

Biot's poroelasticity describes the coupling between pore pressure and stress in rocks. When pore pressure changes and stresses are coupled, fluid diffusion plays an important role making

stability time-dependent. Biot constant (α) was determined in terms of bulk and grain modulus using the expressions in equations 3.11 and in terms of compressibility 3.12 as

$$\alpha = 1 - K_b / K_m \quad 3.11$$

Where K_b and k_m are skeleton bulk and solid grain moduli respectively

$$\alpha = 1 - C_r / C_b \quad 3.12$$

Where C_r and C_b are grain and bulk compressibility respectively.

3.2.2.9 Unconfined Compressive Strength (UCS)

Among the several empirical relationships proposed for application in sandstones, shales and carbonate rocks, the relationship for fine grained, consolidated and unconsolidated sandstones with all porosity ranges suitable for the Niger Delta was adopted as given in equation 3.13, while equation for shale was used for comparison of results as in equation 3.14.

$$UCS = 1200 \exp(-0.036\Delta Tc) \quad 3.13$$

$$UCS = 10(304.8/\Delta Tc - 1) \quad 3.14$$

Where UCS = unconfined compressive strength, ΔTc = compressional wave transit time.

3.2.2.10 Shear Strength

The initial shear strength (τ_i) and in situ rock's tensile strength (T_o) were determined using the empirical relationships in equation 3.15

$$\tau_i = 0.026E/C_b \times 10^6 \{0.008V_{sh} + 0.0045(1 - V_{sh})\} \quad 3.15$$

Where E = Elastic modulus, C_b = bulk compressibility and V_{sh} = volume of shale and in situ rock

Tensile strength (T_o),

$$T_o = C_o / 12 \quad 3.16$$

Where C_o = cohesive strength

$$C_o = 5(V_p - 1) / 0.5(V_p) \quad 3.17$$

3.2.3 Determination of in Situ Stresses Magnitudes and Orientation

Vertical stress (σ_v) was determined by integrating the density (ρ_b) of the materials from surface to the depth of interest as in equation 3.18

Where;

$$\sigma_v = \int z \rho_b(z) g dz \quad 3.18$$

The poroelastic equation which shows the relationship between vertical stress and minimum horizontal stress, Poisson's ratio and pore pressure (p_w) was used together with leak off test to calculate the minimum horizontal stress (σ_H) according to equation 3.19

$$\sigma_H = K (\sigma_v - \alpha p_w) + \alpha p_w \quad 3.19$$

Where α is Biot's coefficient and p_w is mud pressure.

Maximum horizontal stress (S_{Hmax}) was calculated using the relationship in equation 3.20

$$S_{Hmax} = S_{hmin} + \text{tf}^*(S_V - S_{hmin}) \quad 3.20$$

3.2.4 Fracture gradient

Distinguishing between fracture gradient which is practically the minimum horizontal stress and the most likely fracture gradient during drilling as presented equation 3.21

$$P_{FP} = \frac{3v}{2(1-v)(\sigma_v - \alpha P_p)} + \alpha P_p \quad 3.21$$

Where PFP = most likely fracture pressure gradient, σ_v = vertical stress, α = Biot's constant, P_p = pore pressure gradient.

3.2.5 Derivation of Stress Regime

The magnitude of minimum horizontal stress is important to determine the stress regime. Based on the calculated in situ stresses the stress regime for each case study is determined. Identification of stress regime will affect the extent of the mud weight window and the optimum drilling direction in case of deviated wellbores.

For Strike Slip Regime, the order of stress magnitude is

$$\sigma_{Hmax} > \sigma_v > \sigma_{Hmin}$$

For Normal Faulting/Stress Regime, the order of stress magnitude is

$$\sigma_v > \sigma_{Hmax} > \sigma_{Hmin}$$

For Reverse Regime, the order of stress magnitude is

$$\sigma_{Hmax} > \sigma_{Hmin} > \sigma_v$$

3.2.6 Determination of the Local Stresses

The redistributed stresses during the drilling process around the borehole section considered in this work can be calculated/accounted for. Local stresses induced by in-situ stress and hydraulic effects at the wellbore wall ($r = r_w$), for vertical well can be described by (Pasic, 2007) as follow:

$$\sigma_r = P_w \tag{3.22}$$

$$\sigma_t = (\sigma_x + \sigma_y) - (\sigma_x - \sigma_y)\cos 2\theta - P_w \tag{3.23}$$

$$\sigma_a = \sigma_z - 2(\sigma_x - \sigma_y)v\cos 2\theta \tag{3.24}$$

Where:

r_w = the radius of the wellbore,

r = distance from the borehole,

P_w = the internal wellbore pressure,

v = poisson's ratio, angle θ is measured clockwise from x-axis, σ_r is the radial stress, σ_t is tangential stress, σ_a is axial stress

For deviated well, the local stresses induced by in-situ stress and hydraulic effect at the wellbore, can be expressed using the following equation:

$$\sigma_r = P_w \tag{3.25}$$

$$\sigma_t = (\sigma_x + \sigma_y) - 2(\sigma_x + \sigma_y)\cos 2\theta - 4r_{xy} * \sin\theta - P_w \tag{3.26}$$

$$\sigma_a = \sigma_z - v(2(\sigma_x - \sigma_y)\cos\theta + 4r_{xy} * 2\sin 2\theta) \tag{3.27}$$

$$r_{\theta z} = 2(r_{xy}\cos\theta - r_{yz} * \sin\theta) \tag{3.28}$$

$$r_{r\theta} = r_{rz} = 0 \quad 3.29$$

3.2.7 Rock Failure Criterion

Wellbore failure can be caused by many different mechanisms as mentioned in previous sections, To predict the wellbore stability, an appropriate failure criterion should be used and representing the true in situ stress and pore pressure conditions. Several rock failure criteria exists, however for this study the Mogi-Coulomb Shear and Tensile failure criterion are coupled and were used for case study analysis.

The Mogi-Coulomb Shear failure criterion is given by:

$$F = a + b\sigma_{m,2} - \tau_{oct} \quad 3.30$$

Where:

$$\tau_{oct} = \frac{1}{3}\sqrt{(\sigma_1 - \sigma_3)^2 + (\sigma_1 - \sigma_2)^2 + (\sigma_2 - \sigma_3)^2} \quad 3.31$$

$$a = \frac{2\sqrt{2}}{3}c\cos\varphi \quad 3.32$$

$$b = \frac{2\sqrt{2}}{3}c\sin\varphi \quad 3.33$$

$$\sigma_{m,2} = \frac{\sigma_1 + \sigma_2}{2} \quad 3.34$$

Where c is the natural cohesion of the rock, φ is the angle of internal friction of the rock, τ_{oct} is the octahedral shear stress, $\sigma_{m,2}$ is the mean stress and the principal stresses defined as: the maximum principal stress σ_1 , the intermediate principal stress σ_2 and the minimum principal stress σ_3 .

In Eq. 3.30, Shear failure will occur when $F \leq 0$

The Mogi-Coulomb Tensile failure criterion is given by:

$$F = \tau_{t\min} + T_s \quad 3.35$$

In this criterion, the formation will fail in tensile mode when the least compressive principle stress at the wellbore exceeds the tensile strength of the rock.

Where

$\tau_{t \min}$ =Effective minimum compressional principle stress at the wellbore

T_s =Tensile strength of formation.

The effective minimum compressional principal stress is given by σ_3 least total stress minus the pore pressure(P_p)

$\tau_{t \min}$ Is given as:

$$\tau_{t \min} = \sigma_3 - P_p \quad 3.36$$

Substituting equation 3.36 in to in equation 3.35, the Tensile Failure Criterion becomes:

$$F = \sigma_3 - P_p + T_s \quad 3.37$$

In Eq 3.37, Tensile failure will occur when $F \leq 0$

To generate a Criterion as a single linear expression which can determine suitable mud weight window is based on coupling the Mogi Coulomb Shear and Tensile failure criterion.

$$a + b\sigma_{m,2} - \tau_{oct} = \sigma_3 - P_p + T_s \quad 3.38$$

$$F = \sigma_3 - P_p + T_s - a - b\sigma_{m,2} + \tau_{oct} \quad 3.39$$

In Eq 3.39, Shear and Tensile failure will occur when $F \leq 0$

3.2.8 Determination of Safe Mud Weight Window

Based on solution of the poro-elastic relations, it's seen that radial, tangential and axial stresses are functions of the wellbore pressure. Accordingly, to obtain the minimum and maximum limits of safe mud window an iterative procedure is developed using the coupled failure criterion.

The wellbore pressure can have values ranging from the original pore pressure value to the minimum in situ stress value. The minimum in situ stress may be the minimum horizontal stress or vertical stress based on the faulting regime. To analyze wellbore stability, the estimated principal stresses is introduced into the Coupled Mogi-Coulomb rock failure criterion.

The procedure of safe mud weight determination at first step involves setting the wellbore pressure P_w equals the pore pressure (if well is still on planning stage) or the mud weight at which a failure occurs. The stresses around the wellbore are calculated for a point in wall circumference of the well ($\theta = 0$) the tangential, vertical and radial stresses are applied into the failure criterion to see if the rock fails. This step is repeated for the half of wall circumference due to symmetry. In each step, 2.5° added to the angle of θ till it reaches to 180. If the rock fails at any angle, 0.0026psi is added to mud pressure (P_w), stresses are determined and the procedure is repeated. This process continues till the rock failure does not occur around the wellbore. This process with some differences is used to gain the maximum limit and minimum of mud weight. These procedures were carried out carefully for the five (5) case study considered and the safe mud weight window was gotten for each case

3.2.8 Model and Results Comparison

To ascertain the applicability of this coupled Mogi-Coulomb Failure, the upper and lower limits of the determined mud weight window will be compared to those predicted by Mohr-Coulomb linear poro-elastic failure criterion which is another widely used failure criterion. The Mohr-Coulomb criterion used to determine collapse pressure (critical wellbore pressure) is given as:

$$P_c = \{1.5 \sigma_{H_{max}} - 0.5 \sigma_{H_{min}} \alpha_{pp} (1-2\nu/1-\nu) - 1.732\tau_i\} / 1 - 0.5\alpha (1-2\nu/1-\nu) \quad 3.40$$

Where τ_i the initial shear strength

$$r_i = \frac{0.026E}{C_b} * 10^6 (0.008V_{sh} + 0.0045(1 - V_{sh})) \quad 3.41$$

Where E = Elastic modulus C_b = bulk compressibility, V_{sh} = volume of shale, ν = Poisson ratio, α = Biot's coefficient, $\sigma_{H_{max}}$ = maximum horizontal stress, $\sigma_{H_{min}}$ = minimum horizontal stress and P_p = Pore pressure

Zhang (2013) proposed equations for determining maximum and minimum mud weight based on Mohr-Coulomb failure criterion which was also used.

The Minimum mud weight is given as:

$$P_{min} = \frac{\{\sigma_{max} + \sigma_{min} - 2(\sigma_{max} - \sigma_{min})\cos 2\theta - UCS + \alpha(q-1)P_p\}}{q+1} \quad 3.42$$

Where

P_m = Minimum Mud weight or Shear failure pressure to prevent collapse

$$UCS = \frac{2c\cos\theta}{1-\sin\theta} \quad 3.43$$

$$q = \frac{1+\sin\theta}{1-\sin\theta} \quad 3.44$$

α = Biots Coefficient, c = Rock Cohesion and P_p = Pore Pressure

The break down pressure or maximum mud weight is determined using the equation 3.45

below:

$$P_{max} = 3\sigma_{hmin} - \sigma_{Hmax} - P_p - T_0 \quad 3.45$$

P_{max} = Maximum mud weight for wellbore stability

σ_{hmin} = minimum horizontal stress,

σ_{Hmax} = maximum horizontal stress,

P_p = Pore pressure,

T_0 = Tensile strength

CHAPTER FOUR
RESULTS AND DISCUSSIONS

4.1 Results

The results of the study on the development of are presented in this chapter. An excel based spreadsheet was developed to perform all calculations and iterations presented in this chapter. It encompasses an integration of results from the several steps in the study work flow, from generating drilled rock in-situ stresses of the 5 cases considered to model validation.

4.1.1 Determination of the In-situ Stresses and Stress Regime

The magnitude and orientation of the in-situ stresses for the 5 cases analyzed are presented in the table 4.1 below. The utilized data are extracted from the drilling report of the individual wells considered, and the ones that are not present in the report are calculated using the mathematical relationship given in this study.

Table 4.1: Results of in-situ stresses for the 5 wells

Parameter	Well T-101 (Deviated)	Well A-33 (Deviated)	Well D-705 (Deviated)	Well Z-47 (Vertical)	Well Q-01 (Vertical)
Depth of Consideration (ft)	12750	9660	10940	8820	6560
Vertical Stress (σ_v) psi/ft	0.823	0.712	0.83	0.831	0.8421
Minimum Horizontal Stress(σ_h) psi/ft	0.671	0.633	0.591	0.568	0.514
Maximum Horizontal Stress(σ_H) psi/ft	0.778	0.827	0.708	0.929	0.722

During drilling of the well phase/depth, the principle stresses which are in equilibrium are redistributed which can lead to shear or tensile failure. The support that is originally offered by the drilled rock formations are displaced by the drilling fluid that creates a hydrostatic pressure that maintains the wellbore.

Identification of stress regime will affect the extent of the mud weight window and the optimum drilling direction in case of deviated wellbores. Given the principal stresses as presented in the Table 4.1 above, the stress regime is identified. This is presented in Table 4.2.

For Strike-Slip Regime, the order of stress magnitude is

$$\sigma_{Hmax} > \sigma_v > \sigma_{Hmin}$$

For Normal Faulting/Stress Regime, the order of stress magnitude is

$$\sigma_v > \sigma_{Hmax} > \sigma_{Hmin}$$

For Reverse Regime, the order of stress magnitude is

$$\sigma_{Hmax} > \sigma_{Hmin} > \sigma_v$$

Table 4.2: Relatives Magnitude and Stress Regimes

Well Name	σ_v	σ_{Hmax}	σ_{Hmin}	Order	Regime
T-101 (D)	0.8236	0.778	0.671	$\sigma_v > \sigma_{Hmax} > \sigma_{Hmin}$	Normal
A-33 (D)	0.7120	0.827	0.633	$\sigma_{Hmax} > \sigma_v > \sigma_{Hmin}$	Strike-Slip
D-705 (D)	0.9132	0.708	0.591	$\sigma_v > \sigma_{Hmax} > \sigma_{Hmin}$	Normal
Z-47 (V)	0.8771	0.929	0.568	$\sigma_{Hmax} > \sigma_v > \sigma_{Hmin}$	Strike-Slip
Q-01 (V)	0.8421	0.722	0.514	$\sigma_v > \sigma_{Hmax} > \sigma_{Hmin}$	Normal

For wells T-101, D-705 and Q-01 where the vertical stress is the largest of the principal stresses, it is defined to be normal faulting stress regime. The maximum horizontal stress at the

considered depths will be the intermediate stress in a normal faulting regime, highest in a strike-slip regime as obtained in wells A-33 and Z-47, and may be the greatest in a reverse faulting regime. In general, vertical wells will be progressively less stable as the regime changes from normal to strike-slip to reverse, and consequently will require higher mud weights to drill.

4.1.2 Output of Calculated Local Stresses

During drilling operations, the principle stresses which are in equilibrium are redistributed which can lead to shear or tensile failure. The support that is originally offered by the drilled rock formations are displaced by the drilling fluid that creates a hydrostatic pressure that maintains the wellbore. Using equations presented by Pasic et al. (2007) in chapter 3 for vertical and deviated well, the local stresses induced by in-situ stress and hydraulic effect at the wellbore were calculated. The table 4.3 below shows the calculated local stresses for the 5 wells at the wellbore failure depth.

Table 4.3: Results of the local stresses for the 5 wells

Parameter	Well T-101 (Deviated)	Well A-33 (Deviated)	Well D-705 (Deviated)	Well Z-47 (Vertical)	Well Q-01 (Vertical)
Depth of Consideration (ft)	12750	9660	10940	8820	6560
Radial Stress (σ_{rr}) psi/ft	0.53768	0.49348	0.48516	0.46644	0.49244
Tangential Stress (σ_{tt}) psi/ft	0.69732	0.57852	0.57984	0.30856	0.32756
Axial Stress (σ_{zz}) psi/ft	0.76308	0.61112	0.7713596	0.604292	0.70482

These wellbore stresses as given in Table 4.3 are calculated for a point in wall circumference of the well at($\theta = 0$), thus as the mud pressure increases or decreases, the wellbore stresses will vary. Failure type will depend on the orientation and magnitude of these wellbore stress, hence in order to evaluate the potential for wellbore stability these computed stresses and strains must then be compared against a given failure criterion.

4.1.3 Determination of Safe Mud Weight Window (SMWW)

The coupled Mogi-Coulomb failure criterion was used to predict the safe mud weight window by utilizing the local wellbore stresses from the individual wells, Tensile strength of the formations considered and the mud weights in an iterative manner. The iteration is calculated for several point in wall circumference of the well at($\theta = 0$ to 180°) and different trajectories for the deviated wells. The plots of the safe mud weight window for the 5 wells considered are given in figures 4.1 to 4.5

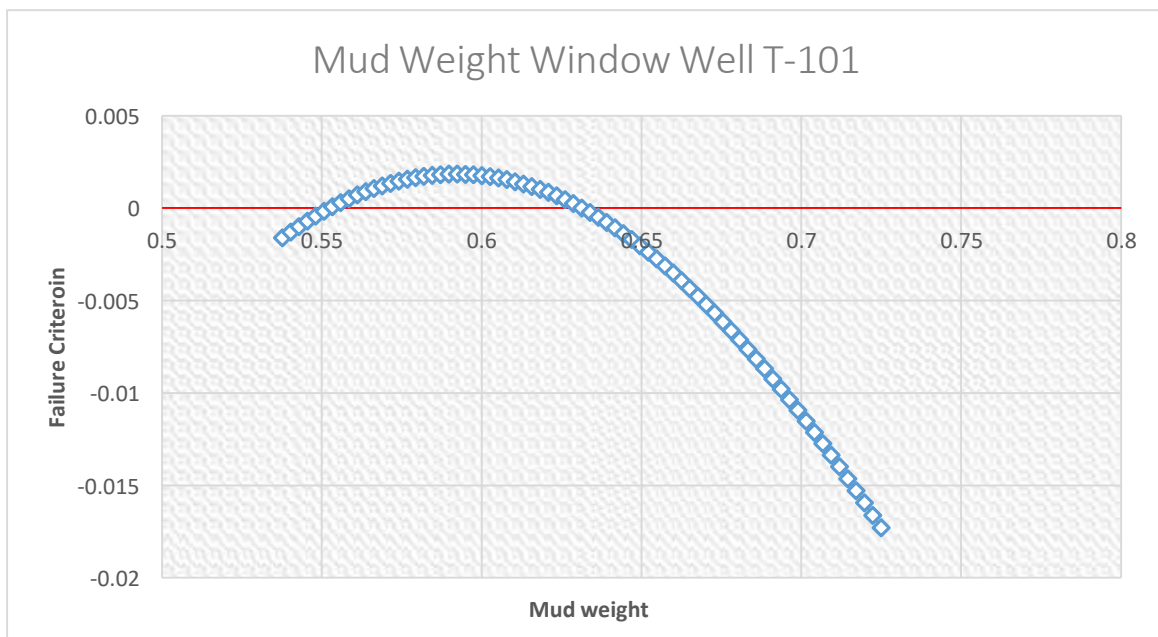


Figure 4.1: Plot of Failure Criterion vs Mud Weight for Well T-101

The Safe mud weight window for Well T-101 predicted can be seen from the Fig 4.1 as the mud weight values that falls under the positive X, Y coordinate. Shear and Tensile failure will occur at the wellbore for negative values of the failure criterion $F \leq 0$ thus, from the plot the safe mud weight window falls between 0.553psi/ft. to 0.631psi/ft. Recall that Well T-101

drilled with a mud weight of 10.34ppg (0.537psi/ft.) experienced shear failure in terms of severe hole pack off which lead to stuck BHA at depths around 12500ft. because of mud weight which was thought to be relatively high. From the calculations a safe drilling operation can be achieved by operating within the predicted mud weight window.

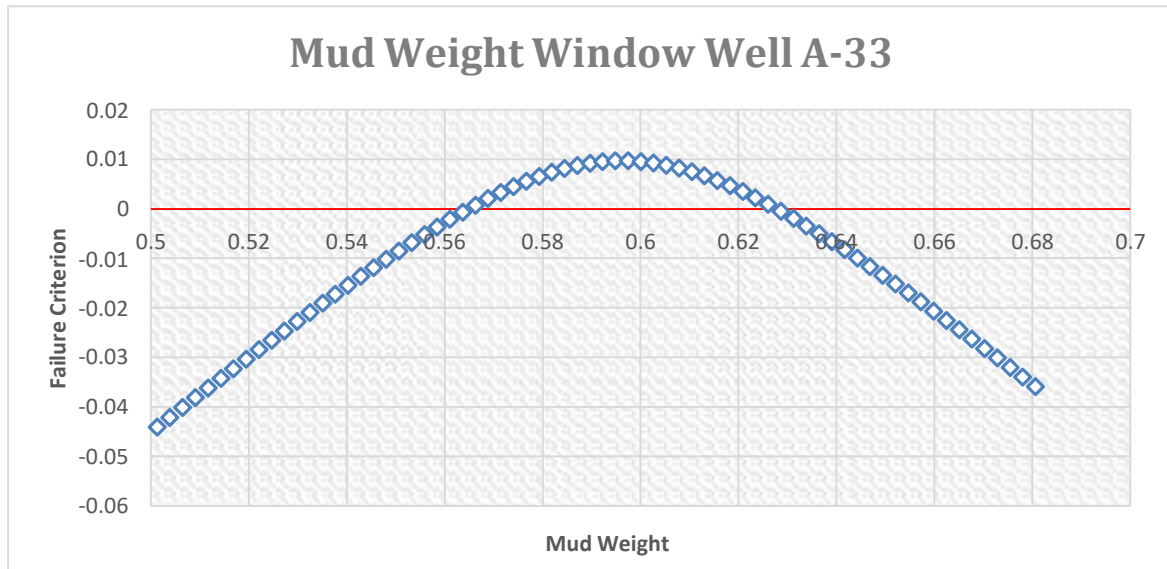


Figure 4.2: Plot of Failure function vs Mud Weight for Well A-33

Shear and Tensile failure will occur at the wellbore of Well A-33 for negative values of the failure criterion $F \leq 0$. The fracture gradient calculated from LOT at 9660ft for well A-33 is 0.652psi/ft. during the drilling phase whereas the mud weight used for this hole section is 9.49ppg (0.493psi/ft.). This mud weight however posed serious hole problems but using the coupled Mogi-Coulomb Failure function, a safe mud weight window between 0.566psi/ft. to 0.6261psi/ft. was predicted as shown in figure 4.2. The wide MW margin can say to have resulted from the rock cohesion and the faulting regime.

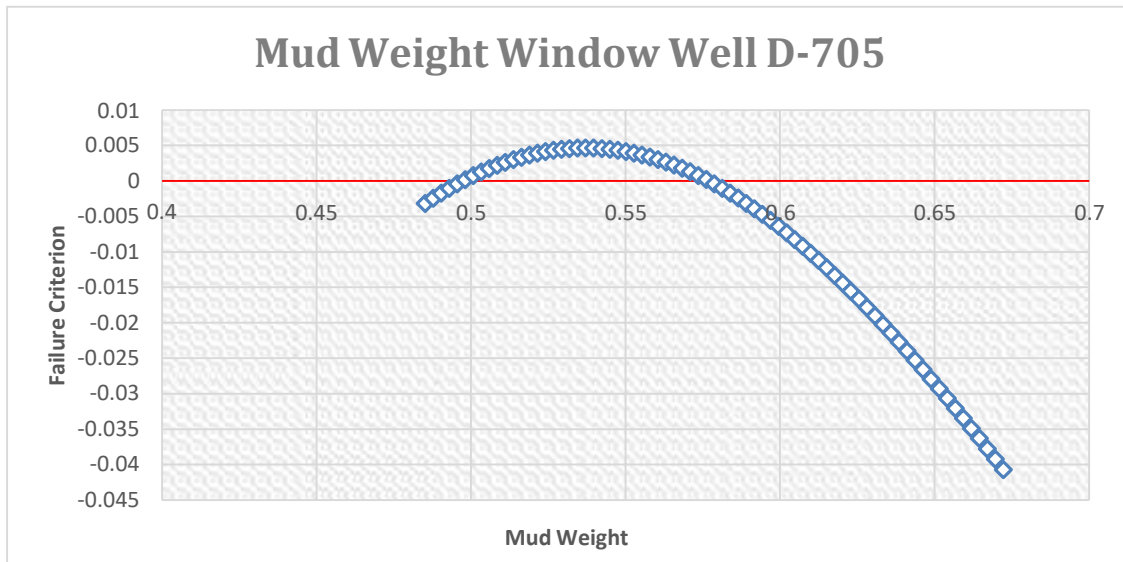


Figure 4.3: Plot of Failure function vs Mud Weight for Well D-705.

The figure 4.3 above shows that well D-705 can be drilled safely without shear or tensile failure if the mud pressure falls between 0.498psi/ft. and 0.576psi/ft. The minimum mud weight predicted from this failure function is very close to the mud weight (9.33ppg/0.485) used ab initio to drill this well at depths around 10400ft and as seen from drilling report of well D-705 was challenged with hole caving and pack off and consequently stuck BHA.

Mud weight selection for this well scenario is critical and will require operating away from lower and upper limits of the mud weight window or simply drill this hole section with in mud weight values that satisfies the coupled Mogi-Coulomb failure criterion ($F \geq 0$).

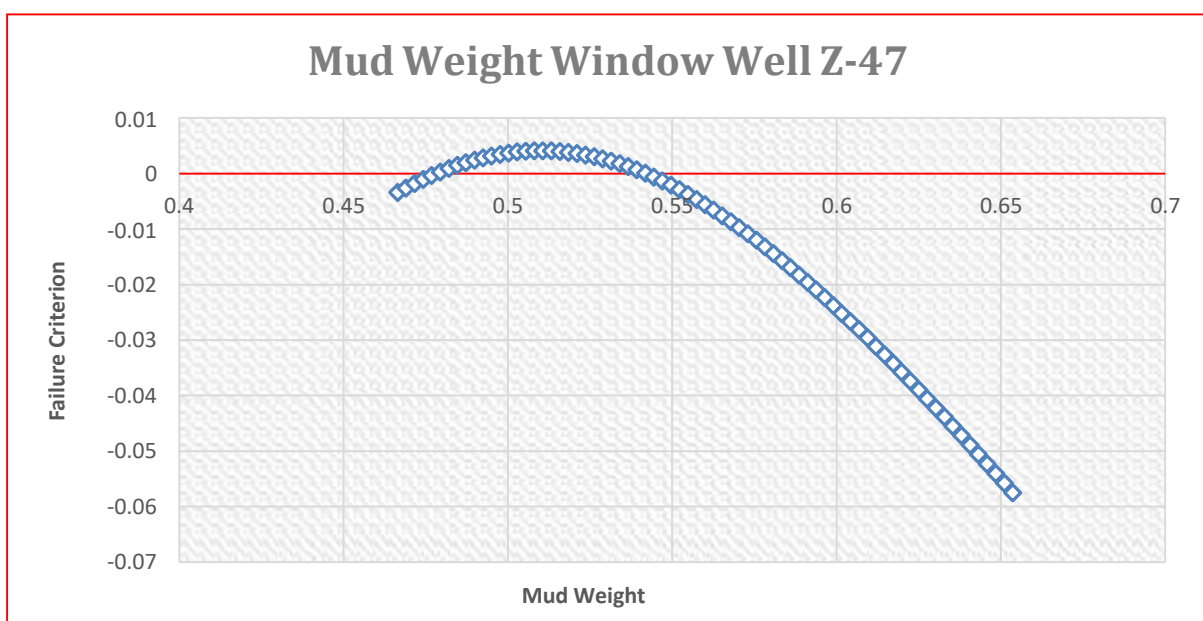


Figure 4.4: Plot of Failure function vs Mud Weight for Well Z-47.

Drilling Reports on Well Z-47 stated that the pore pressure for this well were hydrostatic (0.462psi/ft.) and the mud weight needed from the traditional well design approach was 8.97ppg (0.466ftpsi/ft.) to drill up to 8850ft MD with less than 5degrees inclination. It concluded that mud weight used for this hole section was insufficient in spite of the inhibition of the mud leading to a critical stuck pipe incident. Employing the coupled Mogi-Coulomb failure function. The mud weight window predicted for Well-Z47 as seen in figure 4.4 shows that the well can be safely operated at mud weight values between 0.479psi/ft. and 0.541psi/ft. to prevent borehole collapse or wellbore fracture. Looking at the close difference between the upper limit of the mud weight window and the fracture pressure (0.564psi/ft.) from LOT, it will be in the best interest of the drilling engineer to operate at mud weight values away from the predicted maximum mud weight values to prevent tensile failure.

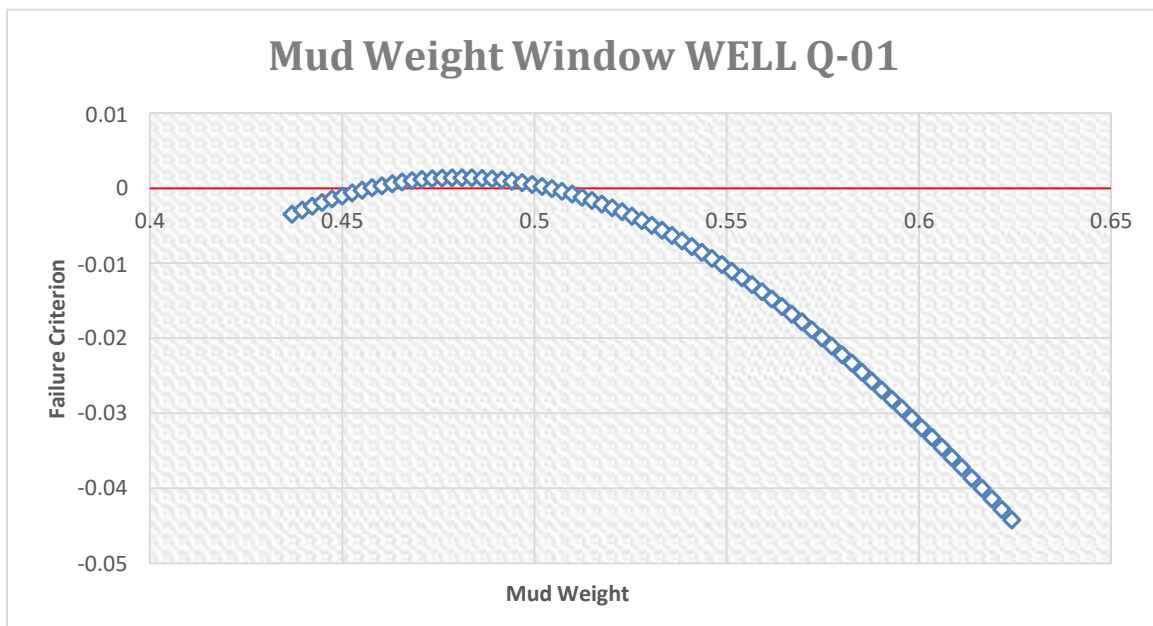


Figure 4.5: Plot of Failure function vs Mud Weight for Well Q-01.

For Well Q-01, during drilling of the pay section with mud weight of 9.47ppg (0.492psi/ft.) caused the formation to fracture at 6560 m MD at shale formation (below the target reservoir) causing a severe lost circulation. Using Coupled Mogi-Coulomb failure function a safe mud weight window was generated for this well as shown in figure 4.5 the Safe MWW falls between

0.458psi/ft. to 0.502psi/ft. Borehole collapse or tensile failure will occur at the wellbore for negative values of the failure criterion $F \leq 0$. The plot of failure function against mud weight for Well Q-01 shows quite a narrow mud weight window with most of the mud weight that satisfies the failure criterion lying almost flat at the X-axis. Looking at the fracture gradient from LOT for this well which is 0.529psi/ft. and the upper limit of the MWW generated for this well, one would expect the original mud weight of 0.492psi/ft. to safely drill the well without any hole problems but on the contrary it did not. One key practice to be adopted considering this scenario is to continuously monitor the equivalent circulating density (ECD) during drilling operation as this resulting tensile failure in Well Q-01 is a clear case of unprecedented increase in mud weight.

4.1.4 Model Results Comparison

The results of the lower limits and upper limits of the mud weight window predicted using coupled Mogi-Coulomb Criterion are compared with those calculated with Mohr-Coulomb Failure criterion and the actual mud weight at different hole inclination (deviated wells) for the 5wells used in case study are presented in below.

Table 4.4 Results of the actual and model predicted mud weight for well T-101

Hole Inclination (Deg)	Coupled Mogi Model (LL) (psi/ft.)	Actual Mudweight (psi/ft.)	Mohr Model (LL) (psi/ft.)	Fracture Gradient (psi/ft.)	Coupled Mogi Model(UL) (psi/ft.)	Mohr Model (UL) (psi/ft.)
0	0.5328	0.53768	0.5446	0.659	0.6353	0.6277
5	0.55488	0.53768	0.5556	0.659	0.6328	0.6227
10	0.54848	0.53768	0.5668	0.659	0.6288	0.6151
15	0.56108	0.53768	0.5706	0.659	0.6298	0.6125
20	0.56368	0.53768	0.5731	0.659	0.6239	0.6099
25	0.56628	0.53768	0.5742	0.659	0.6201	0.6083
30	0.56888	0.53768	0.5766	0.659	0.6176	0.6057
35	0.56648	0.53768	0.5796	0.659	0.6126	0.6041

40	0.57408	0.53768	0.5854	0.659	0.6152	0.6025
45	0.57668	0.53768	0.5843	0.659	0.6143	0.6009
50	0.57928	0.53768	0.5853	0.659	0.6141	0.6025
55	0.58188	0.53768	0.5887	0.659	0.6133	0.6009
60	0.58448	0.53768	0.5893	0.659	0.6117	0.5983
65	0.58708	0.53768	0.5936	0.659	0.6056	0.5967
70	0.58968	0.53768	0.5947	0.659	0.6038	0.5951
75	0.58228	0.53768	0.5956	0.659	0.6025	0.5967
80	0.59488	0.53768	0.5991	0.659	0.6008	0.5951
85	0.59248	0.53768	0.6096	0.659	0.5978	0.5925
90	0.60008	0.53768	0.6106	0.659	0.5953	0.5909

Using the tabulated result presented in this study for Well T-101 which has an inclination of 50degrees, The Coupled Mogi Model predicted 0.579psi/ft. as the minimum allowable mud weight whereas Mohr model predicted 0.585psi/ft. as Minimum allowable mud weight at 50° inclination as against 0.537psi/ft. used mud weight that resulted in the wellbore instability issue. For the maximum allowable mud weight, the coupled-Mogi and Mohr model predicted 0.6141psi/ft. and 0.6025psi/ft. respectively which are still below the fracture pressure. There is difference in mud weight range for every inclination that was calculated for. The significant differences in mud weight calculated are because the well trajectory data were assumed, since the exact coordinates of easting and northing for the well are not available. Also, several parameters at certain point, for example the well inclination and azimuth need to be assumed due to limitation in field data. A mud weight comparison plot is generated for well T-101 as given in the figures below.

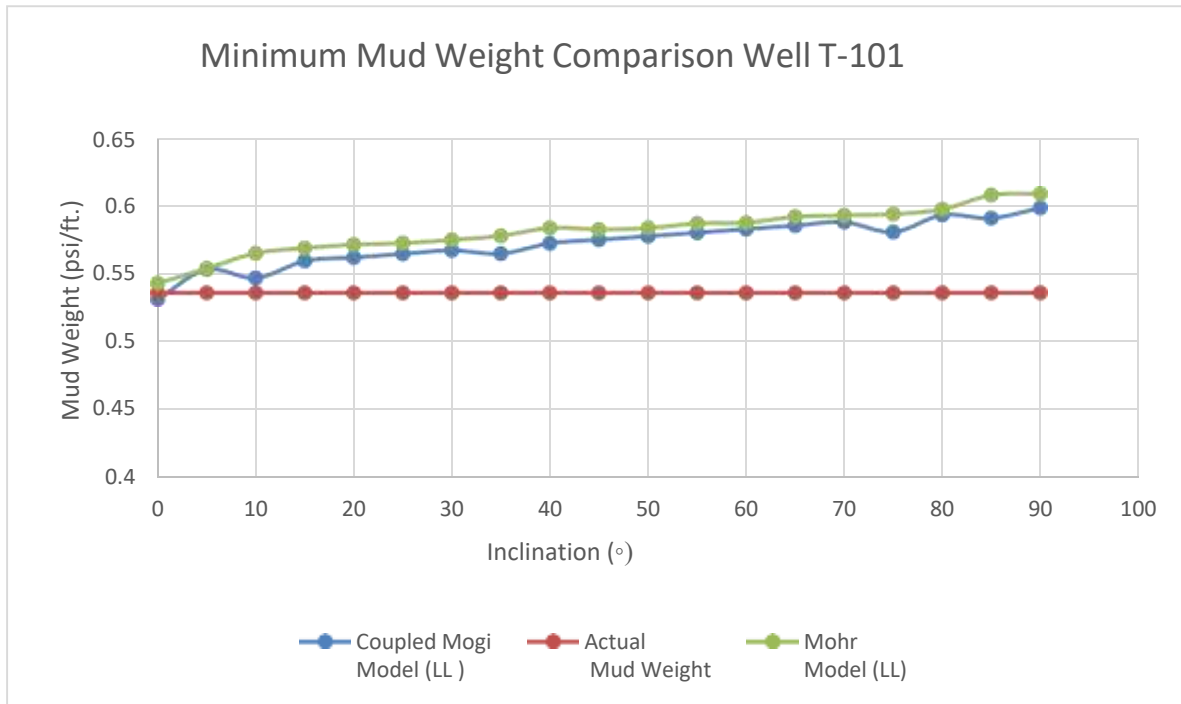


Figure 4.6 Effects of different failure criteria on minimum mud weight for Well T-101

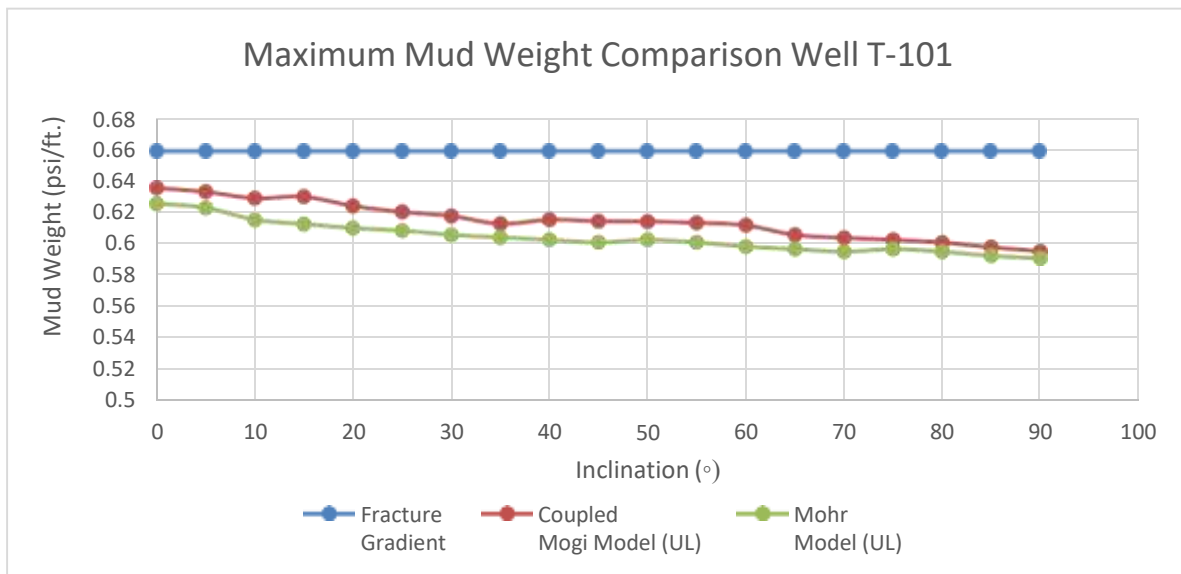


Figure 4.7: Effects of different failure criteria on maximum mud weight for Well T-101

For Well A-33 which is inclined at 35°, the results as tabulated below shows that the coupled Mogi Model predicted 0.548psi/ft. as the minimum allowable mud weight whereas Mohr model predicted 0.561psi/ft. as minimum allowable mud weight both at 35° inclination as against 0.493psi/ft. used mud weight that caused hole pack off for this well.

Table 4.5: Results of the actual and model predicted mud weight for Well A-33

Hole Inclination (Deg)	Coupled Mogi Model (LL)(psi/ft.)	Actual Mudweight (psi/ft.)	Mohr Model (LL) (psi/ft.)	Fracture Gradient (psi/ft.)	Coupled Mogi Model (UL) (psi/ft.)	Mohr Model (UL) (psi/ft.)
0	0.52988	0.49348	0.52987	0.6524	0.62348	0.6317
5	0.53048	0.49348	0.53293	0.6524	0.62608	0.62048
10	0.53508	0.49348	0.53699	0.6524	0.62868	0.62308
15	0.53968	0.49348	0.54105	0.6524	0.62648	0.62368
20	0.54028	0.49348	0.54611	0.6524	0.62428	0.62148
25	0.5492	0.49348	0.55117	0.6524	0.62208	0.61928
30	0.54548	0.49348	0.55623	0.6524	0.61988	0.61708
35	0.54808	0.49348	0.56129	0.6524	0.61768	0.61388
40	0.55968	0.49348	0.56635	0.6524	0.61548	0.61168
45	0.55328	0.49348	0.56941	0.6524	0.61608	0.60948
50	0.54588	0.49348	0.57247	0.6524	0.61668	0.61208
55	0.55848	0.49348	0.57553	0.6524	0.61728	0.61268
60	0.56108	0.49348	0.57859	0.6524	0.61788	0.61328
65	0.56368	0.49348	0.581496	0.6524	0.61328	0.60788
70	0.55988	0.49348	0.584402	0.6524	0.60868	0.60328
75	0.57088	0.49348	0.587308	0.6524	0.60408	0.59868
80	0.56948	0.49348	0.590214	0.6524	0.59948	0.59408
85	0.57086	0.49348	0.593274	0.6524	0.59488	0.58948
90	0.57228	0.49348	0.596334	0.6524	0.59028	0.58488

For the maximum allowable mud weight, the coupled-Mogi and Mohr model predicted 0.618psi/ft. and 0.614psi/ft. respectively which are still within range. The predicted mud weight for Well A-33 at different inclination are presented in the figures below.

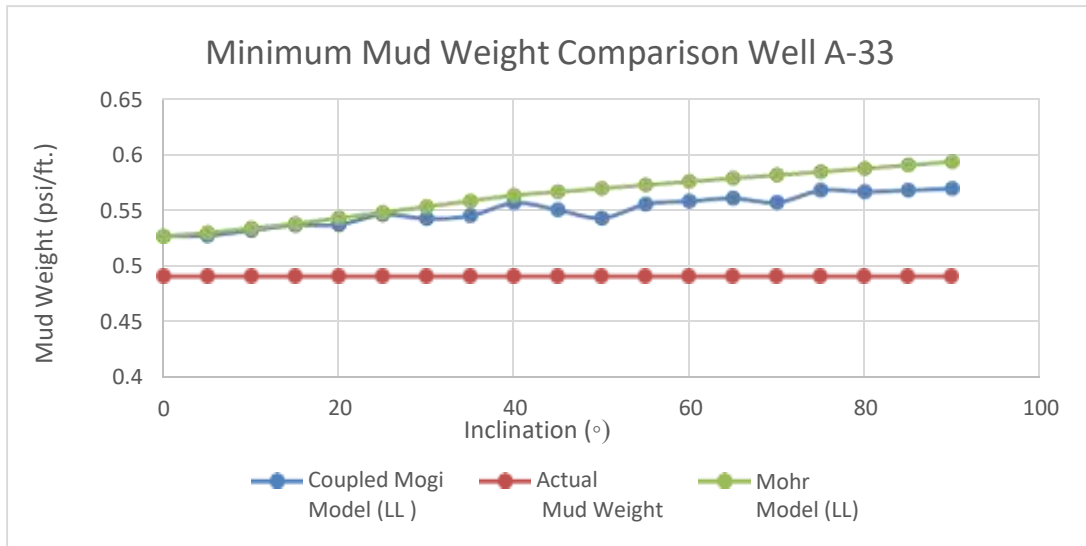


Figure 4.8: Effects of different failure criteria on minimum mud weight for Well A-33

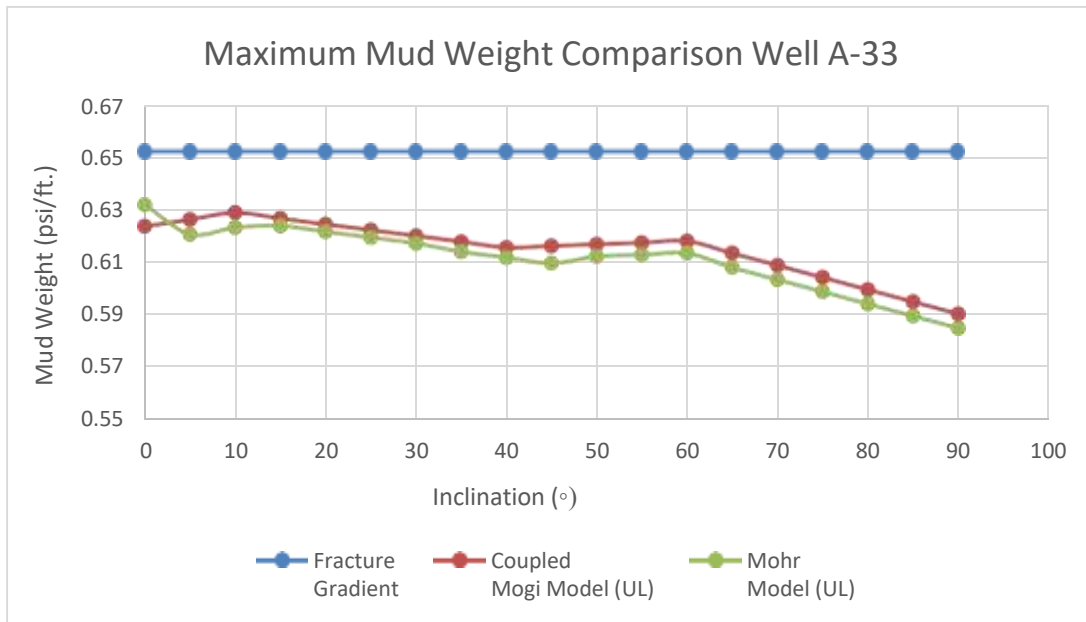


Figure 4.9: Effects of different failure criteria on maximum mud weight for Well A-33

For Well D-705 inclined at 25° at wellbore azimuth of 305°, the predicted mud weight using coupled Mogi-Coulomb Criterion and Mohr-Coulomb Failure criterion gave significant match of the mud weight limits at different wellbore trajectory. The Coupled Mogi Model and Mohr model predicted 0.5074psi/ft. and 0.5251psi/ft. respectively as the minimum allowable mud weight at 25° inclination compared to 0.4852psi/ft. which was the actual mud weight used in the case study to drill this hole section at depths of 10940ft that resulted in the wellbore instability issue.

Table 4.6: Results of the actual and model predicted mud weight for Well D-705

Hole Inclination (Deg.)	Coupled Mogi Model (LL) psi/ft.	Actual MudWeight psi/ft.	Mohr Model (LL) psi/ft.	Fracture Gradient psi/ft.	Coupled Mogi Model (UL) psi/ft.	Mohr Model (UL) psi/ft.
0	0.4981	0.4852	0.5021	0.6233	0.6061	0.6029
5	0.5007	0.4852	0.5108	0.6233	0.5987	0.6017
10	0.5033	0.4852	0.5159	0.6233	0.5913	0.6005
15	0.5059	0.4852	0.5189	0.6233	0.5891	0.5993
20	0.5085	0.4852	0.5205	0.6233	0.5865	0.5965
25	0.5074	0.4852	0.5251	0.6233	0.5831	0.5881
30	0.5085	0.4852	0.5267	0.6233	0.5807	0.5847
35	0.5096	0.4852	0.5243	0.6233	0.5793	0.5831
40	0.5111	0.4852	0.5319	0.6233	0.5757	0.5815
45	0.5215	0.4852	0.5335	0.6233	0.5721	0.5789
50	0.5241	0.4852	0.5371	0.6233	0.5685	0.5763
55	0.5267	0.4852	0.5337	0.6233	0.5649	0.5737
60	0.5293	0.4852	0.5423	0.6233	0.5764	0.5704
65	0.5359	0.4852	0.5449	0.6233	0.5728	0.5698
70	0.5345	0.4852	0.5475	0.6233	0.5692	0.5662
75	0.5361	0.4852	0.5531	0.6233	0.5667	0.5607
80	0.5397	0.4852	0.5507	0.6233	0.5622	0.5599
85	0.5423	0.4852	0.5553	0.6233	0.5607	0.5544
90	0.5479	0.4852	0.5589	0.6233	0.5562	0.5512

For the maximum allowable mud weight, the coupled-Mogi and Mohr model predicted 0.5831psi/ft. and 0.5881psi/ft. respectively at 25°inclination which are still below the fracture pressure. The predicted mud weight for Well D-705 at different inclination are presented in the figures below.

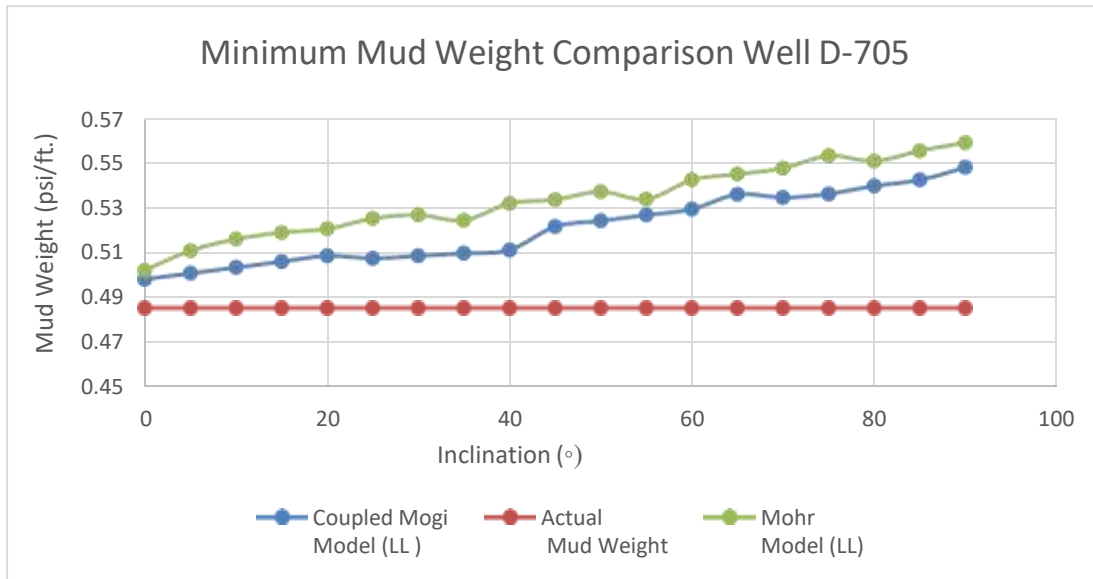


Figure 4.10: Effects of different failure criteria on minimum mud weight for Well D-705

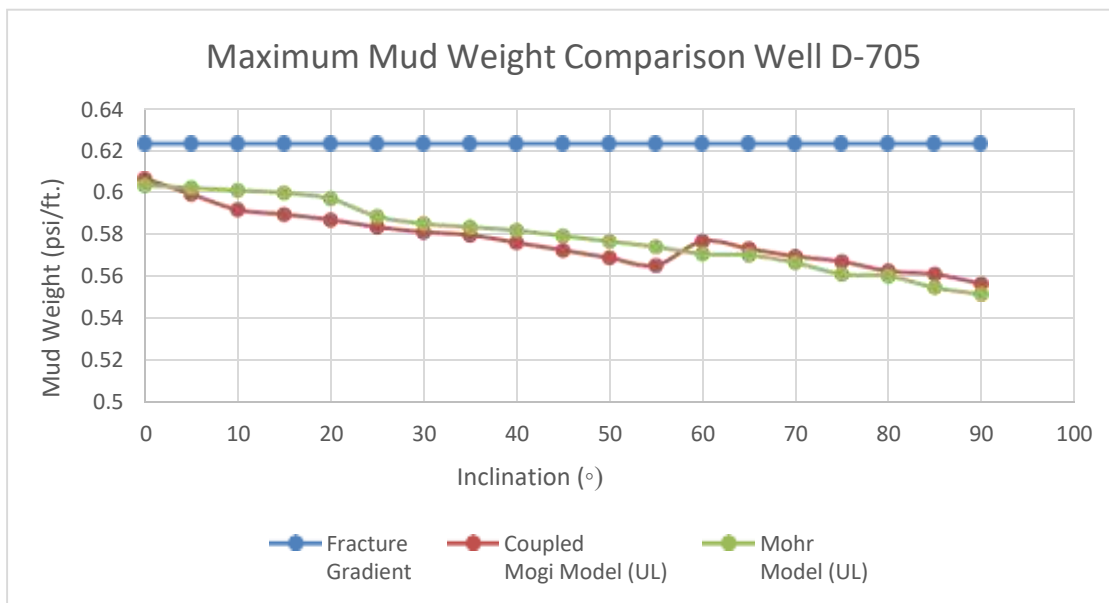


Figure 4.11: Effects of different failure criteria on maximum mud weight for Well D-705

Well Z-47 was planned a vertical well, the pore pressure were hydrostatic (0.437psi/ft.).

The mud weight used for this well was according to the traditional well design approach which was 0.4664psi/ft. required to drill up to 8820ft MD with less than 3° inclination

The Coupled Mogi-Coulomb model and Mohr model predicted 0.4794psi/ft. and 0.4082psi/ft. respectively as the minimum allowable mud weight For Well Z-47 inclined at 0.9° with wellbore azimuth of 17° compared to the actual mud weight of 0.4664psi/ft. that posed the stability problems for this well. For the maximum allowable mud weight, the coupled-Mogi and Mohr model predicted 0.5418psi/ft. and 0.5372psi/ft. respectively which are still within range. The predicted mud weight for Well Z-47 are presented in the table below.

Table 4.7 Results of the actual and model predicted mud weight for Well Z-47

Hole Inclination (Deg.)	Coupled Mogi Model (LL)(psi/ft.)	Actual Mudweight (psi/ft.)	Mohr Model (LL) (psi/ft.)	Fracture Gradient (psi/ft.)	Coupled Mogi Model (UL) (psi/ft.)	Mohr Model (UL) (psi/ft.)
0.9	0.4794	0.46644	0.4802	0.5843	0.54181	0.5372

The table 4.8 present’s mud weight results comparison for Well Q-01 which was drilled a vertical well to a depth of 6560ft with less than 5° inclination. The Coupled Mogi Model predicted 0.458psi/ft. as the minimum allowable mud weight whereas Mohr model predicted 0.45992psi/ft. as minimum allowable mud weight. The actual mud weight used to drill Well Q-01 which is 0.49244psi/ft. initiated tensile failure (fractures) around the wellbore resulting in severe loss circulation. Looking at the table, there is a significant variation between the used mud weight and predicted values of the minimum allowable mud weight. For the maximum allowable mud weight, the coupled-Mogi and Mohr model predicted 0.50181psi/ft. and 0.4927psi/ft. respectively which are almost close to the fracture pressure obtained from

LOT. The optimum mud weight for drilling of this well can be gotten by obtaining the average values of the predicted lower and upper mud weight limits considering the narrow mud weight window nature of this well.

Table 4.8 Results of the actual and model predicted mud weight for Well Q-01

Hole Inclination (Deg.)	Coupled Mogi Model (LL) (psi/ft.)	Actual Mudweight (psi/ft.)	Mohr Model (LL) (psi/ft.)	Fracture Gradient (psi/ft.)	Coupled Mogi Model (UL) (psi/ft.)	Mohr Model (UL) (psi/ft.)
3	0.4578	0.49244	0.45992	0.5293	0.50181	0.4927

The variations in field data and methods employed for determining the safe mud weight window for Wells considered in this study had produced variation in the results. However, the results obtained in this project are still within the range of mud weight. As Mohr-Coulomb failure criterion is independent of the intermediate principal stress, it presents the narrowest allowable pressure window.

CHAPTER FIVE

CONCLUSIONS AND RECOMMENDATIONS

5.1 CONCLUSIONS

The objective of this research has been achieved which was to develop a suitable criteria for selecting sufficient mud weights for drilling operations in the Niger Delta Region. From this extensive study the following conclusions were made:

- a. In this research, no core samples or data was available to be used in the study. However, the study was conducted satisfactorily utilizing well log data, drilling reports, geo-mechanical and geological data to create a wellbore stability model applicable in the study area. Frequent updating of the geo-mechanical model will aid drilling engineers to navigate safely between the collapse stress gradient and fracture gradient to avoid shear and tensile failure initiation.
- b. The coupled Mogi-Coulomb criterion developed for this work predicts the safe mud weight window in an iterative manner and describes the rock failure more accurately than does the traditional Mohr-Coulomb criterion which is independent of the intermediate principal stress, and presents a very slim mud weight window. For rock analysis applications therefore, it would be advantageous to employ this rock criterion.
- c. It was determined through the problem diagnosis that shale formation in the studied wells is a problematic zone with high frequency of wellbore breakout.
- d. It was found that the well trajectory, drilling fluid density, sand type, stress regime, stress magnitude and orientation have significant impact on the wellbore stability in the study area.

- e. The two dominant stress regime around the 5wells studied are normal faulting and strike slip faulting. This can vary on other Niger Delta wells/formation depending on the highest of the three principal or in situ stresses.
- f. The mud is designed inside a safe range called the mud weight window. For deviated well drilling, as the wellbore deviates, the stability envelope will narrow dramatically which will increase the possibility of wellbore instability if the mud is not designed properly. Thus the need for the suitable failure criteria developed in this work.
- g. Rock and sand formation varies, thus every well should be evaluated individually based on some criteria: the type of anticipated problems, their potential severity, the quantity and quality of data needed for a proper analysis, time and budget, and the success of previous analyses of particular type.

5.2 RECOMMENDATIONS

- a. Numerous problems in well drilling, production, work over, well intervention and injection can be addressed prior to commencement by engaging in detailed rock mechanics studies can. Geo-mechanics studies are recommended as a pre design management tool not just for well path and well bore stability analysis but production, injection, sand control, reservoir management and environmental issues such as carbon capture/geo-sequestration guaranteeing environmental safety.
- b. It is suggested that simulations can be applied using some real field data to distinguish the fact that how calculations may differ by taking into account the temperature difference between formation and drilling fluid. In addition, other factors which may induce stress around the wellbore such as chemical reactions should be considered.
- c. There is a need to further validate the results obtained from the model using other linear elastic constitutive model and the borehole failure criteria (Modified Lade, Drucker Prager Criterion etc.).

5.3 CONTRIBUTION TO KNOWLEDGE

A suitable failure model has been developed in this work to predict the safe mud weight window in an iterative manner. It has the advantage of predicting the lower and upper limit for the mud weight as much as the safe mud weight window in one single chart. Results of this study can help well trajectory optimization, proper mud weight determination, and reduce non-productive time (NPT) while drilling.

REFERENCES

- Aadnoy, B.S. and Looyeh, R. (2011). *Petroleum Rock Mechanics: Drilling Operations and Well Design*, first edition. Oxford: Gulf Professional Publishing.
- Al-Ajmi, A.M, and R.W. Zimmerman. (2005). Relation between the Mogi and the Coulomb Failure Criteria. *International Journal of Rock Mechanics & Mining Sciences*. Res. 42: 431–439.
- Al-Ajmi, A.M, R.W. Zimmerman. (2006). Stability Analysis of Deviated Boreholes Using the Mogi-Coulomb Failure Criterion, with Applications to some North Sea and Indonesian Reservoirs. SPE-104035. In proceeding of the IADC/SPE Asia Pacific Drilling Technology Conference and Exhibition, Bangkok, Thailand, November 13-15, 2006.
- Azar, J. J. and Robello Samuel, G., (2007). *Drilling Engineering*. Penn Well Corporation, Tulsa, Oklahoma.
- Barker. J.W. and Gomez. R.K, (1989). Formation of Hydrates during Deepwater Drilling Operations. *JPT* 297-302; *Trans., AIME*. 287.
- Barker, C., (1990). Calculated Volume and Pressure Changes during the Thermal Cracking of Oil to Gas in Reservoirs: *AAPG Bull.*, 74, 1254-1261.
- Brace, W.F. (1960). An Extension of the Griffith Theory of Fracture to Rocks. *J. Geophysical Research*. Res. 65:3477-3480.

- Berg, R. R., and Gangi, A.F., (1999). Primary migration by Oil-Generation Microfracturing in Low-Permeability Source Rocks: Application to the Austin chalk, Texas: AAPG Bull., **83**, no. 5, 727–756.
- Benz, T., R. Schwab. (2008). A Quantitative Comparison of Six Rock Failure Criteria. International Journal of Rock Mechanics & Mining Sciences. Res. 45: 1176–1186.
- Caenn, R., Darley, H. C. H. and Gray, G. R., (2011). Composition and Properties of Drilling and Completion Fluids. 6th ed. Elsevier, Waltham, USA.
- Chen, G., Chenevert, M.E., Sharma, M.M. et al. (2001). The Poroelastic, Chemical, and Thermal Effect on Wellbore Stability in Shales. Presented at the 38th US Rock Mechanics Symposium in Washington D.C., 7-10 July. ARMA-01-0011.
- Colmenares, L.B., M.D. Zoback. (2002). A Statistical Evaluation of Intact Rock Failure Criteria Constrained by Polyaxial Test Data for Five Different Rocks. International Journal of Rock Mechanics & Mining Sciences. Res. 39: 695–729.
- Devereux, S., (1999). Drilling Technology: In Nontechnical Language, Penn Well Books.
- Darley, H. C. H. and Gray, G. R., (1988). Composition and Properties of Drilling and Completion Fluids. 5th ed. Gulf Publishing Company, Houston, Texas.
- Drucker, D.C, W. Prager, (1952). Soil Mechanics and Plastic Analysis of Limit Design. Journal of Quarterly of Applied Mathematics. Res. 10: 157–165.
- Dutta, N. C., (1983). Shale Compaction and Abnormal Pore Pressures: A model of Geopressures in the Gulf of Mexico Basin, 53rd Ann, SEG Meeting.
- Economides, M. J., Watters, L. T. and Dunn-Norman, S., (1998). Petroleum Well Construction. John Ziley & Sons, Ltd, Chichester, England.

- Ewy, R.T. (1999). Wellbore-Stability Predictions by Use of a Modified Lade Criterion. *Journal of SPE Drilling & Completion*. SPE-56862. Res. 14: 85–91.
- Fink, J., (2011). *Petroleum Engineer's Guide to Oil Field Chemicals and Fluids*, Access Online Via Elsevier.
- Fjaer, E., R.M. Holt, P. Horsrud, A.M. Raaen, R. Risnes. (2008). *Petroleum Related Rock Mechanics*, 2nd ed. Elsevier.
- Griffith, A.A. (1921). The Phenomena of Rupture and Flow in Solids. *Journal of Philosophical Transactions of the Royal Society of London*. Res. 221: 163–198.
- Hoek, E., E.T. Brown (1980). Empirical Strength Criterion for Rock Masses. *Journal of Geotechnical Engineering Div.* Res. 106: 1013–1035
- Hawker, D., (2001). *Drilling Fluid Hydraulics*
- Higgins, S.M. (2000). *Geomechanical Modeling as a Reservoir Characterization tool at Rulison Field, Piceance Basin, Colorado*, M.S. Dissertation, Colorado School of Mine, Golden,
- Hubbert, M.K. and Willis, D.G., (1957). Mechanics of Hydraulic Fracturing. *AIME Petroleum Transactions*, **210**, 153-168.
- Joshi, S.D. (2003, may 19-24). Cost/benefits of horizontal wells, SPE Western Regional/AAPG Pacific Section Joint Meeting, pp. 1.
- Jaeger, J.C., N.G.W. Cook, R.W. Zimmerman. (2007). *Fundamentals of Rock Mechanics*, 4rd ed. Blackwell Publishing.
- Kelly, J. (1968). Drilling Problem Shales. *Oil & Gas Journal*, 67-70.

- Kadyrov, T. (2012). Integrated Wellbore Stability Analysis for Well Trajectory Optimization and Field Development: The West Kazakhstan Field. MS thesis, Colorado School of Mines, Golden, Colorado.
- Leuterman, A.J. et al. (1989). New Drilling Fluid Additive Toxicity Data Developed. *Offshore* 31-37.
- Lade, P.V. (1977). Elasto-Plastic Stress-Strain Theory for Cohesionless Soil with Curved Yield Surfaces. *Journal Solid Structures*. Res. 13: 1019–1035.
- Law, B. E., Ulmishek, G. F., and Slavin, V. I. (eds.), 1998, Abnormal pressures in hydrocarbon environments: AAPG Memoir **70**.
- Lorenz, H.: (1980, May 12). Field Experience Pins Down Uses for Air Drilling Fluids," *Oil & Gas Journal* 132-39.
- Luo, X., and Vasseur, G., (1996). Geopressuring Mechanism of Organic Matter Cracking: Numerical Modeling, *AAPG Bull.*, **80**, 856-874.
- Mogi, K. (1971). Fracture and Flow under High Triaxial Compression. *Journal of Geophysical Research*. Res. 76: 1255–1269.
- McLean, M.R., M.A. Addis. (1990). Wellbore Stability Analysis: A Review of Current Methods of Analysis and their Field Application. IADC/SPE 19941. Proceeding of the IADC/SPE Drilling Conference, Houston, Texas, and February 27- March 2.
- Max R. Annis, M.V.S., (1996). *Drilling Fluid Technology Exxon Manual*.
- Mitchell, R. F. and Miska, S. Z., (2011). *Fundamentals of Drilling Engineering*. SPE Textbook Series, Vol. 12. Society of Petroleum Engineers, Richardson, Texas.

- McClintock, F.A., J.B. Walsh. (1962). Friction on Griffith Cracks Under Pressure. Proceeding of the 4th U.S. National Congress of Applied Mechanics. P 1015–1021, Berkeley, California.
- Murrell, S.A.F. (1963). A Criterion for Brittle Fracture of Rocks and Concrete under Triaxial Stress and the Effect of Pore Pressure on the Criterion.
- Fairhurst, C. (Ed.), (1962). Rock Mechanics. Proceeding of 5th Symposium on Rock Mechanics, the University of Minnesota, Minneapolis Pergamon Press, New York, pp. 563–577.
- Mann, D. M., and Mackenzie, A. S., (1990). Prediction of Pore Fluid Pressures in Sedimentary Basins: Marine And Petroleum Geology, **7**, 55-65.
- Mese, A.I. and Tutuncu, A.N. (2011). Impact of Fluids and Formation Anisotropy on Acoustic, Deformation and Failure Characteristics of Reservoir Shales and Pure Clay Minerals. Presented at the International Society of Rock Mechanics Congress, Beijing, China, and 16-21 October. ISRM-12CONGRESS-2011-242.
- Nawrocki, P.A (2010, Oct 23 - 27). Critical Wellbore Pressures Using Different Rock Failure Criteria. ARMA/USRMS 05-794. Proceeding of ISRM International Symposium and 6th Asian Rock Mechanics Symposium, New Delhi, India.
- Nas, S., (2011, April 5 – 6). Kick Detection and Well Control in a Closed Wellbore, IADC/SPE Managed Pressure Drilling and Underbalance Operations Conference and Exhibition, pp. 3.
- Pasic, B., Gaurina-Medimurec, N., and Matanovic, D. (2007). Wellbore Instability: Causes and Consequences. Rudarsko-geološko-naftni zbornik **19**: 87-98.

- Potash, M.S. & Nygren, R.T., (1993). Multiple integrated document assembly data processing system.
- Rasouli, V., Zacharia, J., and Elike (2010). Optimum Well Trajectory Design in a Planned Well in Blacktip Field, Australia, APPEA Journal, Pg 535-548.
- Robertson, R. E. and Stiff, H. A., (1976). An Improved Mathematical Model for Relating Shear Stress to Shear Rate in Drilling Fluid and Cement Slurries. Society of Petroleum Engineers Journal, 16:1, pg. 31-36.
- Stassi D'Alia, F. (1967). Flow and Fracture of Materials According to a New Limiting Condition of Yielding. J. Mechanica. Res. 2: 178–195.
- Skalle, P., (2010). Drilling Fluid Engineering, Bookboon
- Skjeggstad, O., (1989). Boreslam Teknologi. Alma Mater Forlag AS, Bergen.
- Smith, J. E., (1971). The Dynamics of Shale Compaction and Evolution of Pore-Fluid Pressure, Math. Geol., **3**, 239-263.
- Seeberger, M.H., Matlock, R.W., and Hanson, P.M (1989, Feb. 28-March 3). Oil Muds in Large Diameter, Highly Deviated Wells: Solving the Cuttings Removal Problem. Paper SPE 18635 presented at the 1989 SPE/IADC Drilling Conference, New Orleans.
- Tutuncu, A.N. (2014). Advanced Well Integrity: Course Notes. Colorado School of Mines, Golden, Colorado.
- Tutuncu, A.N. (2015). Advanced Well Integrity: Course Notes. Colorado School of Mines, Golden, Colorado.
- Van Dyke, K. & Baker, R., (1998). Drilling Fluids, Mud Pumps, and Conditioning Equipment, University of Texas at Austin Petroleum.

- Vieira, M. G. and Peres, A. E. C., (2012). Effect of Reagents on the Rheological Behavior of an Iron Ore Concentrate Slurry. *International Journal of Mining Engineering and Mineral Processing*, 1(2): p. 38-42.
- Versan, M. and Tolga, A, (2005). Effect of Polymers on the Rheological Properties of KCl/Polymer Type Drilling Fluids. *Energy Sources*, 27:5, p. 405-415.
- Veeken, C.A.M., J.V. Walters, C.J. Kenter, D.R. Davies (1989, Aug. 30 – Sep. 2). Use of Plasticity Models for Predicting Borehole Stability. ISRM-IS-1989-106. Proceeding of the ISRM International Symposium, Pau, France.
- Westennark, R.V. (1986, Feb. 10 - 12). Drilling With a Parasite Aerating String in the Disturbed Belt. Gallatin County, Montana. SPE 14734 presented at the 1986 IADC, ISPE Drilling Conference in Dallas.
- Wiebols, G.A., N.G.W. Cook. (1968). An Energy Criterion for the Strength of Rock in Polyaxial Compression. *International Journal of Rock Mechanics & Mining Sciences*. Res. 5: 529–549.
- Yi, X., S.H. Ong, and J.E. Russel (2005, June 25 -29). Improving Borehole Stability Analysis by Quantifying the Effects of Intermediate Principal Stress using Polyaxial Rock Strength Test Data. ARMA/USRMS 05-794. Proceeding of the 40th U.S. Symposium on Rock Mechanics (USRMS), Anchorage, Alaska.
- Zamora, M. and Power, D., (2002.) Making a Case for AADE Hydraulics and the Unified Rheological Model. AADE Technology Conference “Drilling & Completion Fluids and Waste Management”, Houston, Texas.

Zhang, L., P. Cao, K.C. Radha. (2010). Evaluation of rock strength criteria for wellbore stability analysis. *International Journal of Rock Mechanics & Mining Sciences*. Res. 47: 1304–1316.

Zoback, M.D. (2007). *Reservoir Geomechanics*, Cambridge University Press.

Zhou, S. (1994). A Program to Model the Initial Shape and Extent of Borehole Breakout. *Journal of Computers and Geosciences*. Res. 20: 1143–1160.

NOMENCLATURE

A = area, m²

a = coefficient, unitless

a = radius of the wellbore, inches

a_{w,df} = chemical activity of the fresh water, unitless

a_{w,sh} = chemical activity of shale or formation pore water, unitless

b = coefficient, unitless

b = Coulomb strength parameter, MPa (psi)

c = coefficient, unitless

C = formation cohesion, MPa (psi)

E = Young's modulus, GPa (Mpsi)

F = force, N (kg.m/s²)

F_n = normal force, N (kg.m/s²)

F_s = parallel force, N (kg.m/s²)

E_d = dynamic Young's modulus, GPa (Mpsi)

E_s = static Young's modulus, GPa, (Mpsi)

r = outer radius, inches

g = gravitational acceleration, m/s²

GR = gamma ray, gAPI

G = shear modulus, GPa (Mpsi)

I_m = reactivity coefficient, unitless

K = bulk modulus, GPa, (Mpsi)

K_d = dynamic bulk modulus, GPa (Mpsi)

M = compressional modulus, GPa (Mpsi)

MTV = minimum transport velocity, ft/sec

P_p = pore pressure, MPa (psi)

P_{wb1} = critical wellbore breakout pressure, MPa (psi)

P_{wf1} = critical wellbore breakdown pressure, MPa (psi)

Q_{crit} = critical mud flow rate, gpm

R = the universal gas constant, (J/K.mole)

S = stress tensor, MPa (psi)

S_{Hmax} = maximum horizontal stress, MPa (psi)

S_{Hmin} = minimum horizontal stress, MPa (psi)

S_v = overburden stress, MPa (psi)

T = circulation temperature, °K

T_o = absolute temperature, °K

T_s = tensile strength, MPa (psi)

UCS = uniaxial compressive strength, MPa (psi)

V_p = compressional-wave velocity, m/sec (ft/sec)

V_s = shear-wave velocity, m/sec (ft/sec)

z = depth, m (ft)

z_w = water depth, m (ft)

α = Biot's coefficient, unitless

β = compaction strain-hardening coefficient, unitless

γ = wellbore inclination from the vertical, degrees

ΔP = difference between wellbore pressure and pore pressure, MPa (psi)

Δt_{co} = compressional-wave slowness, $\mu\text{sec}/\text{ft}$ ($\mu\text{sec}/\text{m}$)

Δt_s = shear-wave slowness, $\mu\text{sec}/\text{ft}$ ($\mu\text{sec}/\text{m}$)

$\Delta \Pi$ = osmotic pressure, MPa (psi)

ρ = bulk density, g/cm^3 (kg/m^3)

ρ_w = water density, g/cm^3 (kg/m^3)

σ = stress, MPa (psi)

σ_1 = maximum principle stress, MPa (psi)

σ_2 = intermediate principle stress, MPa (psi)

σ_3 = minimum principle stress, MPa (psi)

σ_{eff} = effective stress, MPa (psi)

$\sigma_{m,2}$ = effective mean stress, MPa (psi)

σ_{max} = effective stress required to reduce the mineral porosity to zero, MPa (psig)

σ_n = normal stress, MPa (psi)

σ_r = radial stress at the wellbore, MPa (psi)

σ_{rr} = radial effective principle stress at the wellbore, MPa (psi)

σ_r' = radial stress alteration due to the introduction of osmotic pressure, MPa (psi)

σ_r'' = radial stress alteration due to the flow-induced stress effect, MPa (psi)

σ_T = thermal stress, MPa (psi)

σ_{tmax} = maximum effective principle stress at the wellbore, MPa (psi)

σ_{tmin} = minimum effective principle stress at the wellbore, MPa (psi)

σ_x = stress in x-axis in Cartesian coordinate system, MPa (psi)

σ_y = stress in y-axis in Cartesian coordinate system, MPa (psi)

σ_z = axial stress at the wellbore, MPa (psi)

σ_{zz} = stress in z-axis in Cartesian coordinate system, MPa (psi)

σ_z' = axial stress alteration due to the introduction of osmotic pressure, MPa (psi)

σ_z'' = axial stress alteration due to the flow-induced stress effect, MPa (psi)

$\sigma_{\theta\theta}$ = hoop stress at the wellbore, MPa (psi)

$\sigma_{\theta\theta}'$ = hoop stress alteration due to the introduction of osmotic pressure, MPa (psi)

$\sigma_{\theta\theta}''$ = hoop stress alteration due to the flow-induced stress effect, MPa (psi)

τ = shear stress, MPa (psi)

τ_{max} = maximum shear stress, MPa (psi)

τ_{oct} = octahedral shear stress, MPa (psi)

τ_{xy} = shear stress in x-y plane, MPa (psi)

τ_{xz} = shear stress in x-z plane, MPa (psi)

τ_{yz} = shear stress in y-z plane, MPa (psi)

τ_{rz} = shear stress in r-z plane, MPa (psi)

$\tau_{r\theta}$ = shear stress in r- plane, MPa (psi)

$\tau_{\theta z}$ = shear stress in θ -z plane, MPa (psi)

ν = Poisson's ratio, unitless

Φ = internal friction angle, degrees

φ = wellbore azimuth from the direction of , degrees

\emptyset = formation porosity, fraction

APPENDIX 1

Parameter	Well T-101 (Deviated)	Well A-33 (Deviated)	Well D-705 (Deviated)	Well Z-47 (Vertical)	Well Q-01 (Vertical)
Depth of Consideration (ft)	12750	9660	10940	8820	6560
Formation/Sand Type	Shale/Sstone	Shale/Sanstone	Shale/Sstone	Sandstone	Shale
Hole Inclination (Deg)	50	35	25	0.9	3
Wellbore Azimuth(Deg)	80	98	305	17	26
Poisson Ration (v)	0.28	0.26	0.2506	0.314	0.33
Shear Modulus(G)psi	702525	80910	50750	253750	435000
Bulk Modulus(Kb)psi	1297315	21520.9	333500	288550	1370975
Matrix/Grain Modulus(Km) psi	101500	3429.25	210250	14210	35235
Young Modulus(E) psi	1785240	7999215	4112000	2760030	2703380
Bulk Compressibility (Cb) psi	0.00076995	0.42195	0.09802	0.0078735	0.03741
Rock Compressibility (Cr) psi	0.087	-0.0018995	0.0111128	0.00794354	0.00007337

Biot					
Constant (α)	0.9	0.87	0.791	0.912	1
Uniaxial Compressive Strength(UCS)psi	7698.05	5611.5	4655.95	4502.25	3617.75
Cohesion (Co) psi/ft	0.251	0.105	0.1134	0.1008	0.1266
Tensile Strength psi	640.9	735.15	564.05	572.75	613.35
Shear Strength (τ)psi	5.7855E+16	2.581E-11	4.988E-09	2.8826E-07	1247
VerticalStress (σv)psi/ft	0.823	0.712	0.83	0.831	0.8421
Minimum Horizontal Stress(σh)psi/ft	0.671	0.633	0.591	0.568	0.514
Maximum Horizontal Stress(σH)psi/ft	0.778	0.827	0.708	0.929	0.722
Fracture Gradient psi/ft	0.659	0.652	0.623	0.584	0.5293
Mud Weight(Pc) ppg	10.34	9.49	9.33	8.97	9.47
Pore Pressure Gradient psi/ft	0.531	0.484	0.477	0.458	0.437
Pore Pressure psi	6770.25	4675.44	5218.38	4039.56	2866.72

Friction					
Angle(Deg)	27	24.5	19	25	19
Shale					
Content (%)	0.2991	0.3222	0.3519	0.2822	0.3782
Mud Weight					
Gradient Psi/ft	0.53768	0.49348	0.48516	0.46644	0.49244
Radial Stress	0.53768	0.49348	0.48516	0.46644	0.49244
Tangential Stress	0.69732	0.57852	0.57984	0.30856	0.32756
Axial Stress	0.76308	0.61112	0.7713596	0.604292	0.70482
A	-0.069133209	0.079830467	0.105706905	0.09419911	0.118011412
B	0.226321648	-0.058541409	0.016024054	-0.0125781	0.017889287
Mean Stress	0.7245	0.73	0.6495	0.7485	0.618
Octahedral Stress	0.09464229	0.049591365	0.119049136	0.12082434	0.154422144
Mogi Failure					
Criterion	0.000194535	-0.012496126	0.002934608	-0.0360399	-0.02535515

	WELL T-101				
Angle 0 to 360 Deg	F -Criterion T-101	Tangential Stress	Axial Stress	Octo Stress	Mw
10	0.000194535	0.69732	0.76308	0.09464229	0.53768
10	-0.033859791	0.821390439	0.798547723	0.12869662	0.54028
10	-0.033175681	0.818790439	0.798547723	0.12801251	0.54288

10	-0.032499692	0.816190439	0.798547723	0.12733652	0.54548
10	-0.031831956	0.813590439	0.798547723	0.12666878	0.54808
10	-0.031172604	0.810990439	0.798547723	0.12600943	0.55068
10	-0.030521767	0.808390439	0.798547723	0.12535859	0.55328
10	-0.029879579	0.805790439	0.798547723	0.1247164	0.55588
10	-0.029246174	0.803190439	0.798547723	0.124083	0.55848
10	-0.028621688	0.800590439	0.798547723	0.12345851	0.56108
10	-0.028006256	0.797990439	0.798547723	0.12284308	0.56368
10	-0.027400016	0.795390439	0.798547723	0.12223684	0.56628
10	-0.026803104	0.792790439	0.798547723	0.12163993	0.56888
10	-0.026215659	0.790190439	0.798547723	0.12105248	0.57148
10	-0.025637819	0.787590439	0.798547723	0.12047464	0.57408
10	-0.025069723	0.784990439	0.798547723	0.11990655	0.57668
10	-0.02451151	0.782390439	0.798547723	0.11934833	0.57928
10	-0.023963319	0.779790439	0.798547723	0.11880014	0.58188
10	-0.023425291	0.777190439	0.798547723	0.11826212	0.58448
10	-0.022897563	0.774590439	0.798547723	0.11773439	0.58708
10	-0.022380276	0.771990439	0.798547723	0.1172171	0.58968
10	-0.021873568	0.769390439	0.798547723	0.11671039	0.59228
10	-0.021377578	0.766790439	0.798547723	0.1162144	0.59488
10	-0.020892442	0.764190439	0.798547723	0.11572927	0.59748
10	-0.0204183	0.761590439	0.798547723	0.11525512	0.60008
10	-0.019955285	0.758990439	0.798547723	0.11479211	0.60268
10	-0.019503535	0.756390439	0.798547723	0.11434036	0.60528
10	-0.019063182	0.753790439	0.798547723	0.11390001	0.60788
10	-0.01863436	0.751190439	0.798547723	0.11347119	0.61048

10	-0.018217199	0.748590439	0.798547723	0.11305402	0.61308
10	-0.01781183	0.745990439	0.798547723	0.11264866	0.61568
10	-0.01741838	0.743390439	0.798547723	0.1122552	0.61828
10	-0.017036974	0.740790439	0.798547723	0.1118738	0.62088
10	-0.016667737	0.738190439	0.798547723	0.11150456	0.62348
10	-0.016310789	0.735590439	0.798547723	0.11114761	0.62608
10	-0.01596625	0.732990439	0.798547723	0.11080308	0.62868
10	-0.015634235	0.730390439	0.798547723	0.11047106	0.63128
10	-0.015314859	0.727790439	0.798547723	0.11015168	0.63388
10	-0.01500823	0.725190439	0.798547723	0.10984505	0.63648
10	-0.014714456	0.722590439	0.798547723	0.10955128	0.63908
10	-0.01443364	0.719990439	0.798547723	0.10927047	0.64168
10	-0.014165884	0.717390439	0.798547723	0.10900271	0.64428
10	-0.013911283	0.714790439	0.798547723	0.10874811	0.64688
10	-0.01366993	0.712190439	0.798547723	0.10850675	0.64948
10	-0.013441913	0.709590439	0.798547723	0.10827874	0.65208
10	-0.013227317	0.706990439	0.798547723	0.10806414	0.65468
10	-0.013026222	0.704390439	0.798547723	0.10786305	0.65728
10	-0.012838704	0.701790439	0.798547723	0.10767553	0.65988
10	-0.012664834	0.699190439	0.798547723	0.10750166	0.66248
10	-0.012504678	0.696590439	0.798547723	0.1073415	0.66508
10	-0.012358297	0.693990439	0.798547723	0.10719512	0.66768
10	-0.012225748	0.691390439	0.798547723	0.10706257	0.67028
10	-0.012107083	0.688790439	0.798547723	0.10694391	0.67288
10	-0.012002347	0.686190439	0.798547723	0.10683917	0.67548
10	-0.011911582	0.683590439	0.798547723	0.10674841	0.67808

10	-0.011834823	0.680990439	0.798547723	0.10667165	0.68068
10	-0.011772101	0.678390439	0.798547723	0.10660893	0.68328
10	-0.011723441	0.675790439	0.798547723	0.10656027	0.68588
10	-0.011688861	0.673190439	0.798547723	0.10652569	0.68848
10	-0.011668375	0.670590439	0.798547723	0.1065052	0.69108
10	-0.011661992	0.667990439	0.798547723	0.10649882	0.69368
10	-0.011669715	0.665390439	0.798547723	0.10650654	0.69628
10	-0.011691539	0.662790439	0.798547723	0.10652836	0.69888
10	-0.011727456	0.660190439	0.798547723	0.10656428	0.70148
10	-0.011777453	0.657590439	0.798547723	0.10661428	0.70408
10	-0.011841508	0.654990439	0.798547723	0.10667833	0.70668
10	-0.011919598	0.652390439	0.798547723	0.10675642	0.70928
10	-0.012011691	0.649790439	0.798547723	0.10684852	0.71188
10	-0.012117751	0.647190439	0.798547723	0.10695458	0.71448
10	-0.012237737	0.644590439	0.798547723	0.10707456	0.71708
10	-0.012371601	0.641990439	0.798547723	0.10720843	0.71968
10	-0.012519292	0.639390439	0.798547723	0.10735612	0.72228
10	-0.012680753	0.636790439	0.798547723	0.10751758	0.72488

		WELL A-33		

F -Criterion A-33	Tangential Stress	Axial Stress	Octo Stress	Mw
-0.012496126	0.57852	0.61112	0.049591365	0.49348
-0.089610582	0.805584	0.670832682	0.126705821	0.49608
-0.087493677	0.802984	0.670832682	0.124588916	0.49868
-0.085376979	0.800384	0.670832682	0.122472217	0.50128
-0.083260498	0.797784	0.670832682	0.120355737	0.50388
-0.081144248	0.795184	0.670832682	0.118239487	0.50648
-0.07902824	0.792584	0.670832682	0.116123479	0.50908
-0.076912488	0.789984	0.670832682	0.114007727	0.51168
-0.074797007	0.787384	0.670832682	0.111892246	0.51428
-0.072681811	0.784784	0.670832682	0.109777705	0.51688
-0.070566919	0.782184	0.670832682	0.107662158	0.51948
-0.068452348	0.779584	0.670832682	0.105547586	0.52208
-0.066338117	0.776984	0.670832682	0.103433356	0.52468
-0.064224249	0.774384	0.670832682	0.101319488	0.52728
-0.062110766	0.771784	0.670832682	0.099206005	0.52988
-0.059997693	0.769184	0.670832682	0.097092932	0.53248
-0.057885059	0.766584	0.670832682	0.094980298	0.53508
-0.055772892	0.763984	0.670832682	0.092868131	0.53768
-0.053661226	0.761384	0.670832682	0.090756464	0.54028
-0.051550096	0.758784	0.670832682	0.088645334	0.54288
-0.049439541	0.756184	0.670832682	0.08653478	0.54548
-0.047329605	0.753584	0.670832682	0.084424844	0.54808
-0.045220335	0.750984	0.670832682	0.082315574	0.55068
-0.043111784	0.748384	0.670832682	0.080207022	0.55328

-0.04100401	0.745784	0.670832682	0.078099248	0.55588
-0.038897077	0.743184	0.670832682	0.075992316	0.55848
-0.036791058	0.740584	0.670832682	0.073886297	0.56108
-0.034686033	0.737984	0.670832682	0.071781271	0.56368
-0.032582092	0.735384	0.670832682	0.069677331	0.56628
-0.030479336	0.732784	0.670832682	0.067574575	0.56888
-0.02837788	0.730184	0.670832682	0.065473119	0.57148
-0.026277853	0.727584	0.670832682	0.063373092	0.57408
-0.024179402	0.724984	0.670832682	0.06127464	0.57668
-0.022082694	0.722384	0.670832682	0.059177932	0.57928
-0.019987921	0.719784	0.670832682	0.05708316	0.58188
-0.017895305	0.717184	0.670832682	0.054990544	0.58448
-0.015805102	0.714584	0.670832682	0.052900341	0.58708
-0.013717609	0.711984	0.670832682	0.050812848	0.58968
-0.011633175	0.709384	0.670832682	0.048728414	0.59228
-0.009552209	0.706784	0.670832682	0.046647448	0.59488
-0.007475198	0.704184	0.670832682	0.044570437	0.59748
-0.005402722	0.701584	0.670832682	0.042497961	0.60008
-0.003335477	0.698984	0.670832682	0.040430716	0.60268
-0.00127431	0.696384	0.670832682	0.038369548	0.60528
0.000779746	0.693784	0.670832682	0.036315493	0.60788
0.00282541	0.691184	0.670832682	0.034269828	0.61048
0.004861086	0.688584	0.670832682	0.032234153	0.61308
0.006884754	0.685984	0.670832682	0.030210485	0.61568
0.008893829	0.683384	0.670832682	0.02820141	0.61828
0.010884955	0.680784	0.670832682	0.026210284	0.62088

0.012853709	0.678184	0.670832682	0.02424153	0.62348
0.014794165	0.675584	0.670832682	0.022301074	0.62608
0.016698245	0.672984	0.670832682	0.020396993	0.62868
0.018554739	0.670384	0.670832682	0.0185405	0.63128
0.020347814	0.667784	0.670832682	0.016747425	0.63388
0.02205477	0.665184	0.670832682	0.015040469	0.63648
0.023642786	0.662584	0.670832682	0.013452453	0.63908
0.025064669	0.659984	0.670832682	0.01203057	0.64168
0.026254848	0.657384	0.670832682	0.010840391	0.64428
0.027129956	0.654784	0.670832682	0.009965283	0.64688
0.027602453	0.652184	0.670832682	0.009492786	0.64948
0.027611967	0.649584	0.670832682	0.009483272	0.65208
0.027157169	0.646984	0.670832682	0.00993807	0.65468
0.026296565	0.644384	0.670832682	0.010798674	0.65728
0.025117309	0.641784	0.670832682	0.01197793	0.65988
0.023703316	0.639184	0.670832682	0.013391923	0.66248
0.022120937	0.636584	0.670832682	0.014974302	0.66508
0.020418033	0.633984	0.670832682	0.016677205	0.66768
0.018627917	0.631384	0.670832682	0.018467322	0.67028
0.016773622	0.628784	0.670832682	0.020321616	0.67288
0.014871208	0.626184	0.670832682	0.022224031	0.67548
0.012932037	0.623584	0.670832682	0.024163202	0.67808
0.01096429	0.620984	0.670832682	0.026130948	0.68068

	WELL D-705		
--	-------------------	--	--

F -Criterion D-705	Tangential Stress	Axial Stress	Octo Stress	Mw
-0.002950523	0.5799	0.7713596	0.119065051	0.4851
-0.017858972	0.715808798	0.806069905	0.1339735	0.4877
-0.016392139	0.713208798	0.806069905	0.132506666	0.4903
-0.014943277	0.710608798	0.806069905	0.131057804	0.4929
-0.013512988	0.708008798	0.806069905	0.129627516	0.4955
-0.012101895	0.705408798	0.806069905	0.128216422	0.4981
-0.010710637	0.702808798	0.806069905	0.126825164	0.5007
-0.009339875	0.700208798	0.806069905	0.125454402	0.5033
-0.007990288	0.697608798	0.806069905	0.124104815	0.5059
-0.006662574	0.695008798	0.806069905	0.122777101	0.5085
-0.00535745	0.692408798	0.806069905	0.121471978	0.5111
-0.004075653	0.689808798	0.806069905	0.12019018	0.5137
-0.002817936	0.687208798	0.806069905	0.118932463	0.5163
-0.001585071	0.684608798	0.806069905	0.117699599	0.5189
-0.000377848	0.682008798	0.806069905	0.116492376	0.5215
0.000802928	0.679408798	0.806069905	0.1153116	0.5241
0.001956436	0.676808798	0.806069905	0.114158091	0.5267
0.003081842	0.674208798	0.806069905	0.113032685	0.5293
0.004178299	0.671608798	0.806069905	0.111936229	0.5319
0.005244946	0.669008798	0.806069905	0.110869581	0.5345
0.006280916	0.666408798	0.806069905	0.109833611	0.5371
0.007285333	0.663808798	0.806069905	0.108829195	0.5397
0.008257315	0.661208798	0.806069905	0.107857213	0.5423
0.009195977	0.658608798	0.806069905	0.10691855	0.5449

0.010100435	0.656008798	0.806069905	0.106014093	0.5475
0.010969805	0.653408798	0.806069905	0.105144722	0.5501
0.011803211	0.650808798	0.806069905	0.104311316	0.5527
0.012599784	0.648208798	0.806069905	0.103514743	0.5553
0.013358667	0.645608798	0.806069905	0.10275586	0.5579
0.014079019	0.643008798	0.806069905	0.102035508	0.5605
0.014760019	0.640408798	0.806069905	0.101354508	0.5631
0.015400869	0.637808798	0.806069905	0.100713659	0.5657
0.016000796	0.635208798	0.806069905	0.100113731	0.5683
0.016559063	0.632608798	0.806069905	0.099555465	0.5709
0.017074963	0.630008798	0.806069905	0.099039565	0.5735
0.017547832	0.627408798	0.806069905	0.098566695	0.5761
0.017977048	0.624808798	0.806069905	0.098137479	0.5787
0.018362036	0.622208798	0.806069905	0.097752492	0.5813
0.018702271	0.619608798	0.806069905	0.097412256	0.5839
0.018997283	0.617008798	0.806069905	0.097117244	0.5865
0.01924666	0.614408798	0.806069905	0.096867868	0.5891
0.019450046	0.611808798	0.806069905	0.096664481	0.5917
0.019607153	0.609208798	0.806069905	0.096507375	0.5943
0.019717753	0.606608798	0.806069905	0.096396774	0.5969
0.019781687	0.604008798	0.806069905	0.096332841	0.5995
0.019798861	0.601408798	0.806069905	0.096315667	0.6021
0.019769251	0.598808798	0.806069905	0.096345277	0.6047
0.019692899	0.596208798	0.806069905	0.096421629	0.6073
0.019569917	0.593608798	0.806069905	0.096544611	0.6099
0.019400482	0.591008798	0.806069905	0.096714046	0.6125

0.019184838	0.588408798	0.806069905	0.096929689	0.6151
0.018923293	0.585808798	0.806069905	0.097191235	0.6177
0.018616215	0.583208798	0.806069905	0.097498312	0.6203
0.018264035	0.580608798	0.806069905	0.097850493	0.6229
0.017867236	0.578008798	0.806069905	0.098247292	0.6255
0.017426356	0.575408798	0.806069905	0.098688171	0.6281
0.016941985	0.572808798	0.806069905	0.099172543	0.6307
0.016414755	0.570208798	0.806069905	0.099699772	0.6333
0.015845343	0.567608798	0.806069905	0.100269185	0.6359
0.015234463	0.565008798	0.806069905	0.100880065	0.6385
0.014582863	0.562408798	0.806069905	0.101531664	0.6411
0.013891323	0.559808798	0.806069905	0.102223205	0.6437
0.013160646	0.557208798	0.806069905	0.102953881	0.6463
0.012391661	0.554608798	0.806069905	0.103722867	0.6489
0.011585212	0.552008798	0.806069905	0.104529316	0.6515
0.010742159	0.549408798	0.806069905	0.105372368	0.6541
0.009863375	0.546808798	0.806069905	0.106251152	0.6567
0.008949738	0.544208798	0.806069905	0.10716479	0.6593
0.008002131	0.541608798	0.806069905	0.108112396	0.6619
0.007021441	0.539008798	0.806069905	0.109093087	0.6645
0.00600855	0.536408798	0.806069905	0.110105978	0.6671
0.004964339	0.533808798	0.806069905	0.111150189	0.6697
0.003889682	0.531208798	0.806069905	0.112224845	0.6723

--	--	--	--	--

	WELL Z-47			
F -Criterion Z-47	Tangential Stress	Axial Stress	Octo Stress	Mw
-0.036039912	0.30856	0.604292	0.120824337	0.46644
-0.041034408	0.733324751	0.738484532	0.125818833	0.46904
-0.039218768	0.730724751	0.738484532	0.124003193	0.47164
-0.037413031	0.728124751	0.738484532	0.122197456	0.47424
-0.035617643	0.725524751	0.738484532	0.120402068	0.47684
-0.033833074	0.722924751	0.738484532	0.118617499	0.47944
-0.03205982	0.720324751	0.738484532	0.116844245	0.48204
-0.030298403	0.717724751	0.738484532	0.115082828	0.48464
-0.028549376	0.715124751	0.738484532	0.113333801	0.48724
-0.026813321	0.712524751	0.738484532	0.111597746	0.48984
-0.025090853	0.709924751	0.738484532	0.109875278	0.49244
-0.023382621	0.707324751	0.738484532	0.108167046	0.49504
-0.02168931	0.704724751	0.738484532	0.106473735	0.49764
-0.020011643	0.702124751	0.738484532	0.104796068	0.50024
-0.018350385	0.699524751	0.738484532	0.10313481	0.50284
-0.016706341	0.696924751	0.738484532	0.101490765	0.50544
-0.01508036	0.694324751	0.738484532	0.099864785	0.50804
-0.01347334	0.691724751	0.738484532	0.098257765	0.51064
-0.011886226	0.689124751	0.738484532	0.096670651	0.51324
-0.010320015	0.686524751	0.738484532	0.09510444	0.51584
-0.008775757	0.683924751	0.738484532	0.093560182	0.51844
-0.007254556	0.681324751	0.738484532	0.092038981	0.52104

-0.005757575	0.678724751	0.738484532	0.090542	0.52364
-0.004286035	0.676124751	0.738484532	0.08907046	0.52624
-0.002841218	0.673524751	0.738484532	0.087625643	0.52884
-0.001424467	0.670924751	0.738484532	0.086208892	0.53144
-3.71891E-05	0.668324751	0.738484532	0.084821614	0.53404
0.001319147	0.665724751	0.738484532	0.083465278	0.53664
0.002643008	0.663124751	0.738484532	0.082141417	0.53924
0.003932798	0.660524751	0.738484532	0.080851626	0.54184
0.005186863	0.657924751	0.738484532	0.079597562	0.54444
0.006403485	0.655324751	0.738484532	0.07838094	0.54704
0.007580897	0.652724751	0.738484532	0.077203528	0.54964
0.008717275	0.650124751	0.738484532	0.076067149	0.55224
0.009810756	0.647524751	0.738484532	0.074973669	0.55484
0.010859435	0.644924751	0.738484532	0.07392499	0.55744
0.01186138	0.642324751	0.738484532	0.072923045	0.56004
0.012814638	0.639724751	0.738484532	0.071969787	0.56264
0.01371725	0.637124751	0.738484532	0.071067175	0.56524
0.014567263	0.634524751	0.738484532	0.070217162	0.56784
0.015362745	0.631924751	0.738484532	0.069421679	0.57044
0.016101802	0.629324751	0.738484532	0.068682623	0.57304
0.016782593	0.626724751	0.738484532	0.068001832	0.57564
0.017403353	0.624124751	0.738484532	0.067381072	0.57824
0.017962408	0.621524751	0.738484532	0.066822017	0.58084
0.018458198	0.618924751	0.738484532	0.066326227	0.58344
0.018889295	0.616324751	0.738484532	0.06589513	0.58604
0.019254422	0.613724751	0.738484532	0.065530003	0.58864

0.019552472	0.611124751	0.738484532	0.065231953	0.59124
0.019782521	0.608524751	0.738484532	0.065001903	0.59384
0.019943847	0.605924751	0.738484532	0.064840578	0.59644
0.020035935	0.603324751	0.738484532	0.06474849	0.59904
0.020058489	0.600724751	0.738484532	0.064725936	0.60164
0.020011438	0.598124751	0.738484532	0.064772987	0.60424
0.019894932	0.595524751	0.738484532	0.064889493	0.60684
0.019709345	0.592924751	0.738484532	0.06507508	0.60944
0.019455265	0.590324751	0.738484532	0.06532916	0.61204
0.019133488	0.587724751	0.738484532	0.065650937	0.61464
0.018745002	0.585124751	0.738484532	0.066039423	0.61724
0.018290978	0.582524751	0.738484532	0.066493447	0.61984
0.017772748	0.579924751	0.738484532	0.067011677	0.62244
0.017191788	0.577324751	0.738484532	0.067592637	0.62504
0.0165497	0.574724751	0.738484532	0.068234725	0.62764
0.015848192	0.572124751	0.738484532	0.068936233	0.63024
0.01508906	0.569524751	0.738484532	0.069695365	0.63284
0.014274163	0.566924751	0.738484532	0.070510262	0.63544
0.013405412	0.564324751	0.738484532	0.071379013	0.63804
0.012484748	0.561724751	0.738484532	0.072299676	0.64064
0.011514129	0.559124751	0.738484532	0.073270296	0.64324
0.010495511	0.556524751	0.738484532	0.074288914	0.64584
0.009430842	0.553924751	0.738484532	0.075353583	0.64844
0.008322045	0.551324751	0.738484532	0.07646238	0.65104
0.007171011	0.548724751	0.738484532	0.077613414	0.65364

WELL-Q1				
F -Criterion Q-1	Tangential Stress	Axial Stress	Octo Stress	Mw
-0.011650086	0.383	0.70482	0.140717078	0.437
-0.012531747	0.626637862	0.786078495	0.141598738	0.4396
-0.011398343	0.624037862	0.786078495	0.140465335	0.4422
-0.010288064	0.621437862	0.786078495	0.139355055	0.4448
-0.009201464	0.618837862	0.786078495	0.138268456	0.4474
-0.008139107	0.616237862	0.786078495	0.137206099	0.45
-0.00710156	0.613637862	0.786078495	0.136168552	0.4526
-0.006089395	0.611037862	0.786078495	0.135156387	0.4552
-0.005103186	0.608437862	0.786078495	0.134170178	0.4578
-0.00414351	0.605837862	0.786078495	0.133210501	0.4604
-0.003210943	0.603237862	0.786078495	0.132277935	0.463
-0.002306064	0.600637862	0.786078495	0.131373056	0.4656
-0.001429448	0.598037862	0.786078495	0.13049644	0.4682
-0.000581669	0.595437862	0.786078495	0.12964866	0.4708
0.000236705	0.592837862	0.786078495	0.128830287	0.4734
0.001025108	0.590237862	0.786078495	0.128041883	0.476
0.001782985	0.587637862	0.786078495	0.127284006	0.4786
0.002509787	0.585037862	0.786078495	0.126557204	0.4812
0.003204976	0.582437862	0.786078495	0.125862016	0.4838
0.003868025	0.579837862	0.786078495	0.125198967	0.4864
0.00449842	0.577237862	0.786078495	0.124568572	0.489

0.005095664	0.574637862	0.786078495	0.123971328	0.4916
0.005659275	0.572037862	0.786078495	0.123407717	0.4942
0.006188791	0.569437862	0.786078495	0.122878201	0.4968
0.006683769	0.566837862	0.786078495	0.122383223	0.4994
0.007143788	0.564237862	0.786078495	0.121923204	0.502
0.007568451	0.561637862	0.786078495	0.12149854	0.5046
0.007957387	0.559037862	0.786078495	0.121109605	0.5072
0.00831025	0.556437862	0.786078495	0.120756742	0.5098
0.008626723	0.553837862	0.786078495	0.120440269	0.5124
0.008906518	0.551237862	0.786078495	0.120160474	0.515
0.009149379	0.548637862	0.786078495	0.119917613	0.5176
0.009355081	0.546037862	0.786078495	0.119711911	0.5202
0.009523432	0.543437862	0.786078495	0.119543559	0.5228
0.009654275	0.540837862	0.786078495	0.119412717	0.5254
0.009747485	0.538237862	0.786078495	0.119319507	0.528
0.009802975	0.535637862	0.786078495	0.119264017	0.5306
0.009820692	0.533037862	0.786078495	0.1192463	0.5332
0.009800618	0.530437862	0.786078495	0.119266373	0.5358
0.009742774	0.527837862	0.786078495	0.119324217	0.5384
0.009647214	0.525237862	0.786078495	0.119419777	0.541
0.009514029	0.522637862	0.786078495	0.119552963	0.5436
0.009343344	0.520037862	0.786078495	0.119723648	0.5462
0.009135318	0.517437862	0.786078495	0.119931674	0.5488
0.008890147	0.514837862	0.786078495	0.120176845	0.5514
0.008608057	0.512237862	0.786078495	0.120458935	0.554
0.008289306	0.509637862	0.786078495	0.120777686	0.5566

0.007934184	0.507037862	0.786078495	0.121132808	0.5592
0.00754301	0.504437862	0.786078495	0.121523982	0.5618
0.007116131	0.501837862	0.786078495	0.121950861	0.5644
0.00665392	0.499237862	0.786078495	0.122413072	0.567
0.006156775	0.496637862	0.786078495	0.122910216	0.5696
0.00562512	0.494037862	0.786078495	0.123441872	0.5722
0.005059398	0.491437862	0.786078495	0.124007594	0.5748
0.004460072	0.488837862	0.786078495	0.12460692	0.5774
0.003827626	0.486237862	0.786078495	0.125239366	0.58
0.003162558	0.483637862	0.786078495	0.125904434	0.5826
0.002465382	0.481037862	0.786078495	0.12660161	0.5852
0.001736627	0.478437862	0.786078495	0.127330365	0.5878
0.00097683	0.475837862	0.786078495	0.128090162	0.5904
0.000186541	0.473237862	0.786078495	0.128880451	0.593
-0.000633683	0.470637862	0.786078495	0.129700675	0.5956
-0.001483277	0.468037862	0.786078495	0.130550269	0.5982
-0.002361672	0.465437862	0.786078495	0.131428664	0.6008
-0.003268295	0.462837862	0.786078495	0.132335287	0.6034
-0.004202569	0.460237862	0.786078495	0.133269561	0.606
-0.005163917	0.457637862	0.786078495	0.134230909	0.6086
-0.006151762	0.455037862	0.786078495	0.135218753	0.6112
-0.007165526	0.452437862	0.786078495	0.136232518	0.6138
-0.008204637	0.449837862	0.786078495	0.137271629	0.6164
-0.009268522	0.447237862	0.786078495	0.138335514	0.619
-0.010356615	0.444637862	0.786078495	0.139423607	0.6216
-0.011468353	0.442037862	0.786078495	0.140535345	0.6242

